Wilson, P.A., Lyle, M., and Firth, J.V. (Eds.)
Proceedings of the Ocean Drilling Program, Scientific Results Volume 199

5. Data Report: Late Eocene–Early Oligocene Radiolarians, ODP Leg 199 Holes 1218A, 1219A, and 1220A, Central Pacific[1]

Satoshi Funakawa,[2] Hiroshi Nishi,[3] Theodore C. Moore,[4] and Catherine A. Nigrini[5]

ABSTRACT

During Ocean Drilling Program Leg 199, eight sites (Sites 1215–1222) were cored in the Central Pacific. Late Eocene–early Oligocene thick radiolarian-rich biogenic sediments were collected from Holes 1218A, 1219A, and 1220A. This is the first attempt to calibrate the ages of Paleogene radiolarian events using magnetostratigraphy in this region. A total of 107 species and species groups, which are valuable for stratigraphic correlation, are listed with numeric data and figures. Among these three holes, a total of 77 radiolarian events were recognized and their ages were calibrated by correlation with paleomagnetic events recorded in Hole 1220A.

INTRODUCTION

The Eocene/Oligocene boundary has attracted the attention of many researchers from the viewpoint that it may represent a climatic threshold from the early Paleogene greenhouse earth to the late Neogene icehouse environment. Recently, Ocean Drilling Program (ODP) research cruises in the Southern Ocean have collected and documented microfossil faunal and floral changes in Eocene–Oligocene sediment sequences and correlated these with magnetostratigraphy. Eocene–

[1]Funakawa, S., Nishi, H., Moore, T.C., and Nigrini, C.A., 2006. Data report: Late Eocene–early Oligocene radiolarians, ODP Leg 199 Holes 1218A, 1219A, and 1220A, central Pacific. *In* Wilson, P.A., Lyle, M., and Firth, J.V. (Eds.), *Proc. ODP, Sci. Results*, 199, 1–74 [Online]. Available from World Wide Web: <http://www-odp.tamu.edu/publications/199_SR/VOLUME/CHAPTERS/216.PDF>. [Cited YYYY-MM-DD]
[2]Department of Geology, Faculty of Agriculture, Utsunomiya University, Mine-cho 350, Utsunomiya, Tochigi 321-8505 Japan.
funakawa@msg.biglobe.ne.jp
[3]Department of Earth and Planetary Sciences, Graduate School of Science, Hokkaido University, N10 W8, Sapporo 060-0810 Japan.
[4]Department of Geological Sciences, University of Michigan, 2534 C.C. Little Building, Ann Arbor MI 48109-1063, USA.
[5]161 Morris, Canmore AB T1W 2W7, Canada.

Initial receipt: 4 May 2004
Acceptance: 15 March 2005
Web publication: 10 January 2006
Ms 199SR-216

Oligocene radiolarian faunal change in this region has been discussed by Caulet (1991), Takemura (1992), and Takemura and Ling (1997).

Many Paleogene radiolarians were reported during the Deep Sea Drilling Project (DSDP) from the equatorial Pacific. Riedel and Sanfilippo (1971), Moore (1971), and Johnson (1976) studied late Paleogene radiolarians from the Central Pacific in samples collected during DSDP Legs 7, 8, and 33, respectively. Goll (1972), Dinkelman (1973), and Nigrini (1985) examined Eocene–Quaternary radiolarians in samples collected during DSDP Legs 9, 16, and 85, respectively, from the eastern equatorial Pacific. The many common radiolarian events found among these sites have contributed to establishing a standard low-latitude radiolarian biostratigraphy (Sanfilippo and Riedel in Saunders et al., 1985; Sanfilippo et al., 1985; Sanfilippo and Nigrini, 1998). The time resolution of these events, however, was still uncertain because no chronologic control such as correlative magnetostratigraphy existed in the previous sequences. This research is the first attempt to examine late Paleogene radiolarian faunal change and tie it to a chronologic framework for the Central Pacific region.

Holes 1218A, 1219A, and 1220A were cored during ODP Leg 199 in the Central Pacific (Fig. F1). Radiolarian counts, 77 radiolarian events, and ages are presented here.

F1. Central Pacific map, p. 49.

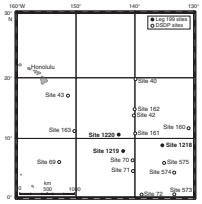

MATERIALS

Paleogene sedimentary sequences from Holes 1218A, 1219A, and 1220A are composed mainly of Oligocene nannofossil-rich calcareous ooze and chalk and underlying Eocene radiolarian-rich biosiliceous ooze and radiolarite.

Hole 1218A

Hole 1218A was drilled at 8°53.378′N, 135°22.00′W (water depth = 4828 m). The 274.3-m-thick lithologic succession overlying middle Eocene basalt basement is subdivided into four units (Shipboard Scientific Party, 2002b):

- Unit I (0–52.1 meters below seafloor [mbsf]): Holocene–early Miocene radiolarian clay, clay with radiolarians, or zeolites;
- Unit II (52.1–216.9 mbsf): early Miocene–early Oligocene nannofossil ooze, clayey radiolarian nannofossil ooze, and chalk;
- Unit III (216.9–252.2 mbsf): earliest Oligocene–middle Eocene radiolarite and nannofossil chalk with thin chert layers; and
- Unit IV (250.2–274.3 mbsf): middle Eocene nannofossil chalk.

A total of 73 samples from the interval spanning Sample 199-1218A-25X-7, 75–77 cm (233.95 mbsf; Unit III), to 22X-1, 30–32 cm (196.20 mbsf; Unit II), were collected for examination of late Eocene–early Oligocene radiolarians (Fig. F2). The average sampling interval was ~0.52 m. Radiolarian preservation is moderate to good throughout the sequence except for Sample 199-1218A-25X-2, 32–34 cm (226.52 mbsf), which is barren of radiolarians.

F2. Radiolarian species and species groups, Hole 1218A, p. 50.

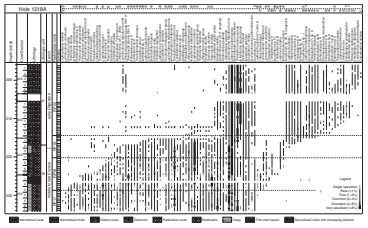

Hole 1219A

Hole 1219A is located at 7°48.019′N, 142°00.940′W (water depth = 5063 m). The 244.8-m-thick sediment overlying early Eocene basalt basement is subdivided into four units (Shipboard Scientific Party, 2002c):

Unit I (0–30.0 mbsf): Holocene–early Miocene radiolarian clay and radiolarian ooze;
Unit II (30.0–150.8 mbsf): early Miocene–early Oligocene nannofossil ooze and nannofossil ooze with radiolarians and clay;
Unit III (150.8–234.2 mbsf): late–middle Eocene radiolarian clay, radiolarian ooze of Subunit IIIA, and middle Eocene radiolarite, chert, and zeolitic clay of Subunit IIIB; and
Unit IV (234.2–44.8 mbsf): early Eocene nannofossil chalk.

A total of 65 samples spanning the interval from Sample 199-1219A-18H-3, 130–132 cm (162.30 mbsf; Subunit IIIA), to 15H-1, 30–34 cm (129.80 mbsf; Unit II), were examined for radiolarians (Fig. F3). The average sampling interval in this hole was ~0.5 m. Radiolarian preservation is good to very good throughout the sequence examined.

F3. Radiolarian species and species groups, Hole 1219A, p. 51.

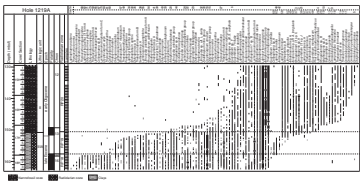

Hole 1220A

Hole 1220A is situated at 10°10.600′N, 142°45.503′W (water depth = 5218 m). The 114.0-m sedimentary sequence of this hole is subdivided into four units (Shipboard Scientific Party, 2002d):

Unit I (0–19.1 mbsf): early Miocene clay and clay with zeolite;
Unit II (19.1–37.2 mbsf): early Miocene–Oligocene radiolarian ooze with clay, nannofossil radiolarian ooze with clay, and nannofossil ooze with clay and radiolarians;
Unit III (37.2–69.2 mbsf): Oligocene nannofossil ooze, radiolarian ooze with clay and nannofossils, and nannofossil diatom ooze; and
Unit IV (Subunit IVA: 69.2–114.0 mbsf): late–middle Eocene radiolarian ooze with clay, clayey radiolarian ooze, and clay with radiolarians.

A total of 81 samples were collected for this study spanning the interval from Sample 199-1220A-9H-7, 63–65 cm (85.63 mbsf; Subunit IVA), to 6H-1, 25–27 cm (47.75 mbsf; Unit III) (Fig. F4). The average sampling interval was ~0.47 m. Preservation of radiolarians in this hole is moderate to very good.

F4. Radiolarian species and species groups, Hole 1220A, p. 52.

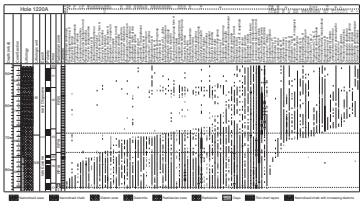

METHODS

Dried and weighed core sediment sample was placed into a beaker with a 3%–5% solution of hydrogen peroxide and sodium diphosphate decahydrate to remove the calcareous fine fraction from radiolarian shells before hydrochloric acid treatment because the calcareous fine fraction sometimes breaks radiolarian shells during intense effervescence in hydrochloric acid solution. After boiling for a few minutes to achieve desegregation of the fine calcareous fraction from radiolarian shells, the sample was sieved and washed through a 63-µm mesh. The

desegregated residue was returned to a beaker containing a 3% solution of hydrochloric acid. After dissolution of the calcareous fraction, the residue was sieved through a 63-µm screen and again returned to the beaker. A solution of ~5% hydrogen peroxide with a little sodium diphosphate decahydrate was added to the beaker and then boiled for 20 min or more. Wet residue sieved through a 63-µm mesh was oven-dried at 60°–70°C. The dried material was divided equally using a simple splitter into parts of sample large enough to obtain several thousand specimens per sample. One portion of the divided material was scattered randomly on a glass slide on which thin gum tragacanth was first spread. Material was mounted using Canada balsam and a 24 mm × 40 mm coverslip.

We counted all specimens to the end of the transverse line at which 500 specimens was exceeded. All specimens mounted on a slide were observed to confirm the occurrence of stratigraphic marker species and groups. Species and species groups that are valuable for stratigraphic correlation are recorded in **"Appendix A,"** p. 15, and illustrated in Plates P1–P17. Radiolarian events recognized in Holes 1218A, 1219A, and 1220A are presented in Table **T1.** Radiolarian count data for each hole are shown in **"Appendix B,"** p. 46, **"Appendix C,"** p. 47, and **"Appendix D,"** p. 48.

RADIOLARIAN FAUNA

The low-latitude radiolarian biostratigraphy (Sanfilippo and Riedel in Saunders et al., 1985) and the code numbers of radiolarian zones (Sanfilippo and Nigrini, 1998) are applied for this study (Figs. **F2, F3, F4, F5, F6, F7, F8**). Zones RP17 (*Cryptocarpium azyx* Interval Zone; Sanfilippo and Riedel in Saunders et al., 1985), RP18 (*Calocyclas bandyca* Concurrent Range Zone; Sanfilippo and Riedel in Saunders et al., 1985), RP19 (*Cryptocarpium ornatum* Interval Zone; Maurrasse and Glass, 1976), and RP20 (*Theocyrtis tuberosa* Interval Zone; Riedel and Sanfilippo, 1978) are identified in this study. The zonal boundaries RP17/RP18, RP18/RP19, and RP19/RP20 are defined by the bottom morphotypic appearance (Bm) of *C. bandyca*, the top morphotypic appearance (Tm) of *Thyrsocyrtis tetracantha*, and the evolutionary transition from *Lithocyclia aristotelis* group to *Lithocyclia angusta*, respectively (see Sanfilippo and Nigrini, 1998).

The uppermost radiolarian zone in each of the examined sediment sequence from Holes 1218A, 1219A, and 1220A is identified to Zone RP20. Zones RP19 and RP18 are identified in the sequences of all three holes. Zone RP17 is the basal part of the examined sequences in Holes 1218A and 1220A.

Middle–upper Eocene Zones RP17, RP18, and RP19 are characterized by relatively larger species numbers than Oligocene Zone RP20 (Figs. **F2, F3, F4**). In general, *T. tuberosa* form A, *L. aristotelis* group, *C. ornatum*, and *Periphaena triactis* are common to abundant from Zones RP17 to RP19, whereas *C. azyx* and *Thyrsocyrtis* spp. are restricted in Zone RP17 and the lower part of Zone RP18. *Lychnocanoma tripodium*, *Lophocyrtis aspera* group, *T. tuberosa* group, and *Stylosphaera coronata laevis* occur from Zone RP17 to Zone RP20. *L. tripodium* is abundant to common in middle–upper Eocene Zones RP17, RP18, and RP19, whereas *L. aspera* group and *T. tuberosa* group are abundant in Oligocene Zone RP20.

T1. Radiolarian events, p. 57.

F5. Stratigraphically valuable species/groups, Hole 1220A, p. 53.

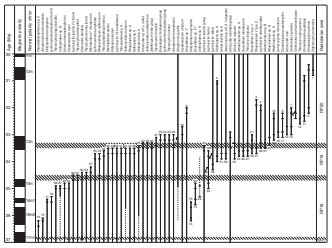

F6. Radiolarian events, Hole 1218A, p. 54.

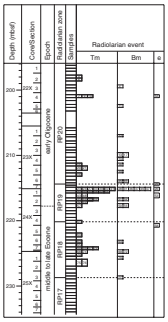

F7. Radiolarian events, Hole 1219A, p. 55.

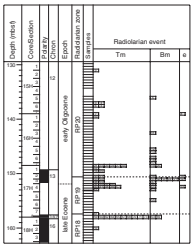

F8. Radiolarian events, Hole 1220A, p. 56.

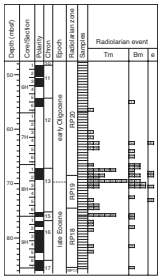

Hole 1218A

The Bm of *C. bandyca* (Zone RP17/RP18 boundary), the Tm of *T. tetracantha* (Zone RP18/RP19 boundary), and the evolutionary transition from *L. aristotelis* group to *L. angusta* (Zone RP19/RP20 boundary) are identified between Samples 199-1218A-25X-3, 120–122 cm, and 25X-3, 75–77 cm (228.90–228.45 mbsf), Samples 24X-4, 121–123 cm, and 24X-4, 75–77 cm (220.41–219.95 mbsf), and Samples 23X-7, 6–8 cm, and 23X-6, 120–122 cm (214.56–214.20 mbsf), respectively (Fig. F2).

The radiolarian fauna from Zone RP17 to lower Zone RP18 is characterized by common to abundant *C. azyx*, *T. tetracantha*, *L. tripodium* group, *T. tuberosa* group, *T. tuberosa* form A, *C. ornatum*, *Thyrsocyrtis lochites*, *P. triactis*, *L. aspera* group, and *Stylosphaera coronata laevis*. This interval is noticeable by the presence of cosmopolitan species, known from equatorial to southern high-latitude areas such as *Thyrsocyrtis* spp., *Eusyringium fistuligerum*, *L. aspera* group, and *T. tuberosa* group. *T. tuberosa* group is abundant in the lowermost part of the examined sequence and decreases in the uppermost part of Zone RP17. In the upper part of Zone RP18, *C. azyx*, *T. tetracantha*, *T. bromia* form A, *T. lochites*, and *S. coronata laevis* decrease in abundance, whereas *C. ornatum* and *L. aspera* group increase.

In the middle–upper part of Zone RP19, *T. tuberosa* form A, *L. tripodium* group, *L. aristotelis* group, *P. triactis*, and *C. ornatum* decrease in abundance and *T. tuberosa* group becomes the dominant species. The radiolarian fauna in Zone RP20 is characterized by very abundant *L. aspera* group, *Artophormis gracilis,* and *T. tuberosa* group.

Hole 1219A

Zones RP18, RP19, and RP20 were distinguished in the analyzed interval from this hole (Fig. F3). The Tm of *T. tetracantha* (Zone RP18/RP19 boundary) is situated between Samples 199-1219A-17H-7, 130–132 cm, and 17H-7, 80–82 cm (157.65–157.15 mbsf), and the evolutionary transition from *L. aristotelis* group to *L. angusta* (Zone RP19/RP20 boundary) is located between Samples 199-1219A-17H-2, 80–82 cm, and 17H-2, 30–32 cm (150.80–150.30 mbsf).

The radiolarian fauna in Zone RP18 is marked by abundant to very abundant occurrences of *C. ornatum*, *L. aspera* group, and *T. lochites* with common occurrences of *L. aristotelis* group, *P. triactis*, *T. tuberosa* form A, and *L. tripodium* group.

In Zone RP19, several species that are abundant in Zone RP18 such as *T. tuberosa* form A, *L. aristotelis* group, *P. triactis*, *C. ornatum*, and *L. tripodium* group decrease, whereas *T. tuberosa* group increases in abundance. In Zone RP20, *L. aspera* group, *T. tuberosa* group, and *A. gracilis* become abundant.

Hole 1220A

In this hole, Zones RP17–RP20 were recognized in the analyzed interval (Fig. F4). Shipboard Scientific Party (2002c) reported the Zone RP17/RP18 boundary between Sections 199-1220A-9H-7, 45 cm, and 9H-6, 45 cm (85.45–83.95 mbsf). In this study, *C. bandyca* is present in Sample 199-1220A-9H-7, 25–27 cm (85.25 mbsf), but is absent from Sample 199-1220A-9H-7, 63–65 cm (85.63 mbsf). Therefore, the Zone RP17/RP18 boundary is located between Section 199-1220A-9H-7, 45 cm, and 9H-7, 25–27 cm (85.45–85.25 mbsf). The Tm of *T. tetracantha* (Zone

RP18/RP19 boundary) is located between Samples 199-1220A-8H-6, 77–79 cm, and 8H-6, 25–27 cm (74.77–74.25 mbsf), and the evolutionary transition from *L. aristotelis* group to *L. angusta* (Zone RP19/RP20 boundary) is placed between Samples 8H-2, 75–77 cm, and 8H-2, 25–27 cm (68.75–68.25 mbsf).

From Zone RP17 to the middle part of Zone RP18, the radiolarian fauna is characterized by abundant *T. lochites*, *L. aristotelis* group, *C. ornatum*, *T. tuberosa* form A, *P. triactis*, *S. coronata laevis*, *L. tripodium* group, and *L. aspera* group. Although their presence persists into the overlying Zone RP19, common to abundant occurrences of *T. lochites* end within Zone RP18. *T. bromia* form A and *Zealithapium mitra* group also decrease in abundance at the same level.

In the middle–upper part of Zone RP19, abundances of *L. aristotelis* group, *C. ornatum*, and *P. triactis* decrease, whereas *T. tuberosa* group increases. In Zone RP20, *L. aspera* group and *A. gracilis* are abundant to very abundant. *T. tuberosa* group is one of the dominant species in the lower–middle part of Zone RP20 but exhibits a sharp decline in abundance in the upper part of Zone RP20.

RADIOLARIAN EVENTS

A total of 77 radiolarian events were recognized within the examined sequences: 26 Bms, 5 evolutionary transitions (e), and 46 Tms (Table **T1**). Of the 77 events, 67 events were recognized in all holes and 9 were recognized in two holes. The distribution of Bms and Tms demonstrates that the interval from the late Eocene to early Oligocene is characterized by Tms rather than Bms (Figs. **F5, F6, F7, F8;** Table **T1**).

Paleomagnetic events were assigned in Holes 1219A and 1220A (Shipboard Scientific Party, 2002c, 2002d). In this study, the Hole 1220A paleomagnetic events that were confirmed from the Chron C11r/C12n to C17n/C17r boundaries throughout the sequence examined were applied for age calibration of the radiolarian events. Ages of radiolarian events were calibrated to the global paleomagnetic timescale of Berggren et al. (1995) and are noted in the right-hand columns in Table **T1.** Ranges of stratigraphically valuable species and species groups in Hole 1220A are shown in Figure **F5.**

Hole 1218A

In Hole 1218A, 25 Bms and 46 Tms were identified (Fig. **F6;** Table **T1**).

In Zones RP18, RP19, and RP20, 12, 22, and 9 Tms are distributed, respectively (Fig. **F6;** Table **T1**). Three intervals featuring concentrations of Tms were distinguished. Ten Tms are observed in the middle–upper part of Zone RP18 from Samples 199-1218A-25X-1, 75–77 cm, to 24X-5, 71–73 cm (225.45–221.41 mbsf), and form an interval of Tm concentration. Across the Eocene/Oligocene boundary from the upper part of Zone RP19 to the lowermost part of Zone RP20 between Samples 199-1218A-24X-2, 118–120 cm (217.38 mbsf), and 23X-4, 118–120 cm (211.18 mbsf), 25 Tms are concentrated. In Zone RP20, 5 Tms are situated within an interval from Sample 199-1218A-22X-4, 75–77 cm, to 22X-1, 120–122 cm (201.15–197.10 mbsf).

In Zones RP18, RP19, and RP20, 4, 10, and 10 Bms are observed, respectively (Fig. **F6;** Table **T1**). One interval characterized by concentration of Bms is recognized around the Eocene/Oligocene boundary from

the upper part of Zone RP19 (Sample 199-1218A-24X-3, 29–31 cm; 217.99 mbsf) to the lower part of Zone RP20 (Sample 23X-3, 107–109 cm; 209.57 mbsf), in which 17 Bms are located.

Hole 1219A

In the examined sequence from this hole, 22 Bms and 44 Tms were identified (Fig. F7; Table T1).

In Zones RP18, RP19, and RP20, 11, 14, and 16 Tms are identified, respectively (Fig. F7; Table T1). In the uppermost part of Zone RP18 between Samples 199-1219A-18H-1, 30–32 cm, and 17H-7, 130–132 cm (158.30–157.65 mbsf), 10 Tms and 2 Bms are concentrated. Because these events are scattered from the middle to upper part of Zone RP19 in Holes 1218A and 1220A (Figs. F6, F8), a possible hiatus covering part of upper Zone RP19 is indicated in this hole. According to age calibration of radiolarian events in Hole 1220A, the estimated age of the lower limit of the hiatus is ~36.1 Ma and that of the upper limit is ~34.7 Ma.

Across the Eocene/Oligocene boundary from the upper part of Zone RP19 to lowermost part of Zone RP20 between Samples 199-1219A-17H-4, 130–132 cm (153.15 mbsf), and 16H-7, 30–32 cm (148.30 mbsf), a total of 25 Tms are situated. In Zone RP20, 6 Tms are located in the interval from Sample 199-1219A-16H-1, 78–80 cm, to 15H-5, 130–134 cm (139.78–136.80 mbsf).

In Zones RP18, RP19, and RP20, 2, 10, and 8 Bms are distributed, respectively (Fig. F7; Table T1). Sixteen Bms are situated around the Eocene/Oligocene boundary from the upper part of Zone RP19 (Sample 199-1219A-17H-4, 130–132 cm; 153.15 mbsf) to the lower part of Zone RP20 (Sample 16H-5, 78–80 cm; 145.78 mbsf).

Hole 1220A

In the examined interval from this hole, 26 Bms and 45 Tms were identified (Fig. F8; Table T1).

In Zones RP18, RP19, and RP20, 10, 16, and 14 Tms are distributed, respectively (Fig. F8; Table T1). In an interval from the upper part of Zone RP18 (Sample 199-1220A-9H-2, 125–127 cm; 78.75 mbsf) to the lowermost part of Zone RP19 (Sample 8H-5, 125–127 cm; 73.75 mbsf), 12 Tms are concentrated. Across the Eocene/Oligocene boundary from the upper part of Zone RP19 to the lowermost of Zone RP20 between Samples 199-1220A-8H-3, 127–129 cm (70.77 mbsf), and 8H-1, 77–79 cm (67.27 mbsf), a total of 22 Tms are distributed.

In Zones RP18, RP19, and RP20, 4, 9, and 10 Bms are observed, respectively (Fig. F8; Table T1). From the upper part of Zone RP19 (Sample 199-1220A-8H-3, 127–129 cm; 70.77 mbsf) to the lower part of Zone RP20 (Sample 7H-7, 35–37 cm; 66.35 mbsf), 16 Bms are distributed; this interval is characterized by Bms.

ACKNOWLEDGMENTS

The authors express their sincere thanks to Annika Sanfilippo of Scripps Institution of Oceanography (La Jolla, California, USA) and Toyosaburo Sakai of Utsunomiya University (Japan) for suggesting species identification of radiolarians. We also thank Christopher J. Hollis of the Institute of Geological and Nuclear Sciences (Lower Hutt, New Zealand) and Lorri Peters of Texas A&M University (ODP, College Sta-

tion, Texas, USA) for reviewing the draft of this report. This work was financially supported by a Grant-in-Aid for Research Fellowships of the Japan Society for the Promotion of Science for Young Scientists (number 1200254) for the first author. Part of this work was carried out at the Satellite Institution (Radiolaria) of Micropaleontological Reference Center in Utsunomiya University, Japan. This research used samples and/or data provided by the Ocean Drilling Program (ODP). ODP is sponsored by the U.S. National Science Foundation (NSF) and participating member countries under management of Joint Oceanographic Institutions (JOI), Inc.

REFERENCES

Abelmann, A., 1990. Oligocene to middle Miocene radiolarian stratigraphy of southern high latitudes from Leg 113, Sites 689–690, Maud Rise. *In* Barker, P.F., Kennett, J.P., et al., *Proc. ODP, Sci. Results,* 113: College Station, TX (Ocean Drilling Program), 675–708.

Abelmann, A., 1992. Early to middle Miocene radiolarian stratigraphy of the Kerguelen Plateau, Leg 120. *In* Wise, S.W., Jr., Schlich, R., et al., *Proc. ODP, Sci. Results,* 120: College Station, TX (Ocean Drilling Program), 757–783.

Berggren, W.A., Kent, D.V., Swisher, C.C., III, and Aubry, M.-P., 1995. A revised Cenozoic geochronology and chronostratigraphy. *In* Berggren, W.A., Kent, D.V., Aubry, M.-P., and Hardenbol, J. (Eds.), *Geochronology, Time Scales and Global Stratigraphic Correlation*. Spec. Publ.—SEPM (Soc. Sediment. Geol.), 54:129–212.

Burma, B.H., 1959. On the status of *Theocampe* Haeckel, and certain similar genera. *Micropaleontology,* 5:325–330.

Bury, P.S., 1862. *Figures of Remarkable Forms of Polycystins, or Allied Organisms, in the Barbados Chalk Deposit:* London (W. Weldon).

Bütschli, O., 1882. Beiträge zur Kenntnis der Radiolarienskelette, insbesondere der Cyrtida. *Z. Wiss. Zool.,* 36:485–540.

Bütschli, O., 1882. Klassen und Ordnungen des Their-Reichs, wissenschaftlich dargestellt in Wort und Bild. *In* Brown, H.G. (Ed.), *Paleontologische Entwicklung der Rhizopoda von C. Schwager.* I. *Abtheilung:* Heidelberg (Sarkodia und Sporozoa), 321–616.

Carnevale, P., 1908. Radiolarie e silicoflagellati di Bergonzano (Reggio Emilia). *Veneto Sci. Lett. Arti Mem.,* 28:1–46.

Caulet, J.P., 1986. Radiolarians from the southwest Pacific. *In* Kennett, J.P., von der Borch, C.C., et al., *Init. Repts. DSDP,* 90: Washington (U.S. Govt. Printing Office), 835–861.

Caulet, J.-P., 1991. Radiolarians from the Kerguelen Plateau, Leg 119. *In* Barron, J., Larsen, B., et al., *Proc. ODP, Sci. Results,* 119: College Station, TX (Ocean Drilling Program), 513–546.

Chen, P.-H., 1975. Antarctic radiolaria. *In* Hayes, D.E., Frakes, L.A., et al., *Init. Repts. DSDP,* 28: Washington (U.S. Govt. Printing Office), 437–513.

Clark, B.L., and Campbell, A.S., 1942. Eocene radiolarian faunas from the Mt. Diablo area, California. *Spec. Pap.—Geol. Soc. Am.,* 39:1–112.

Clark, B.L., and Campbell, A.S., 1945. Radiolaria from the Kreyenhagen Formation near Los Banos, California. *Mem.—Geol. Soc. Am.,* 101:1–66.

De Wever, P., Dumitrica, P., Caulet, J.-P., Nigrini, C., and Caridroit, M., 2001. *Radiolarians in the sedimentary record:* New York (Gordon and Breach Science Publ.).

Deflandre, G., 1953. Radiolaires fossiles. *In* Grassé, P.-P. (Ed.), *Traité de Zoologie* (Vol. 1): 389–436.

Dinkelman, M.G., 1973. Radiolarian stratigraphy: Leg 16, Deep Sea Drilling Program. *In* van Andel, T.H., Heath, G.R., et al., *Init. Repts. DSDP,* 16: Washington (U.S. Govt. Printing Office), 747–813.

Dreyer, F., 1889. Morphologische Radiolarienstudien. 1. Die Pylombildungen in vergleichend-anatomischer und entwicklungsgeschichtlicher Beziehung bei Radiolarien und bei Protisten überhaupt, nebst System und Beschreibung neuer und der bis jetzt bekannten pylomatischen Spumellarien. *Jena. Z. Naturwiss.,* 23:1–138.

Dzinoridze, R.N., Jousé, A.P., Koroleva-Golikova, G.S., Kozlova, G.E., Nagaeva, G.S., Petrushevskaya, M.G., and Strelnikova, N.I., 1978. Diatom and radiolarian Cenozoic stratigraphy, Norwegian Basin; DSDP Leg 38. *In* Talwani, M., Udintsev, G., et al., *Init. Repts. DSDP,* 38, 39, 40, 41 (Suppl.): Washington (U.S. Govt. Printing Office), 289–427.

Ehrenberg, C.G., 1838. Über die Bildung der Kreidefelsen und des Kreidemergels durch sichtbare Organismen. *Abh. Kgl. Preuss.* (Akad. Wiss. Berlin), 59–147.

Ehrenberg, C.G., 1847. Über die mikroskopischen kieselschaligen Polycystinen als mächtige Gebirgsmasse von Barbados und über das Verhältniss deraus mehr als 300 neuen Arten bestehenden ganz eigenthümlichen Formengruppe jener Felsmasse zu den jetzt lebenden Thieren und zur Kreidebildung. Eine neue Anregung zur Erforschung des Erdlebens. *K. Preuss. Akad. Wiss. Berlin, Ber., Jahre 1847*:40–60.

Ehrenberg, C.G., 1854. *Mikrogeologie: Das Erden und Felsen schaffende Wirken des unsichtbar kleinen selbständigen Lebens auf der Erde:* Leipzig (Leopold Voss).

Ehrenberg, C.G., 1873. Grössere Felsproben des Polycystinen-Mergels von Barbados mit weiteren Erläuterungen. *K. Preuss. Akad. Wiss. Berlin, Monatsberichte,* 1873:213–263.

Ehrenberg, C.G., 1875. Fortsetzung der mikrogeologischen Studien als Gesammt-Uebersicht der mikroskopischen Paläontologie gleichartig analysirter Gebirgsarten der Erde, mit specieller Rücksicht auf den Polycystinen-Mergel von Barbados. *Abh. K. Akad. Wiss. Berlin,* 1875:1–225.

Foreman, H.P., 1973. Radiolaria of Leg 10 with systematics and ranges for the families Amphipyndacidae, Artostrobiidae, and Theoperidae. *In* Worzel, J.L., Bryant, W., et al., *Init. Repts. DSDP,* 10: Washington (U.S. Govt. Printing Office), 407–474.

Goll, R.M., 1972. Leg 9 synthesis, radiolaria. *In* Hays, J.D., et al., *Init. Repts. DSDP,* 9: Washington (U.S. Govt. Printing Office), 947–1058.

Haeckel, E., 1862. *Die Radiolarien (Rhizopoda Radiolaria):* Berlin (Reimer).

Haeckel, E., 1879. *Natürliche Schöpfungsgeschichte* (7th ed.): Berlin (Georg Reimer).

Haeckel, E., 1881. Entwurf eines Radiolarien-Systems auf Grund von Studien der Challenger-Radiolarien (Basis for a radiolarian classification from the study of Radiolaria of the Challenger collection). *Jena. Z. Med. Naturwiss.,* 15 (Vol. 8, Pt. 3):418–472.

Haeckel, E., 1887. Report on the radiolaria collected by H.M.S. *Challenger* during the years 1873–1876. *Rep. Sci. Results Voy. H.M.S.* Challenger, *1873–1876, Zool.,* 18:1–1803.

Holdsworth, B.K., 1975. Cenozoic radiolaria biostratigraphy: Leg 30: tropical and equatorial Pacific. *In* Andrews, J.E., Packham, G., et al., *Init. Repts. DSDP,* 30: Washington (U.S. Govt. Printing Office), 499–537.

Hull, D.M., 1993. Quaternary, Eocene, and Cretaceous radiolarians from the Hawaiian Arch, northern equatorial Pacific Ocean. *In* Wilkens, R.H., Firth, J., Bender, J., et al., *Proc. ODP, Sci. Results,* 136: College Station, TX (Ocean Drilling Program), 3–25.

Johnson, D.A., 1974. Radiolaria from the eastern Indian Ocean, DSDP Leg 22. *In* von der Borch, C.C., Sclater, J.G., et al., *Init. Repts. DSDP,* 22: Washington (U.S. Govt. Printing Office), 521–575.

Johnson, D.A., 1976. Cenozoic radiolarians from the central Pacific, DSDP Leg 33. *In* Schlanger, S.O., Jackson, E.D., et al., *Init. Repts. DSDP,* 33: Washington (U.S. Govt. Printing Office), 425–437.

Johnson, D.A., 1978. Cenozoic Radiolaria from the eastern tropical Atlantic, DSDP Leg 41. *In* Lancelot, Y., Seibold, E., et al., *Init. Repts. DSDP,* 41: Washington (U.S. Govt. Printing Office), 763–789.

Kellogg, D.E., 1980. Character displacement and phyletic change in the evolution of the radiolarian subfamily Artiscinae. *Micropaleontology,* 26:196–210.

Kling, S.A., 1971. Radiolaria: Leg 6 of the Deep Sea Drilling Project. *In* Fischer, A.G., Heezen, B.C., et al., *Init. Repts. DSDP,* 6: Washington (U.S. Govt. Printing Office), 1069–1117.

Kozlova, G.E., 1983. Radiolyarievye Kompleksy Borealnogo Nizhnego Paleotchena: rol mikrofauny v izucheni i osadochnykh toltsch kontinentov i morei. *Tr., Vses. Nauchno-Issled. Geologorazved. Neft. Inst.,* 126:84–112. (in Russian)

Kozlova, G.E., 1999. Radiolyarii paleogena borealnoi oblasti rossii: Praktichskoe Rukovodstvo po mikrofaune rossii. *Tr., Vses. Nauchno-Issled. Geologorazved. Neft. Inst.,* 9:1–323. (in Russian)

Ling, H.Y., 1975. Radiolaria: Leg 31 of the Deep Sea Drilling Project. *In* Karig, D.E., Ingle, J.C., Jr., et al., *Init. Repts. DSDP,* 31: Washington (U.S. Govt. Printing Office), 703–761.

Lucchese, C., 1927. Radiolari Miocenici di Salsomaggiore: annali del R. Museo Geologico di Bologna. *G. Geol.,* 2:80–116.

Martin, G.C., 1904. Radiolaria. *In* Clark, W.B., Eastman, C.R., Glenn, L.C., Bagg, R.M., Bassler, R.S., Boyer, C.S., Case, E.C., and Hollick, C.A. (Eds.), *Systematic Paleontology of the Miocene Deposits of Maryland:* Baltimore (Maryland Geol. Surv., Johns Hopkins Press), 447–459.

Mato, C.Y., and Theyer, F., 1980. *Lychnocanoma bandyca* n. sp., a new stratigraphically important late Eocene radiolarian. *In* Sliter, W. V. (Ed.), *Studies in Marine Micropaleontology and Paleoecology: A Memorial Volume to Orville L. Bandy.* Spec. Publ. Cushman Found. Foram. Res., 19:225–229.

Maurrasse, F., and Glass, B.P., 1976. Radiolarian stratigraphy and North American microtektites in Caribbean RC9-58: implications concerning late Eocene radiolarian chronology and the age of the Eocene-Oligocene boundary. *Trans. 7th Caribbean Geol. Conf.,* Guadeloupe, 1974:205–212.

Moore, T.C., 1971. Radiolaria. *In* Tracey, J.I., Jr., Sutton, G.H., et al., *Init. Repts. DSDP,* 8: Washington (U.S. Govt. Printing Office), 727–775.

Moore, T.C., 1972. Mid-Tertiary evolution of the radiolarian genus *Calocycletta. Micropaleontology,* 18:144–152.

Moore, T.C., 1973. Radiolaria from Leg 17 of the Deep Sea Drilling Project. *In* Winterer, E.L., Ewing, J.I., et al., *Init. Repts. DSDP,* 17: Washington (U.S. Govt. Printing Office), 797–869.

Müller, J., 1858. Über die Thalassicollen, Polycystinen und Acanthometren des Mittelmeeres. *K. Preuss. Akad. Wiss. Berlin, Abh.,* 1–62.

Murray, J., 1895. A summary of the scientific results obtained at the sounding, dredging, and trawling stations of the *HMS Challenger. Rep. Sci. Results Voyage HMS Challenger,* 2:817–822.

Nigrini, C., 1974. Cenozoic Radiolaria from the Arabian Sea, DSDP Leg 23. *In* Davies, T.A., Luyendyk, B.P., et al., *Init. Repts. DSDP,* 26: Washington (U.S. Govt. Printing Office), 1051–1121.

Nigrini, C., 1977. Tropical Cenozoic Artostrobiidae (Radiolaria). *Micropaleontology,* 23:241–269.

Nigrini, C., 1985. Radiolarian biostratigraphy in the central equatorial Pacific, Deep Sea Drilling Project Leg 85. *In* Mayer, L.A., Theyer, F., Thomas, E., et al., *Init. Repts. DSDP,* 85: Washington (U.S. Govt. Printing Office), 511–551.

Nigrini, C., and Sanfilippo, A., 2000. Paleogene radiolarians from Sites 998, 999, and 1001 in the Caribbean. *In* Leckie, R.M., Sigurdsson, H., Acton, G.D., and Draper, G. (Eds.), *Proc. ODP, Sci. Results,* 165, 57–81 [CD-ROM]. Available from: Ocean Drilling Program, Texas A&M University, College Station, TX 77845-9547, U.S.A.

Nishimura, A., 1987. Cenozoic Radiolaria in the western North Atlantic, Site 603, Leg 93 of the Deep Sea Drilling Project. *In* van Hinte, J.E., Wise, S.W., Jr., et al., *Init. Repts. DSDP,* 93 (Pt. 2): Washington (U.S. Govt. Printing Office), 713–737.

O'Connor, B., 1997. Lower Miocene Radiolaria from Te Kopua Point, Kaipara Harbour, New Zealand. *Micropaleontology,* 43:101–128.

O'Connor, B.M., 1999. Radiolaria from the late Eocene Oamaru diatomite, South Island, New Zealand. *Micropaleontology,* 45:1–55.

Palmer, A., 1987. Cenozoic radiolarians from Deep Sea Drilling Project Sites 612 and 613 (Leg 95, New Jersey Transect) and Atlantic Slope Project Site ASP 15. *In* Poag, C.W., Watts, A.B., et al., *Init. Repts. DSDP,* 95: Washington (U.S. Govt. Printing Office), 339–357.

Petrushevskaya, M.G., 1971. Radiolarii Nassellaria v planktone Mirovogo Okeana. *Issled. Fauny Morey, Nauka,* 9:5–294. (in Russian)

Petrushevskaya, M.G., 1975. Cenozoic radiolarians of the Antarctic, Leg 29, DSDP. *In* Kennett, J.P., Houtz, R.E., et al., *Init. Repts. DSDP,* 29: Washington (U.S. Govt. Printing Office), 541–675.

Petrushevskaya, M.G., and Kozlova, G.E., 1972. Radiolaria, Leg 14, Deep Sea Drilling Project. *In* Hayes, D.E., Pimm, A.C., et al., *Init. Repts. DSDP,* 14: Washington (U.S. Govt. Printing Office), 495–648.

Popova, I.M., Baumgartner, P.O., Guex, J., Tochilina, S.V.,and Glezer, Z.I., 2002. Radiolarian biostratigraphy of Paleogene deposits of the Russian platform (Voronesh anticline). *Geodiversitas,* 24:7–59.

Renz, G.W., 1984. Cenozoic radiolarians from the Barbados Ridge, Lesser Antilles subduction complex, Deep Sea Drilling Project Leg 78A. *In* Biju-Duval, B., Moore, J.C., et al., *Init. Repts. DSDP,* 78: Washington (U.S. Govt. Printing Office), 447–462.

Riedel, W.R., 1957. Eocene Radiolaria. *Geol. Surv. Prof. Pap. U.S.,* 280G:257.

Riedel, W.R., 1957. Radiolaria: a preliminary stratigraphy. *In* Petterson, H. (Ed.), *Rep. Swed. Deep-Sea Exped., 1947–1948* (Vol. 6): Goteborg (Elanders Boktryckeri Aktiebolag), 59–96.

Riedel, W.R., 1959. Oligocene and Lower Miocene Radiolaria in tropical Pacific sediments. *Micropaleontology,* 5:285–302.

Riedel, W.R., 1967. Subclass Radiolaria. *In* Harland, W.B., Holland, C.H., House, M.R., Hughes, N.F., Reynolds, A.B., Rudwick, M.J.S., Satterthwaite, G.E., Tarlo, L.B.H., and Willey, E.C. (Eds.), *The Fossil Record.* Geol. Soc. London, 291–298.

Riedel, W.R., and Funnell, B.M., 1964. Tertiary sediment cores and microfossils from the Pacific Ocean floor. *Q. J. Geol. Soc. London,* 120:305–368.

Riedel, W.R., and Hays, J.D., 1969. Cenozoic Radiolaria from Leg 1. *In* Ewing, M., and Worzel, J.L., et al., *Init. Repts. DSDP,* 1: Washington (U.S. Govt. Printing Office), 400–402.

Riedel, W.R., and Sanfilippo, A., 1970. Radiolaria, Leg 4, Deep Sea Drilling Project. *In* Bader, R.G., Gerard, R.D., et al., *Init. Repts. DSDP,* 4: Washington (U.S. Govt. Printing Office), 503–575.

Riedel, W.R., and Sanfilippo, A., 1971. Cenozoic Radiolaria from the western tropical Pacific, Leg 7. *In* Winterer, E.L., Riedel, W.R., et al., *Init. Repts. DSDP,* 7 (Pt. 2): Washington (U.S. Govt. Printing Office), 1529–1672.

Riedel, W.R., and Sanfilippo, A., 1973. Cenozoic Radiolaria from the Caribbean, Deep Sea Drilling Project, Leg 15. *In* Edgar, N.T., Saunders, J.B., et al., *Init. Repts. DSDP,* 15: Washington (U.S. Govt. Printing Office), 705–751.

Riedel, W.R., and Sanfilippo, A., 1978. Stratigraphy and evolution of tropical Cenozoic radiolarians. *Micropaleontology,* 24:61–96.

Riedel, W.R., and Sanfilippo, A., 1986. Morphological characters for a natural classification of Cenozoic Radiolaria, reflecting phylogenies. *Mar. Micropaleontol.,* 11:151–170.

Sanfilippo, A., 1990. Origin of the subgenera *Cyclampterium, Paralampterium* and *Sciadiopeplus* from *Lophocyrtis* (*Lophocyrtis*) (Radiolaria, Theoperidae). *Mar. Micropaleontol.,* 15:287–312.

Sanfilippo, A., and Caulet, J.P., 1998. Taxonomy and evolution of Paleogene Antarctic and tropical Lophocyrtid radiolarians. *Micropaleontology,* 44:1–43.

Sanfilippo, A., and Nigrini, C., 1995. Radiolarian stratigraphy across the Oligocene/Miocene transition. *Mar. Micropaleontology,* 24:239–285.

Sanfilippo, A., and Nigrini, C., 1998. Code numbers for Cenozoic low latitude radiolarian biostratigraphic zones and GPTS conversion tables. *Mar. Micropaleontol.,* 33:109–156.

Sanfilippo, A., and Riedel, W.R., 1973. Cenozoic Radiolaria (exclusive of theoperids, artostrobiids and amphipyndacids) from the Gulf of Mexico, Deep Sea Drilling Project Leg 10. *In* Worzel, J.L., Bryant, W., et al., *Init. Repts. DSDP,* 10: Washington (U.S. Govt. Printing Office), 475–611.

Sanfilippo, A., and Riedel, W.R., 1974. Radiolaria from the west-central Indian Ocean and Gulf of Aden, DSDP Leg 24. *In* Fisher, R.L., Bunce, E.T., et al., *Init. Repts. DSDP,* 24: Washington (U.S. Govt. Printing Office), 997–1035.

Sanfilippo, A., and Riedel, W.R., 1979. Radiolaria from the northeastern Atlantic Ocean, DSDP Leg 48. *In* Montadert, L., Roberts, D. G., et al., *Init. Repts., DSDP,* 48: Washington (U.S. Govt. Printing Office), 493–511.

Sanfilippo, A., and Riedel, W.R., 1980. A revised generic and suprageneric classification of the Artiscins (Radiolaria). *J. Paleontol.,* 54:1008–1011.

Sanfilippo, A., and Riedel, W.R., 1982. Revision of the radiolarian genera *Theocotyle, Theocotylissa,* and *Thyrsocyrtis*. *Micropaleontology,* 28:170–188.

Sanfilippo, A., and Riedel, W.R., 1992. The origin and evolution of Pterocorythidae (Radiolaria): a Cenozoic phylogenetic study. *Micropaleontology,* 38:1–36.

Sanfilippo, A., Westberg-Smith, M.J., and Riedel, W.R., 1981. Cenozoic Radiolarians at Site 462, Deep Sea Drilling Project Leg 61, Western Tropical Pacific. *In* Larson, R.L., Schlanger, S.O., et al., *Init. Repts. DSDP,* 61: Washington (U.S. Govt. Printing Office), 495–505.

Sanfilippo, A., Westberg-Smith, M.J., and Riedel, W.R., 1985. Cenozoic radiolaria. *In* Bolli, H.M., Saunders, J.B., and Perch-Nielsen, K. (Eds.), *Plankton Stratigraphy:* Cambridge (Cambridge Univ. Press), 631–712.

Saunders, J.B., Bernoulli, D., Mueller-Merz, E., Oberhänsli, H., Perch-Nielsen, K., Riedel, W.R., Sanfilippo, A., and Torrini, R., Jr., 1984. Stratigraphy of the late middle Eocene to early Oligocene in the Bath Cliff section Barbados, West Indies. *Micropaleontology,* 30:390–425.

Shilov, V.V., 1995. Eocene–Oligocene radiolarians from Leg 145, North Pacific. *In* Rea, D.K., Basov, I.A., Scholl, D.W., and Allan, J.F. (Eds.), *Proc. ODP, Sci. Results,* 145: College Station, TX (Ocean Drilling Program), 117–132.

Shipboard Scientific Party, 2002a. Leg 199 summary. *In* Lyle, M., Wilson, P.A., Janecek, T.R., et al., *Proc. ODP, Init. Repts.,* 199: College Station TX (Ocean Drilling Program), 1–87.

Shipboard Scientific Party, 2002b. Site 1218. *In* Lyle, M., Wilson, P.A., Janecek, T.R., et al., *Proc. ODP, Init. Repts.,* 199, 1–125 [CD-ROM]. Available from: Ocean Drilling Program, Texas A&M University, College Station TX 77845-9547, USA.

Shipboard Scientific Party, 2002c. Site 1219. *In* Lyle, M., Wilson, P.A., Janecek, T.R., et al., *Proc. ODP, Init. Repts.,* 199, 1–128 [CD-ROM]. Available from: Ocean Drilling Program, Texas A&M University, College Station TX 77845-9547, USA.

Shipboard Scientific Party, 2002d. Site 1220. *In* Lyle, M., Wilson, P.A., Janecek, T.R., et al., *Proc. ODP, Init. Repts.,* 199, 1–92 [CD-ROM]. Available from: Ocean Drilling Program, Texas A&M University, College Station TX 77845-9547, USA.

Takemura, A., 1992. Radiolarian Paleogene biostratigraphy in the southern Indian Ocean, Leg 120. *In* Wise, S.W., Jr., Shlich, R., et al., *Proc. ODP, Sci. Results,* 120: College Station, TX (Ocean Drilling Program), 735–756.

Takemura, A., and Ling, H.Y., 1997. Eocene and Oligocene radiolarian biostratigraphy from the Southern Ocean: correlation of ODP Legs 114 (Atlantic Ocean) and 120 (Indian Ocean). *Mar. Micropaleontol.,* 30:97–116.

Takemura, A., and Ling, H.Y., 1998. Taxonomy and phylogeny of the genus *Theocorys* (*Nassellaria,* radiolaria) from the Eocene and Oligocene sequences in the Antarctic region. *Paleontol. Res.,* 2:155–169.

Theyer, F., Mato, C.Y., and Hammond, S.R., 1978. Paleomagnetic and geochronologic calibration of latest Oligocene to Pliocene radiolarian events, equatorial Pacific. *Mar. Micropaleontol.,* 3:377–395.

Vinassa de Regny, P.E., 1900. Radiolari Miocenici Italiani. *Mem. R. Acad. Sci. Inst. Bologna, Ser. 5,* 8:227–257.

Weaver, F.M., 1983. Cenozoic radiolarians from the southwest Atlantic, Falkland Plateau region, Deep Sea Drilling Project Leg 71. *In* Ludwig, W.J., Krasheninnikov, V.A., et al., *Init. Repts. DSDP,* 44: Washington (U.S. Govt. Printing Office), 667–686.

Weaver, F.M., and Dinkelman, M.G., 1978. Cenozoic radiolarians from the Blake Plateau and the Blake–Bahama Basin, DSDP Leg 44. *In* Benson, W.E., Sheridan, R.E., et al., *Init. Repts. DSDP,* 44: Washington (U.S. Govt. Printing Office), 865–885.

Westberg-Smith, M.J., and Riedel, W.R., 1984. Radiolarians from the western margin of the Rockall Plateau: Deep Sea Drilling Project Leg 81. *In* Roberts, D.G., Schnitker, D., et al., *Init. Repts. DSDP,* 81: Washington (U.S. Govt. Printing Office), 479–501.

Wiseman, J.D., and Riedel, W.R., 1960. Tertiary sediments from the floor of the Indian Ocean. *Deep-Sea Res.,* 7: 215–217.

APPENDIX A

Species List

Descriptions and illustrations of the species in the present study are found in the publications cited. In this study, classification of family by De Wever et al. (2001) was applied.

Subclass RADIOLARIA Müller, 1858
Superorder POLYCYSTINA Ehrenberg, 1838, emend. Riedel, 1967
Order NASSELLARIA Ehrenberg, 1875
Family Acanthodesmiidae Haeckel, 1881, emend. Riedel, 1967

***Dendrospyris* sp. A**
(Pl. P1, figs. 1a–3)

Remarks: Lattice shell is elliptical in ventral and dorsal views with constriction along sagittal ring. Lattice pores are subcircular and irregularly distributed; relatively large ones are attached to sagittal ring. Surface of lattice shell is somewhat thorny without apical horn. Several rodlike appendages extend from oval basal ring. Median bar is located in higher horizon than basal ring. Primary lateral spines extend downward and, in most specimens, are not attached to basal ring.

This species is distinguished from *Dendrospyris anthocyrtoides* by larger size of subcircular pores in the thick shell wall.

***Dorcadospyris circulus* (Haeckel) group**
(Pl. P1, figs. 4a–5b)

Gamospyris circulus Haeckel, 1887, p. 1042, pl. 83, fig. 19; Goll, 1972, p. 965, pl. 59, fig. 1; pl. 60, figs. 1–3; pl. 61, fig. 1; pl. 62, figs. 1–3.

Dorcadospyris circulus (Haeckel): Moore, 1971, p. 739, pl. 8, figs. 3–5; Sanfilippo and Riedel, 1973, p. 528; Riedel and Sanfilippo, 1973, p. 738, pl. 1, fig. 8; Dinkelman, 1973, p. 770, pl. 4, figs. 6, 7; Nigrini, 1974, p. 1066, pl. 2B, fig. 4; Johnson, 1974, p. 546, pl. 6, fig. 16; 1976, p. 435; 1978, p. 781; Holdsworth, 1975, p. 529; Sanfilippo and Nigrini, 1995, p. 276, pl. 2, figs. 7, 9, 10.

Dorcadospyris sp(p).: Riedel and Sanfilippo, 1973, p. 710, pl. 1, figs. 9, 10.

Questionable form of *Dorcadospyris circulus* (Haeckel): Sanfilippo and Nigrini, 1995, pl. 2, figs. 8, 11.

Remarks: Sanfilippo and Nigrini (1995) excluded a form without an apical horn from *D. circulus*. In Hole 1220A this form with or without a tiny apical horn occurred from the upper part of the examined section, where the typical form of this species with a stout apical horn also occurred. In this study, we included these two forms because the variation of the apical horn from long and robust, like the typical form, to short and narrow makes difficult to subdivide them completely.

***Dorcadospyris pseudopapilio* Moore**
(Pl. P1, figs. 8, 9)

Dorcadospyris pseudopapilio Moore, 1971, p. 738, pl. 6, figs. 7, 8; Sanfilippo and Riedel, 1973, p. 528; Riedel and Sanfilippo, 1973, p. 738; Dinkelman, 1973, p. 769, pl. 4, figs. 2, 3; Sanfilippo et al., 1985, p. 664, figs. 10.1a, 10.1b; Sanfilippo and Nigrini, 1995, p. 278; Nigrini and Sanfilippo, 2000, p. 73.

P1. *Dendrospyris, Dorcadospyris, Nephrospyris,* p. 58.

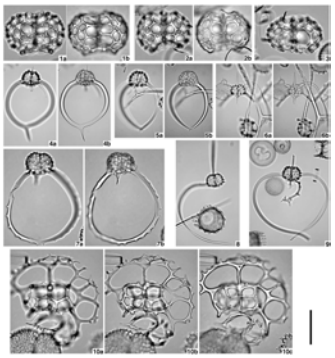

Remarks: In some specimens, secondary feet and meshwork are not preserved (Pl. P1, fig. 8).

***Dorcadospyris quadripes* Moore**
(Pl. P1, figs. 6a, 6b)

Dorcadospyris quadripes Moore, 1971, p. 738, pl. 7, figs. 3–5; Dinkelman, 1973, p. 769, pl. 4, figs. 4, 5; Johnson, 1976, p. 435; 1978, p. 781.

***Dorcadospyris spinosa* Moore**
(Pl. P1, figs. 7a, 7b)

Dorcadospyris spinosa Moore, 1971, p. 739, pl. 7, figs. 1, 2; Sanfilippo and Riedel, 1973, p. 528; 1974, p. 1022; Riedel and Sanfilippo, 1973, p. 738, pl. 2, fig. 2; Dinkelman, 1973, p. 769, pl. 4, figs. 8, 9; Nigrini, 1974, p. 1066, pl. 2B, fig. 4; Johnson, 1974, p. 546, pl. 6, fig. 18; 1976, p. 435; 1978, p. 781.

Dorcadospyris spinosa Moore group: Holdsworth, 1975, p. 529.

Remarks: Usually nonjoined primary feet are present, but in some specimens, they are broken off (Pl. P1, figs. 7a, 7b).

***Nephrospyris* sp. A**
(Pl. P1, figs. 10a–10c)

Remarks: Shell composed of outer lenticular to flat discoidal lattice and central lattice including sagittal ring. Lattice pores in central part are large and polygonal. Outer lattice is three to four times as broad as the central one that has variably sized rounded pores.

This species is distinguished from other acanthodesmiids by the outer lattice shell extending from central lattice.

Family Artostrobiidae Riedel, 1967

***Dictyoprora amphora* (Haeckel) group**
(Pl. P2, figs. 1a–2b)

Dictyocephalus amphora Haeckel, 1887, p. 1305, pl. 62, fig. 4.

Dictyocephalus lipogaster Clark and Campbell, 1945, p. 42, pl. 6, fig. 9.

Lithomitra sp. aff. *L. lineata* (Ehrenberg) group: Riedel and Sanfilippo, 1971, pl. 3E, fig. 18.

Theocampe aff. *mongolfieri* (Ehrenberg): Petrushevskaya and Kozlova, 1972, pl. 23, figs. 1, 2.

Theocampe sp.: Petrushevskaya and Kozlova, 1972, pl. 23, fig. 12.

Theocampe amphora (Haeckel) group: Foreman, 1973, p. 431, pl. 8, figs. 7, 9–13; Riedel and Sanfilippo, 1973, p. 740; Nigrini, 1974, p. 1070, pl. 1M, figs. 1–5; pl. 2E, fig. 7; Johnson, 1974, p. 552, pl. 2, fig. 4; pl. 4, fig. 2; 1976, p. 436; 1978, p. 782; Sanfilippo and Riedel, 1974, p. 1025.

Theocampe armadillo (Ehrenberg): Ling, 1975, p. 732, pl. 13, fig. 15.

Theocampe mongolfieri (Haeckel): Ling, 1975, p. 732, pl. 13, figs. 16, 17.

Dictyoprora amphora (Haeckel) group: Nigrini, 1977, p. 250, pl. 4, figs. 1, 2; Sanfilippo et al., 1985, fig. 33.3; Nishimura, 1987, p. 725, pl. 2, fig. 3; Riedel and Sanfilippo, 1986, pl. 3, fig. 8; Nigrini and Sanfilippo, 2000, p. 72.

P2. *Dictyoprora, Phormostichoartus, Siphocampe, Theocamptra, Centrobotrys,* p. 59.

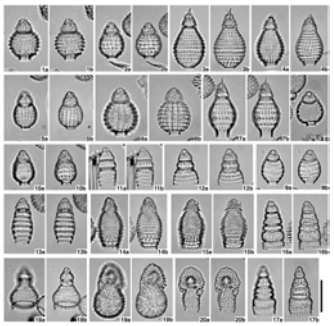

Dictyoprora amphora (Haeckel): Caulet, 1991, p. 538.

Dictyoprora mongolfieri (Haeckel): Shilov, 1995, p. 126, pl. 2, fig. 6.

***Dictyoprora armadillo* (Ehrenberg)**
(Pl. **P2,** figs. 3a–4b)

Eucyrtidium armadillo Ehrenberg, 1873, p. 225; 1875, pl. 9, fig. 10.

Theocampe armadillo (Ehrenberg) group: Riedel and Sanfilippo, 1971, p. 1601, pl. 3E, figs. 3, 5 (partim); 1973, p. 740; Johnson, 1974, p. 552; 1976, p. 436; 1978, p. 782; Holdsworth, 1975, p. 532.

Dictyoprora armadillo (Ehrenberg): Nigrini, 1977, p. 250, pl. 4, fig. 4; Renz, 1984, p. 458; Sanfilippo et al., 1985, fig. 33.5; Nigrini and Sanfilippo, 2000, p. 72.

Dictyoprora armadillo (Ehrenberg) group: Renz, 1984, p. 458.

***Dictyoprora mongolfieri* (Ehrenberg)**
(Pl. **P2,** figs. 5a–6b)

Eucyrtidium mongolfieri Ehrenberg, 1854, pl. 36, fig. 18, B lower; 1873, p. 230; 1875, p. 72, pl. 10, fig. 3.

Sethamphora costata Haeckel, 1887, p. 1251, pl. 62, fig. 3.

Sethamphora mongolfieri (Ehrenberg): Haeckel, 1887, p. 1251; Riedel, 1957b, p. 81, pl. 1, fig. 7.
Theocampe costata Haeckel, 1887, p. 1426, pl. 66, fig. 24.

Theocampe mongolfieri (Ehrenberg): Burma, 1959, p. 329; Riedel and Sanfilippo, 1970, p. 536, pl. 12, fig. 9; 1971, pl. 3E, fig. 13; 1973, p. 740; 1978, p. 76, p. 9, fig. 13; Moore, 1971, p. 744, pl. 2, fig. 3; Petrushevskaya and Kozlova, 1972, p. 538, pl. 23, figs. 3–5; Foreman, 1973, p. 432, pl. 8, fig. 6; pl. 9, fig. 17; Dinkelman, 1973, p. 789; Nigrini, 1974, p. 1070, pl. 1M, figs. 7–10; pl. 2E, fig. 9; Johnson, 1974, p. 552, pl. 2, figs. 3, 5; pl. 5, fig. 1; 1976, p. 436; 1978, p. 782; Sanfilippo and Riedel, 1974, p. 1023; Holdsworth, 1975, p. 532.

Dictyoprora mongolfieri (Ehrenberg): Nigrini, 1977, p. 250, pl. 4, fig. 7; Weaver, 1983, p. 675; Renz, 1984, p. 458; Sanfilippo and Riedel in Saunders et al., 1985, p. 412; Sanfilippo et al., 1985, p. 702, figs. 33.1a–33.1d; Riedel and Sanfilippo, 1986, pl. 3, fig. 9; Takemura, 1992, p. 743, pl. 7, fig. 12; Takemura and Ling, 1997, p. 111; Nigrini and Sanfilippo, 2000, p. 72, pl. 1, fig. 10; pl. 2, fig. 9.

?*Eucyrtidium gemmatum* Ehrenberg, 1873, p. 229, 1875, pl. 10, fig. 6.

***Dictyoprora ovata* (Haeckel)**
(Pl. **P2,** figs. 7a, 7b)

Theocampe ovata Haeckel, 1887, p. 1416, pl. 69, fig. 16.

Theocampe armadillo (Ehrenberg) group: Riedel and Sanfilippo, 1971, p. 1601, pl. 3E, figs. 4, 6 (partim); Nigrini, 1974, p. 1070, pl. 1M, fig. 6; pl. 2E, fig. 7.

Theocampe sp. aff. *T. gemmata* (Ehrenberg): Petrushevskaya and Kozlova, 1972, p. 538, pl. 23, fig. 10.

Theocampe exvellens (Ehrenberg): Petrushevskaya and Kozlova, 1972, p. 538, pl. 23, fig. 7.

Dictyoprora ovata (Haeckel): Nigrini, 1977, p. 251, pl. 4, figs. 5, 6.

?*Theocampe calimorphos* (Clark and Campbell): Petrushevskaya and Kozlova, 1972, p. 538, pl. 23, fig. 8.

***Dictyoprora pirum* (Ehrenberg)**
(Pl. P2, figs. 8–9b)

Eucyrtidium pirum Ehrenberg, 1873, p. 232; 1875, pl. 10, fig. 14.

Theocampe pirum (Ehrenberg): Haeckel, 1887, p. 1423; Riedel and Sanfilippo, 1971, p. 1601, pl. 3E, figs. 10, 11; 1973, p. 740; Nigrini, 1974, p. 1070, pl. 2E, fig. 10; Johnson, 1974, p. 552. pl. 6, fig. 14; 1976, p. 436; 1978, p. 782; Sanfilippo and Riedel, 1974, p. 1023; Holdsworth, 1975, p. 532; Ling, 1975, p. 732, pl. 13, fig. 18.

Dictyoprora pirum (Ehrenberg): Nigrini, 1977, p. 251, pl. 4, fig. 8; Sanfilippo and Riedel in Saunders et al., 1985, p. 412; Sanfilippo et al., 1985, p. 703, figs. 33.2a, 33.2b; Takemura, 1992, p. 743, pl. 5, fig. 11; Takemura and Ling, 1997, p. 111; Nigrini and Sanfilippo, 2000, p. 72.

***Dictyoprora* sp. A**
(Pl. P2, figs. 10a, 10b)

Remarks: This species has shorter abdomen with maximum breadth at the distal part rather than at the median and is distinguished from *Dictyoprora urceolus* (Haeckel) by these characteristics.

***Phormostichoartus marylandicus* (Martin)**
(Pl. P2, figs. 11a–12b)

Lithocampe marylandica Martin, 1904, p. 450, pl. 130, fig. 4.

Artostrobium sp. aff. *A. doliolum* Riedel and Sanfilippo, 1971, pl. 1H, fig. 4; pl. 2I, figs. 1–8; pl. 3E, figs. 7–9.

Theocamptra marylandica (Martin) Petrushevskaya and Kozlova, 1972, p. 538, pl. 23, figs. 20, 21.

Theocamptra sp. aff. *T. marylandica* (Martin) Petrushevskaya and Kozlova, 1972, p. 538, pl. 23, figs. 22, 23.

Theocamptra ovata (Haeckel) Petrushevskaya and Kozlova, 1972, p. 538, pl. 23, figs. 17, 18.

Theocamptra sp. aff. *T. ovata* (Haeckel) Petrushevskaya and Kozlova, 1972, p. 538, pl. 23, figs. 15, 16; pl. 24, fig. 6.

Phormostichoartus marylandicus (Martin) Nigrini, 1977, p. 253, pl. 2, figs. 1–3; Nigrini, 1985, p. 522; Caulet, 1991, p. 539.

?*Lithocampe ovata* Haeckel, 1887, p. 1504, pl. 77, fig. 1.

?*Theocampe collaris* Haeckel, 1887, p. 1425, pl. 66, fig. 18.

***Siphocampe* sp. aff. *S. acephala* (Ehrenberg)**
(Pl. P2, figs. 13a, 13b)

aff. *Eucyrtidium acephalum* Ehrenberg, 1873, p. 224; 1875, pl. 11, fig. 5.

aff. *Eucyrtidium ?obstipum* Ehrenberg, 1873, p. 231; 1875, pl. 11, fig. 17.

aff. *Lithomitra acephala* Bütschli, 1882, p. 529; Haeckel, 1887, p. 1484.

aff. *Siphocampe acephala* (Ehrenberg,) Nigrini, 1977, p. 254, pl. 3, fig. 5; Takemura, 1992, p. 743, pl. 6, fig. 9; Takemura and Ling, 1997, p. 114.

Remarks: This species is distinguished from *Siphocampe acephala* by a symmetrically positioned cephalis.

***Siphocampe quadrata* (Petrushevskaya and Kozlova)**
(Pl. P2, figs. 14a–15b)

Lithamphora sacculifera quadrata Petrushevskaya and Kozlova, 1972, p. 539, pl. 30, figs. 4–6.

Lithamphora(?) sp. Petrushevskaya and Kozlova, 1972, p. 539, pl. 30, fig. 2

Lithomitra docilis Foreman, 1973, p. 431, pl. 8, figs. 20–22; pl. 9, figs. 3–5; Johnson, 1974, p. 552, pl. 3, fig. 16.

Siphocampe (?)*quadrata* (Petrushevskaya and Kozlova): Nigrini, 1977, p. 257, pl. 3, fig. 12; Caulet, 1991, p. 539; Takemura, 1992, p. 743, pl. 7, fig. 7; Takemura and Ling, 1997, p. 114.

Lithamphora sp. aff. *L. quadrata* Petrushevskaya: Dzinoridze et al., 1978, pl. 29, fig. 1; pl. 33, fig. 1.

?*Lithomitra sacculifera* Clark and Campbell, 1945, p. 50, pl. 7, fig. 18.

?*Artostrobium miralestense* (Campbell and Clark): Riedel and Sanfilippo, 1971, p. 1599, pl. 3E, fig. 12 (partim).

?*Theocampe amphora* (Haeckel) group: Chen, 1975, p. 456, pl. 2, fig. 3 (partim).

***Siphocampe* sp. A**
(Pl. P2, figs. 16a–17b)

Remarks: Shell is composed of three segments. Cephalis is sub- or hemispherical with few subcircular pores. Ventral tube, if observed, is directed upward. Collar stricture is indistinct externally. Thorax is truncate conical to inflated cylindrical, with two or three transverse rows of subcircular pores. Lumbar stricture is indistinct. Abdomen usually bears 3–5 rounded constrictions without internal rings. Pores in abdomen are transversely aligned or randomly distributed. Indistinct sculpture of longitudinal ridge is present in upper abdomen. Distal end of shell is fully opened and ragged.

This species is distinguished from all other artostrobiids in this study by 3–5 rounded constrictions in abdomen.

***Theocamptra formaster* Petrushevskaya and Kozlova**
(Pl. P2, figs. 18a, 18b)

Phormostichoartus sp. aff. *P. corona* Haeckel: Riedel and Sanfilippo, 1971, pl. 3F, figs. 4, 5 (partim).

Theocamptra formaster Petrushevskaya in Petrushevskaya and Kozlova, 1972, p. 539, pl. 23, figs. 26, 27.

Family Cannobotryidae Haeckel, 1881

***Centrobotrys gravida* Moore**
(Pl. P2, figs. 19a, 19b)

Centrobotrys gravida Moore, 1971, p. 744, pl. 5, fig. 8; Sanfilippo and Riedel, 1973, p. 532; Riedel and Sanfilippo, 1973, p. 738; 1978, p. 67, pl. 4, fig. 8; 1986, pl. 1, fig. 14; Dinkelman, 1973, p. 789, pl. 5, fig. 6; Holdsworth, 1975, p. 533; Sanfilippo et al., 1985, p. 704, figs. 35.1a, 35.1b; Nigrini and Sanfilippo, 2000, p. 72.

***Centrobotrys petrushevskayae* Sanfilippo and Riedel**
(Pl. P2, figs. 20a, 20b)

Centrobotrys(?) sp. A: Riedel and Sanfilippo, 1971, p. 1602, pl. 3F, figs. 15, 16.

Centrobotrys sp.: Petrushevskaya and Kozlova, 1972, pl. 39, fig. 11.

Centrobotrys petrushevskayae Sanfilippo and Riedel, 1973, p. 532, pl. 36, figs. 12, 13; 1974, p. 1021; Riedel and Sanfilippo, 1973, p. 738; 1986, pl. 1, fig. 15; Johnson, 1974, p. 552; 1976, p. 435; 1978, p. 781; Holdsworth, 1975, p. 533, pl. 2, figs. 23–25; Sanfilippo et al., 1985, p. 704, figs. 35.2a, 35.2b; Sanfilippo and Nigrini, 1995, p. 275, pl. 1, figs. 18–20; Nigrini and Sanfilippo, 2000, p. 72.

Family Lophophaenidae Haeckel, 1881, emend. Petrushevskaya, 1971

***Lophophaena apiculata* Ehrenberg**
(Pl. P3, figs. 1a–2b)

Lophophaena apiculata Ehrenberg, 1873, p. 242; 1875, pl. 8, fig. 11.

***Lophophaena capito* Ehrenberg group**
(Pl. P3, figs. 3a–4b)

Lophophaena capito Ehrenberg, 1873, p. 242; 1875, pl. 8, fig. 6.

Lophophaena ?capito Ehrenberg group: Petrushevskaya and Kozlova, 1972, p. 535, pl. 33, figs. 20–23; Johnson, 1974, p. 552; 1976, p. 436; Petrushevskaya, 1975, pl. 9, fig. 21.

Lamptonium sanfilippoae Foreman: Ling, 1975, p. 729, pl. 9, figs. 23–25.

***Lophophaena radians* Ehrenberg**
(Pl. P3, figs. 5a–6b)

Lophophaena radians Ehrenberg, 1873, p. 243; 1875, pl. 8, figs. 7–9.

Lophophaenoma radians (Ehrenberg): Haeckel, 1887, p. 1304; Caulet, 1991, p. 538.

***Pseudodictyophimus* sp. C**
(Pl. P3, figs. 7a–9b)

Remarks: Shell is composed of cephalis and thorax. Cephalis is semispherical with almost hyaline wall perforated by several small subcircular pores. Apical horn extends from internal apical spine, three-bladed and robust, two to three times as long as cephalic height. Collar stricture is distinct. Upper thorax is truncated conical with three ridges extending to three feet, which are three-bladed, more than two times as long as thoracic height, and curved convexly

P3. *Lophophaena, Pseudodictyophimus,* Sethoperid, p. 60.

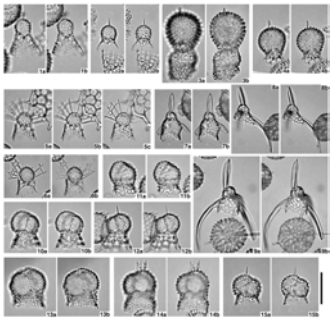

outward. Lower thorax is conical. Subcircular pores are randomly distributed in thoracic wall. Distal part of thorax is fully opened.

This species is distinguished from other *Pseudodictyophimus* by long feet. A long and robust apical horn is also a distinguishing characteristic from other lophophaenids.

Family Sethoperidae Haeckel, 1881, emend. Petrushevskaya, 1971

Sethoperid sp. A
(Pl. P3, figs. 10a–12b)

Remarks: Shell is composed of cephalis and thorax. Cephalis is subspherical, with constrictions along internal connecting arches, with or without tiny thorns. Apical horn is not observed. Collar stricture is distinct. Thorax is truncated conical with subcircular pores. Distal end of thorax is fully opened without feet.

This species is distinguished from other sethoperids by its footless thorax.

Sethoperid sp. B
(Pl. P3, figs. 13a–15b)

Remarks: Mostly similar to Sethoperid sp. A and distinguished from it by relatively larger cephalis and by smaller subcircular pores in thorax. According to morphologic similarity and their stratigraphic distributions, this species is descendant of Sethoperid sp. A.

Family Eucyrtidiidae Ehrenberg, 1847

***Artophormis barbadensis* (Ehrenberg)**
(Pl. P4, figs. 1a, 1b)

P4. *Artophormis, Thyrsocyrtis,* p. 61.

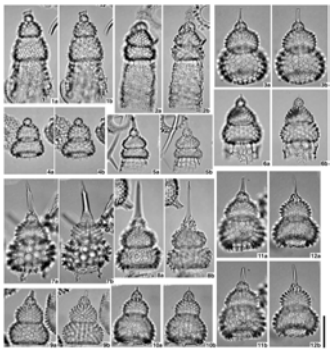

Calocyclas barbadensis Ehrenberg, 1873, p. 217; 1875, pl. 18, fig. 8.

Artophormis barbadensis (Ehrenberg): Riedel and Sanfilippo, 1970, p. 532, pl. 13, fig. 5; 1971, p. 1592, pl. 3B, figs. 8, 9; 1973, p. 737; Moore, 1971, p. 742, pl. 5, fig. 9; Johnson, 1974, p. 547, pl. 5, fig. 6; 1978, p. 780; Holdsworth, 1975, p. 529; Ling, 1975, p. 728, pl. 9, figs. 9, 10; Sanfilippo and Riedel in Saunders et al., 1985, p. 411; Sanfilippo et al., 1985, p. 666, figs. 12.1a, 12.1b.

***Artophormis dominasinensis* (Ehrenberg)**
(Pl. P6, figs. 5a–6b)

Podocyrtis dominasinensis Ehrenberg, 1873, p. 250; 1875, pl. 14, fig. 14.

Podocyrtis brevipes Ehrenberg, 1873, p. 249; 1875, pl. 16, fig. 6.

Artophormis dominasinensis (Ehrenberg): Riedel and Sanfilippo, 1970, p. 532.

***Artophormis gracilis* Riedel group**
(Pl. P4, figs. 2a–6b)

Artophormis gracilis Riedel, 1959, p. 300, pl. 2, figs. 12, 13; Riedel and Sanfilippo, 1970, p. 532, pl. 13, figs. 6, 7; 1971, p. 1592, pl. 3B, figs. 5–7; pl. 6, fig. 7; 1973, p. 737; 1986, pl. 3, figs. 15, 16; Kling, 1971, p. 1088, pl. 5, fig. 7; Moore, 1971, p. 742, pl. 5, figs. 10, 11; Goll, 1972, p. 958; Dinkelman, 1973, p. 774; Nigrini, 1974, p. 1066, pl. 2C, figs. 1–5; 1985, p. 522; Johnson, 1974, p. 547, pl. 6, fig. 1; 1976, p. 435; 1978, p. 780; Sanfilippo and Riedel, 1974, p. 1000; Holdsworth, 1975, p. 529; Ling, 1975, p. 728, pl. 9, fig. 11; Weaver, 1983, p. 675; Renz, 1984, p. 455; Sanfilippo and Riedel in Saunders et al., 1985, p. 411; Sanfilippo et al., 1985, p. 666, figs. 12.2a–12.2c; Abelmann, 1990, p. 697, pl. 7, fig. 5;

1992, p. 776; Sanfilippo and Nigrini, 1995, p. 272, pl. 1, figs. 1–5; Nigrini and Sanfilippo, 2000, p. 72.

?*Cyrtophormis gracilis* (Riedel): Petrushevskaya and Kozlova, 1972, p. 547, pl. 28, figs. 13–15.

Calocyclas bandyca **(Mato and Theyer)**
(Pl. **P5,** figs. 1a–3)

Lychnocanoma bandyca Mato and Theyer, 1980, p. 225, pl. 1, figs. 1–6; Sanfilippo et al., 1985, p. 676, figs. 19.3a, 19.3b.

Calocyclas bandyca (Mato and Theyer): Renz, 1984, p. 455; Sanfilippo and Riedel in Saunders et al., 1985, p. 411, pl. 5, figs. 1, 5, 6; Riedel and Sanfilippo, 1986, pl. 2, fig. 12; Nigrini and Sanfilippo, 2000, p. 72.

Calocyclas hispida **(Ehrenberg)**
(Pl. **P5,** figs. 4a, 4b)

Anthocyrtis hispida Ehrenberg, 1873, p. 216; 1875, pl. 8, fig. 2.

Cycladophora hispida (Ehrenberg): Riedel and Sanfilippo, 1970, p. 529, pl. 10, fig. 9; 1971, p. 1593, pl. 3B, figs. 10, 11; 1978, p. 65, pl. 3, fig. 6; Moore, 1971, p. 741, pl. 4, figs. 6, 7; Dinkelman, 1973, p. 774.

Calocyclas hispida (Ehrenberg): Foreman, 1973, p. 434, pl. 1, figs. 12–15; pl. 9, fig. 18; Riedel and Sanfilippo, 1973, p. 737; Nigrini, 1974, p. 1067, pl. 1F, figs. 5–8; Johnson, 1974, p. 547, pl. 4, fig. 1; 1976, p. 435; 1978, p. 780; Sanfilippo and Riedel, 1974, p. 1020; Chen, 1975, p. 459, pl. 3, fig. 10; Holdsworth, 1975, p. 529; Ling, 1975, p. 728, pl. 9, fig. 12; Renz, 1984, p. 455; Sanfilippo and Riedel in Saunders et al., 1985, p. 412; Sanfilippo et al., 1985, figs. 15.2a, 15.2b; Riedel and Sanfilippo, 1986, pl. 2, fig. 10; Hull, 1993, p. 12, pl. 7, fig. 1; Nigrini and Sanfilippo, 2000, p. 72.

Calocyclas turris **Ehrenberg**
(Pl. **P5,** figs. 5a, 5b)

Calocyclas turris Ehrenberg, 1873, p. 218; 1875, pl. 18, fig. 7; Riedel, 1957b, p. 89, pl. 3, fig. 8; pl. 4, figs. 1, 2; Riedel and Sanfilippo, 1973, p. 738; 1978, p. 65, pl. 3, figs. 7, 8; 1986, pl. 2, fig. 11; pl. 5, fig. 3; Foreman, 1973, p. 434; Nigrini, 1974, p. 1067, pl. 2C, fig. 6; Johnson, 1974, p. 547, pl. 5, fig. 2; 1976, p. 435; 1978, p. 780; Sanfilippo and Riedel, 1974, p. 1020; Holdsworth, 1975, p. 529; Ling, 1975, p. 728, pl. 9, fig. 13; Renz, 1984, p. 455; Sanfilippo and Riedel in Saunders et al., 1985, p. 412, pl. 5, fig. 12; Sanfilippo et al., 1985, p. 669, figs. 15.1a–15.1c; Nigrini and Sanfilippo, 2000, p. 72.

Cycladophora stiligera Ehrenberg, 1873, p. 223; 1875, pl. 18, fig. 3.

Cycladophora turris (Ehrenberg): Riedel and Sanfilippo, 1970, p. 529, pl. 13, figs. 3, 4; 1971, p. 1593; Moore, 1971, p. 741, pl. 4, fig. 8; Dinkelman, 1973, p. 774,

Eucyrtidium ?hillaby **Ehrenberg group**
(Pl. **P5,** figs. 6a–8b)

Eucyrtidium hillaby Ehrenberg, 1873, p. 229; 1875, pl. 11, fig. 8.

Pterocyrtidium barbadense Ehrenberg group: Petrushevskaya and Kozlova, 1972, p. 552, pl. 27, figs. 18, 19.

P5. *Calocyclas, Eucyrtidium,* p. 62.

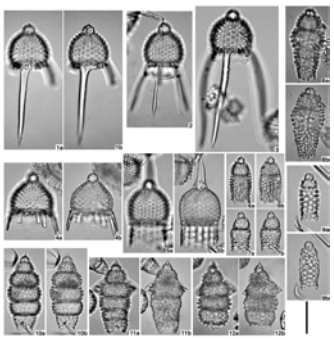

Eucyrtidiidae gen. sp. aff. *Pterocyrtidium barbadense* Ehrenberg: Petrushevskaya and Kozlova, 1972, pl. 22, fig. 10.

Theoperid gen. et sp. indet.: Johnson, 1974, pl. 2, figs. 14, 15; pl. 6, fig. 11.

?Theoperid gen. et sp. indet: Johnson, 1974, pl. 5, fig. 17.

Pterocyrtidium sp.: Ling, 1975, p. 729, pl. 10, fig. 19 (partim).

Remarks: This group includes two morphotypes, one has a relatively large shell with three lateral wings (Pl. **P5,** figs. 8a, b) and the other has no lateral appendages (Pl. **P5,** figs. 6a–7b). The development of three wings varies between these two types. In the late form, the abdomen has a shallow stricture without internal ring. This group is distinguished from *Lophocyrtis barbadense* by its long cylindrical to wavy abdomen.

Eucyrtidium montiparum **Ehrenberg**
(Pl. **P5,** figs. 10a, 10b)

Eucyrtidium montiparum Ehrenberg, 1873, p. 230; 1875, pl. 9, fig. 11.

Lithocampe subligata Stöhr group: Petrushevskaya and Kozlova, 1972, p. 546, pl. 25, figs. 7–10.

Theoperid gen. et sp. indet.: Johnson, 1974, pl. 6, figs. 12, 13.

Remarks: This species has a similar skeletal character to the Miocene *Stichocorys delmontensis*, which is evolved from *Stichocorys wolfii* near the Oligocene/Miocene boundary. The range of this species is significantly different from that of *S. delmontensis*.

Eucyrtidium ?panthera **Ehrenberg**
(Pl. **P5,** figs. 9a, 9b)

Eucyrtidium panthera Ehrenberg, 1873, p. 231; 1875, pl. 11, fig. 18.

?*Eucyrtidium* sp. cf. *E. panthera* Ehrenberg: Ling, 1975, pl. 12, fig. 18.

Remarks: This species is distinguished from *E. ?hillaby* by the hyaline shell wall of abdomen and larger size of abdominal pores.

Eucyrtidium **sp. F**
(Pl. **P6,** figs. 1a–3b)

Cyrtophormis sp. Ch: Petrushevskaya and Kozlova, 1972, p. 547, pl. 26, fig. 1; Dzinoridze et al., 1978, pl. 28, fig. 3.

Theoperid. gen. et sp. indet.: Johnson, 1974, pl. 4, figs. 13, 14.

Eucyrtidium sp. A: Ling, 1975, p. 731, pl. 12, fig. 20.

Cyrtophormis (?) *alta* (Moksjakova): Kozlova, 1999, p. 155, pl. 30, figs. 7, 9; pl. 46, fig. 4.

?*Eucyrtidium* sp. aff. *E. montiparum* Ehrenberg: Petrushevskaya and Kozlova, 1972, p. 548, pl. 26, figs. 2–4.

Remarks: Multisegmented shell is composed of cephalis, thorax, abdomen, and one or two post-abdominal segments. Cephalis is subspherical, perforated by circular pores. Apical horn is three-bladed, almost the same length as cephalic height. Collar stricture is indistinct externally. Thorax is truncated conical to

P6. *Eucyrtidium, Artophormis, Theocorys, Dictyopodium,* p. 63.

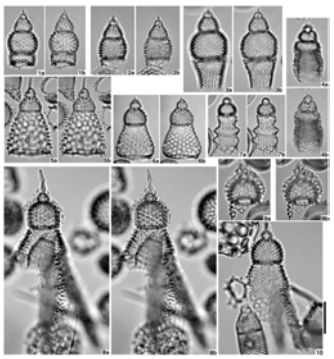

campanulate. Pores in thorax are circular to subcircular, roughly arranged hexagonally. Lumbar stricture is distinct. Abdomen is inflated cylindrical to truncate conical. Breadth of shell reaches maximum at abdomen. Pores in abdomen are circular to subcircular, larger than those in thorax, and arranged hexagonally. Post-abdominal segments are cylindrical. Later form has single post-abdominal segment, its breadth decreases downward. Height is variable.

This species is distinguished from *E. montiparum* by larger abdomen, which is the widest segment in the shell.

***Eucyrtidium* sp. F1**
(Pl. P5, figs. 11a–12b)

Remarks: Multisegmented thick shell is composed of cephalis, thorax, abdomen, and three or more post-abdominal segments. Cephalis is subspherical, perforated by small circular pores, with three-bladed short apical horn, length of which is less than the height of cephalis. Collar stricture is distinct. Thorax is campanulate. Pores in thorax are weakly arranged hexagonally. Lumbar stricture is distinct. Abdomen is inflated cylindrical. Pores in abdomen are roughly arranged hexagonally and larger than those in thorax. Three trigonal wings, attached to lower thorax to abdomen, are one-fifth to one-fourth as long as abdominal breadth. Post-abdominal segments are cylindrical to subcylindrical. Breadth of shell reaches maximum at first post-abdominal segment and then decreases downward. Pores are somewhat larger than those in abdomen, usually of uniform size, and weakly arranged hexagonally or randomly distributed.

This species is distinguished from *E. montiparum* by the presence of three well-developed wings.

***Eucyrtidium* (?) sp. J**
(Pl. P6, figs. 4a, 4b)

Remarks: Shell is composed of three segments. Cephalis is subspherical and perforated by very small pores, with a tiny apical horn, which is shorter than height of cephalis. Collar stricture is distinct. Thorax is campanulate to cup-shaped. Pores are roughly arranged hexagonally. Lumbar stricture is shallow. Abdomen is subcylindrical externally. Upper abdomen has tubercular surface. Pores are subcircular, smaller than those in thorax, and randomly distributed. Lower abdomen is covered with spongy meshwork and distinguished from upper part by decreasing breadth.

This species is distinguished from *E. ?hillaby* by the spongy layers of abdomen. This species is distinguished from the Antarctic Eocene *Eucyrtidium nishimurae* by the relatively smaller shell without post-abdominal segments and spongy abdomen.

***Theocorys bianulus* O'Connor**
(Pl. P6, figs. 7a, 7b)

Eucyrtidium sp. cf. *E. "rocket"*: Ling, 1975, p. 731, pl. 12, fig. 19.

Theocorys bianulus O'Connor, 1997, p. 84, pl. 4, figs. 1–4; pl. 10, figs. 1–4; pl. 11, fig. 5.

?Eucyrtidiidae gen. sp. "rocket": Petrushevskaya and Kozlova, 1972, p. 547, pl. 28, figs. 2, 3.

***Theocorys spongoconus* Kling**
(Pl. P8, figs. 11a, 11b)

Theocorys spongoconus Kling, 1971, p. 1087, pl. 5, fig. 6; Weaver, 1983, p. 678; Nigrini and Sanfilippo, 2000, p. 74.

Theocorys (?) *spongoconum* Kling: Foreman, 1973, p. 440.

Theocorys spongoconum Kling: Riedel and Sanfilippo, 1971, p. 1596, pl. 2F, fig. 4; pl. 3C, fig. 3; 1973, p. 740, pl. 2, fig. 1; 1978, p. 76, pl. 9, fig. 16; Nigrini, 1974, p. 1068, pl. 2D, fig. 5; Johnson, 1974, p. 549, pl. 6, fig. 2; 1976, p. 436; 1978, p. 782; Sanfilippo and Riedel, 1974, p. 1023; Holdsworth, 1975, p. 531; Ling, 1975, p. 730, pl. 11, fig. 13; Renz, 1984, p. 460.

Family Lophocyrtiidae Sanfilippo and Caulet, 2001

***Dictyopodium eurylophus* Ehrenberg**
(Pl. P6, figs. 8a–10)

Dictyopodium eurylophus Ehrenberg, 1873, p. 223; 1875, pl. 19, fig. 4.

***Dictyopodium oxylophus* Ehrenberg**
(Pl. P7, figs. 1a–3b)

Dictyopodium oxylophus Ehrenberg, 1873, p. 223; 1875, pl. 19, fig. 5.

Dictyopodium sp. aff. *D. oxylophus* Ehrenberg: Chen, 1975, p. 460, pl. 4, figs. 1, 2.

***Lophocyrtis* (*Apoplanius*) *aspera* (Ehrenberg)**
(Pl. P7, figs. 4a–7b)

Eucyrtidium asperum Ehrenberg, 1873, p. 226; 1875, pl. 8, fig. 15.

Calocyclas asperum (Ehrenberg): Petrushevskaya and Kozlova, 1972, p. 548, pl. 28, figs. 16–18; Johnson, 1978, p. 780; Dzinoridze et al., 1978, pl. 28, fig. 15; Caulet, 1991, p. 537; Shilov, 1995, p. 126; Kozlova, 1999, p. 153, pl. 46, fig. 10 (partim).

Calocyclas sp. B; Takemura, 1992, p. 745, pl. 5, fig. 13; Takemura and Ling, 1997, p. 111, pl. 1, fig. 14.

Lophocyrtis (*Apoplanius*) *aspera* (Ehrenberg): Sanfilippo and Caulet, 1998, p. 14, pl. 3A, figs. 5–10; pl. 3B, figs. 1, 2, 5–9; pl. 6, figs. 6–8.

Theocorys minuta Takemura and Ling, 1998, p. 162, figs. 3.16–3.21, 5.5, 5.6.

Calocyclas sp. cf. *C. asperum* (Ehrenberg): Kozlova, 1999, pl. 28, fig. 14.

***Lophocyrtis* (*Apoplanius*) *nomas* Sanfilippo and Caulet**
(Pl. P7, figs. 8a–9b)

Lophocyrtis (*Apoplanius*) *nomas* Sanfilippo and Caulet, 1998, p. 15, pl. 3A, figs. 1–4; pl. 3B, figs. 3, 4; pl. 6, figs. 1a–5b.

Calocyclas sp. A: Takemura, 1992, p. 745, pl. 1, figs. 3, 4; Takemura and Ling, 1997, p. 111, pl. 1, fig. 15.

Theocorys saginata Takemura and Ling, 1998, p. 164, figs. 4.7–4.14, 5.9, 5.10.

?*Calocyclas asperum* (Ehrenberg): Kozlova, 1999, p. 153, pl. 35, fig. 6 (partim).

Remarks: This species and the ancestral *L. aspera* are counted together in numeric data because of the common occurrence of broken specimens without cephalis throughout sequence.

P7. *Dictyopodium, Lophocyrtis,* p. 64.

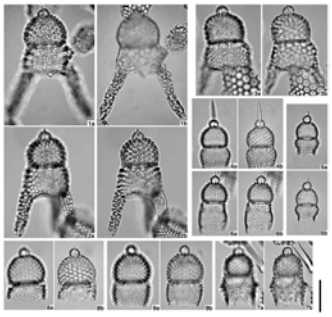

***Lophocyrtis* (*Cyclampterium*) *hadra* Riedel and Sanfilippo**
(Pl. P8, figs. 1a–2b)

Lophocyrtis hadra Riedel and Sanfilippo, 1986, p. 168, pl. 7, figs. 12–15.

Lophocyrtis (*Cyclampterium*) *hadra* Riedel and Sanfilippo: Sanfilippo, 1990, p. 304, pl. 1, figs. 11, 12.

***Lophocyrtis* (*Cyclampterium*) *milowi* (Riedel and Sanfilippo)**
(Pl. P8, fig. 3)

Cyclampterium (?) *milowi* Riedel and Sanfilippo, 1971, p. 1593, pl. 7, figs. 8, 9; 1973, p. 738; Dinkelman, 1973, p.776, pl. 2, fig. 1; Chen, 1975, p. 460, pl. 2, figs. 4, 5; Holdsworth, 1975, p. 529; Ling, 1975, p. 731, pl. 12, fig. 15; Johnson, 1976, p. 435; 1978, p. 781; Nigrini, 1985, p. 523.

Cyclampterium milowi Riedel and Sanfilippo: Renz, 1984, p. 457; Riedel and Sanfilippo, 1986, pl. 1, fig. 3.

Lophocyrtis (*Cyclampterium*) *milowi* (Riedel and Sanfilippo): Riedel and Sanfilippo, 1978, p. 67, pl. 4, fig. 14; Sanfilippo, 1990, p. 306, pl. I, figs. 13–16; plate II, figs. 1, 2; Sanfilippo and Nigrini, 1995, p. 279; Nigrini and Sanfilippo, 2000, p. 73.

?*Cyclampterium* ?sp.: Sanfilippo and Riedel, 1970, pl. 2, fig. 7.

***Lophocyrtis* (*Lophocyrtis*?) *barbadense* (Ehrenberg)**
(Pl. P8, figs. 4a–5b)

Pterocanium barbadense Ehrenberg, 1873, p. 254; 1875, pl. 17, fig. 6.

Pterocyrtidium sp.: Petrushevskaya and Kozlova, 1972, p. 552, pl. 27, fig. 15.

Pterocyrtidium sp. Ling, 1975, p. 729, pl. 10, fig. 18 (partim).

Lophocyrtis (*Lophocyrtis*?) *barbadense* (Ehrenberg): Sanfilippo and Caulet, 1998, p. 8, pl. 4, figs. 9–10b.

?Theoperid gen. et sp. indet.: Johnson, 1974, pl. 2, figs. 16, 17.

***Lophocyrtis* (*Lophocyrtis*) *jacchia* (Ehrenberg)**
(Pl. P8, figs. 6a–7b)

Thyrsocyrtis jacchia Ehrenberg, 1873, p. 261; 1875, pl. 12, fig. 7.

Eucyrtidium stephanophorum Ehrenberg, 1873, p. 233; 1875, pl. 8, fig. 14.

Lophocyrtis (?) *jacchia* (Ehrenberg): Riedel and Sanfilippo, 1970, p. 530; 1971, p. 1594, pl. 3C, figs. 4, 5; pl. 7, fig. 16; 1973, p. 739; 1978, p. 70, pl. 7, fig. 1; 1986, pl. 7, fig. 10; Moore, 1971, p. 742, pl. 5, figs. 4, 7; Dinkelman, 1973, p. 780, pl. 2, fig. 6; Johnson, 1974, p. 548, pl. 5, fig. 5; 1978, p. 781; Nigrini, 1974, p. 1067, pl. 2C, fig. 10; Chen, 1975, pl. 3, figs. 5, 6; Holdworth, 1975, p. 530; Ling, 1975, p. 729, pl. 10, fig. 7; Sanfilippo et al., 1981, p. 504; Renz, 1984, p. 459; Sanfilippo and Riedel in Saunders et al., 1985, p. 412; Westberg-Smith and Riedel, 1985, p. 493; Caulet, 1986, p. 853; Palmer, 1987, p. 356.

Lophocyrtis jacchia (Ehrenberg): Sanfilippo and Riedel, 1979, p. 504; Renz, 1984, p. 459; Riedel and Sanfilippo, 1986, pl. 7, fig. 10.

Lophocyrtis ?*jacchia* (Ehrenberg) group: Petrushevskaya and Kozlova, 1972, p. 542, pl. 28, fig. 21.

P8. *Lophocyrtis, Theocorys,* p. 65.

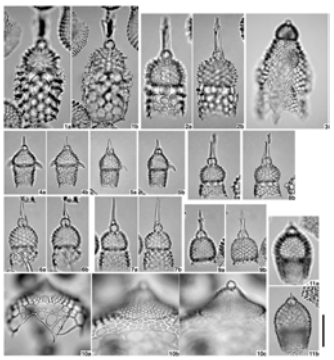

Theoperid gen. et sp. indet.: Johnson, 1974, pl. 3, fig. 17.

Lophocyrtis (*Lophocyrtis*) *jacchia* (Ehrenberg): Sanfilippo, 1990, p. 302, pl. I, figs. 5–10; pl. III, fig. 6; Caulet, 1991, p. 538.

Lophocyrtis (*Lophocyrtis*) *jacchia jacchia* (Ehrenberg) sensu Sanfilippo and Caulet, 1998, p. 10, pl. 4, figs. 1a, 1b.

***Lophocyrtis jacchia*(?) (Ehrenberg) form A**
(Pl. P8, figs. 8a–9b)

Remarks: This group is characterized by distally thorned apical horn. On the basis of the lack of large pores immediately below the lumbar stricture and/or the lack of arches at the base of apical horn in several specimens, the species is questionably identified to *L. jacchia*. In this study, the range of the species and *L. jacchia* without distally thorned apical horn is different; therefore, this group is counted separately from the typical form.

***Lophocyrtis* (*Sciadiapeplus*) *oberhaensliae* Sanfilippo**
(Pl. P8, figs. 10a–10c)

Lophocyrtis (*Sciadiapeplus*) *oberhaensliae* Sanfilippo, 1990, p. 310, pl. 2, figs. 10–14.

Family Pterocorythidae Haeckel, 1881, emend. Moore, 1972

***Anthocyrtidium adiaphorum* Sanfilippo and Riedel**
(Pl. P9, figs. 1a, 1b)

Anthocyrtidium adiaphorum Sanfilippo and Riedel, 1992, p. 25, pl. 1, figs. 14, 15; pl. 4, figs. 1, 2.

?*Podocyrtis coronatus* (Ehrenberg): Petrushevskaya and Kozlova, 1972, p.543, pl. 35, fig. 3.

?*Podocyrtis* sp. aff. *P. coronatus* (Ehrenberg): Petrushevskaya and Kozlova, 1972, pl. 35, fig. 4.

***Anthocyrtidium stenum* Sanfilippo and Riedel**
(Pl. P9, figs. 2a, 2b)

Anthocyrtidium stenum Sanfilippo and Riedel, 1992, p. 24, pl. 1, figs. 16, 17; pl. 4, fig. 3.

***Arbatrossidium* sp. A**
(Pl. P9, figs. 4a, 4b)

Arbatrossidium sp.: Sanfilippo and Riedel, 1992, pl. 1, fig. 8.

Remarks: Shell is composed of three segments. Cephalis is cylindrical and perforated by small circular pores, with tubercular surface. Apical horn is three-bladed and 2–3 times as long as height of cephalis. Collar stricture is indistinct. Thorax is inflated campanulate. Pores are circular to subcircular, roughly aligned longitudinally. Lumbar stricture is indistinct externally. Abdomen is cylindrical. Pores are circular to subcircular, larger than those in thorax, and roughly aligned longitudinally. Distal end of abdomen is fully opened and has peristomial teeth.

This species is distinguished from *Calocycletta parva* by the larger shell with a long apical horn.

P9. *Anthocyrtidium, Arbatrossidium, Cryptocarpium, Lamprocyclas, Podocyrtis,* p. 66.

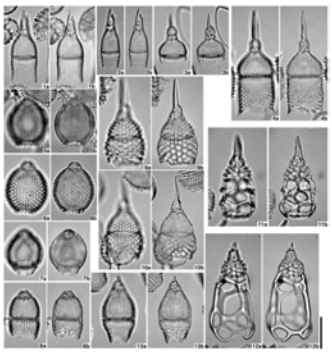

***Arbatrossidium* sp. B**
(Pl. P9, figs. 3a, 3b)

?*Calocycletta parva* Moore, 1972, p. 148, pl. 1, figs. 1–5; Dinkelman, 1973, p. 788, pl. 7, figs. 1, 2; Sanfilippo and Riedel, 1992, pl. 1, figs. 3–5; pl. 2, fig. 9; Sanfilippo and Nigrini, 1995, pl. 2, figs. 4, 5.

?*Theocyrtis* sp.: Riedel and Sanfilippo, 1978, pl. 1, fig. 12.

Remarks: This species is mostly similar to *Arbatrossidium* sp. A but distinguished from it by its relatively smaller shell.

***Cryptocarpium azyx* (Sanfilippo and Riedel)**
(Pl. P9, figs. 5a, 5b)

Carpocanistrum (?) *azyx* Sanfilippo and Riedel, 1973, p. 530, pl. 35, fig. 9.

Carpocanistrum azyx Sanfilippo and Riedel: Holdsworth, 1975, p. 532; Johnson, 1978, p. 781; Riedel and Sanfilippo, 1978, p. 67, pl. 4, fig. 5.

"*Carpocanistrum*" *azyx* Sanfilippo and Riedel: Renz, 1984, p. 456; Sanfilippo and Riedel in Saunders et al., 1985, p. 412, pl. 5, figs. 2, 3; Sanfilippo et al., 1985, p. 690, figs. 27.1a, 27.1b.

Cryptocarpium azyx (Sanfilippo and Riedel): Sanfilippo and Riedel, 1992, p. 6, pl. 2, fig. 21; Nigrini and Sanfilippo, 2000, p. 72, pl. 2, figs. 4–6.

***Cryptocarpium ornatum* (Ehrenberg)**
(Pl. P9, figs. 6a–8b)

Cryptoprora ornata Ehrenberg, 1873, p. 222; 1875, pl. 5, fig. 8; Riedel and Sanfilippo, 1971, pl. 3D, figs. 10, 11; Johnson, 1974, p. 550, pl. 5, fig. 9; 1978, p. 781; Renz, 1984, p. 457; Sanfilippo and Riedel in Saunders et al., 1985, p. 412, pl. 5, fig. 4; Sanfilippo et al., 1985, p. 693, figs. 27.2a, 27.2b.

Theocapsomma ornata (Ehrenberg): Petrushevskaya and Kozlova, 1972, p. 535, pl. 22, fig. 1.

Theocapsomma sp. F group: Petrushevskaya and Kozlova, 1972, p. 535, pl. 22, fig. 3.

Theocapsomma sp. aff. *T. ornata* (Ehrenberg): Petrushevskaya and Kozlova, 1972, pl. 22, fig. 2.

Carpocanistrum (?) *azyx* Sanfilippo and Riedel: Riedel and Sanfilippo, 1973, p. 738. pl. 2, fig. 4.

Cryptoprora sp. cf. *C. ornata* Ehrenberg: Johnson, 1974, pl. 2, figs. 18–20.

Cryptocarpium ornatum (Ehrenberg): Sanfilippo and Riedel, 1992, p. 6, pl. 2, figs. 18–20; Nigrini and Sanfilippo, 2000, p. 72.

***Lamprocyclas rhinoceros* (Haeckel)**
(Pl. P9, figs. 9a, 9b)

Lamprocyclas rhinoceros (Haeckel): Petrushevskaya and Kozlova, 1972, p. 544, pl. 36, figs. 1–3.

Lamprocyclas spp.: Sanfilippo and Riedel, 1992, pl. 1, fig. 11.

***Lamprocyclas* sp. A**
(Pl. P9, figs. 10a, 10b)

Remarks: Shell is composed of three segments. Cephalis is cylindrical to truncate conical. Cephalic wall is smooth, partly hyaline, and partly perforated by small circular pores. Collar stricture is indistinct. Thorax is campanulate with longitudinal aligned circular to subcircular pores. Lumbar stricture is indistinct externally. Abdomen is inflated cylindrical. Circular to subcircular pores, larger than those in thorax, are aligned in longitudinal rows. Distal end of abdomen is fully opened with semidifferentiated hyaline peristome.

This species is distinguished from *L. rhinoceros* by the smaller size and larger number of thoracic and abdominal pores.

***Podocyrtis* (*Lampterium*) *chalala* Riedel and Sanfilippo**
(Pl. P9, figs. 11a, 11b)

Podocyrtis (*Lampterium*) *chalala* Riedel and Sanfilippo, 1970, p. 535, pl. 12, figs. 2, 3; 1971, p. 1598; 1978, p. 71, pl. 8, fig. 3, text-fig. 3; 1986, pl. 2, fig. 14; Moore, 1971, p. 743, pl. 3, figs. 5, 6; Sanfilippo and Riedel, 1973, p. 532; Dinkelman, 1973, p. 788; Johnson, 1974, p. 551; 1976, p. 436; 1978, p. 781; Holdsworth, 1975, p. 532; Sanfilippo et al., 1985, p. 697, fig. 30.11; Nigrini and Sanfilippo, 2000, p. 73.

Lampterium chalala (Riedel and Sanfilippo): Petrushevskaya and Kozlova, 1972, p. 543, pl. 32, fig. 12.

Podocyrtis chalala Riedel and Sanfilippo: Riedel and Sanfilippo, 1973, p. 739; 1986, pl. 3, figs. 10, 11; Renz, 1984, p. 459; Sanfilippo and Riedel in Saunders et al., 1985, p. 412.

***Podocyrtis* (*Lampterium*) *goetheana* (Haeckel)**
(Pl. P9, figs. 12a, 12b)

Cycladophora goetheana Haeckel, 1887, p. 1376, pl. 65, fig. 5.

Podocyrtis (*Lampterium*) *goetheana* (Haeckel): Riedel and Sanfilippo, 1970, p. 535; 1971, p.1598, pl. 8, fig. 13; 1978, p. 72, pl. 8, fig. 6; Moore, 1971, p. 743, pl. 3, figs. 7, 8; Sanfilippo and Riedel, 1973, p. 532; 1974, p. 1023; Dinkelman, 1973, p. 788; Johnson, 1974, p. 551; 1976, p. 436; 1978, p. 781; Holdsworth, 1975, p. 532; Sanfilippo et al., 1985, p. 697, fig. 30.12; Nigrini and Sanfilippo, 2000, p. 73.

Podocyrtis goetheana (Haeckel): Riedel and Sanfilippo, 1973, p. 739; 1986, pl. 3, fig. 12; Renz, 1984, p. 459; Sanfilippo and Riedel in Saunders et al., 1985, p. 412.

Lampterium goetheanum (Haeckel): Petrushevskaya and Kozlova, 1972, p. 543.

?*Lampterium* sp. aff. *Lampterium goetheanum* (Haeckel): Petrushevskaya and Kozlova, 1972, pl. 32, figs. 13, 14.

***Podocyrtis* (*Podocyrtis*) *papalis* Ehrenberg**
(Pl. P9, figs. 13a, 13b)

Podocyrtis papalis Ehrenberg, 1847, p. 55, fig. 2; 1854, pl. 36, fig. 23; 1873, p. 251; Riedel and Hays, 1969, pl. 1, fig. C; Riedel and Sanfilippo, 1973, p. 739; Renz, 1984, p. 460.

Podocyrtis fasciata Clark and Campbell, 1942, p. 80, pl. 7, figs. 29, 33.

Podocyrtis (*Podocyrtis*) *papalis* Ehrenberg: Riedel and Sanfilippo, 1970, p. 533, pl. 11, fig. 1; 1971, p. 1598, pl. 3E, fig. 1; 1986, pl. 7, fig. 1; Moore, 1971, p. 743, pl. 2, fig. 4; Petrushevskaya and Kozlova, 1972, p. 544, pl. 35, fig. 1; Sanfilippo and Riedel, 1973, p. 531, pl. 20, figs. 11–14; pl. 36, figs. 2, 3; 1974, p. 1023; Dinkelman, 1973, p. 788; Nigrini, 1974, p. 1069, pl. 1K, figs. 7–10; Johnson, 1974, p. 551, pl. 4, fig. 12; 1976, p. 436; 1978, p. 782; Ling, 1975, p. 731, pl. 13, fig. 5; Sanfilippo et al., 1985, fig. 30.1; Nishimura, 1987, p. 727, pl. 2, fig. 17; Hull, 1993, p. 13, pl. 7, figs. 7, 8; pl. 8, fig. 10; Kozlova, 1999, p. 151, pl. 15, fig. 6; pl. 24, figs. 16, 17; Nigrini and Sanfilippo, 2000, p. 74, pl. 2, fig. 11; pl. 3, figs. 6, 7.

Theocyrtis tuberosa Riedel emend. Sanfilippo et al. group
(Pl. **P10,** figs. 1a–6b)

P10. *Theocyrtis,* p. 67.

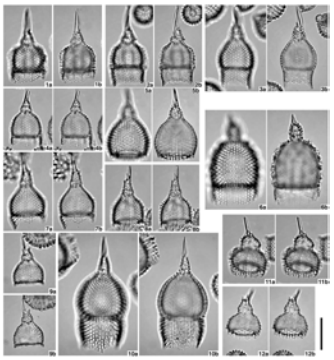

Theocyrtis tuberosa Riedel, 1959, p. 298, pl. 2, fig. 10, 11; Riedel and Sanfilippo, 1970, p. 535, pl. 13, figs. 8–10; 1971, p. 1598, pl. 3D, figs. 14, 15; 1973, p. 740; 1978, p. 78, pl. 1, fig. 11; Moore, 1971, p. 743, pl. 5, figs. 5, 6; Goll, 1972, p. 958, pl. 19, fig. 1; Sanfilippo and Riedel, 1973, p. 532; 1974, p. 1023; Dinkelman, 1973, p. 789; Nigrini, 1974, p. 1070, pl. 2E, figs. 5, 6; 1985, p. 523; Johnson, 1974, p. 551; 1976, p. 436; 1978, p. 782; Holdsworth, 1975, p. 532; Ling, 1975, p. 731, pl. 13, fig. 7; Weaver, 1983, p. 678; Renz, 1984, p. 460; Sanfilippo and Riedel in Saunders et al., 1985, p. 413, pl. 5, figs. 9–11; Sanfilippo et al., 1985, p. 701, figs. 32.1a–32.1d; Takemura, 1992, p. 744, pl. 6, figs. 1, 2; Sanfilippo and Nigrini, 1995, p. 283; Takemura and Ling, 1997, p. 114, pl. 1, fig. 8; Nigrini and Sanfilippo, 2000, p. 74.

Calocycletta tuberosa (Riedel): Petrushevskaya and Kozlova, 1972, p. 544, pl. 35, figs. 11–14.

Remarks: This species group includes *Theocyrtis tuberosa* (Pl. **P10,** figs. 6a, 6b), *T. tuberosa* variant A (Pl. **P10,** figs. 1a–2b, 4a, 4b) of Nigrini and Sanfilippo (this volume), and a form with smooth thorax with apically closed cephalis.

Theocyrtis (?) *tuberosa* Riedel emend. Sanfilippo et al. form A
(Pl. **P10,** figs. 7a–10b)

Eucyrtidium acanthocephala Ehrenberg, 1873, p. 225; 1875, pl. 9, fig. 8.

Theocyrtis sp. aff. *T. tuberosa* Riedel: Riedel and Sanfilippo, 1971, pl. 3D, figs. 16–18.

Theocyrtis sp.: Riedel and Sanfilippo, 1978, pl. 1, fig. 10.

Calocycletta acanthocephala (Ehrenberg): Petrushevskaya and Kozlova, 1972, p. 544, pl. 35, figs. 5–7.

Calocycletta virginis Haeckel: Petrushevskaya and Kozlova, 1972, p. 544, pl. 35, figs. 8–10.

Remarks: This form is distinguished from *T. tuberosa* group by a pore at the apex of cylindrical cephalis with or without two or three thorns surrounding the pore. This form includes *Theocyrtis* sp. A of Nigrini and Sanfilippo (this volume) (Pl. **P10,** figs. 7a–9b) and *Calocycletta robusta* early variant of Nigrini and Sanfilippo (this volume) (Pl. **P10,** figs. 10a, 10b).

Theocyrtis (?) *tuberosa* Riedel emend. Sanfilippo et al. form B
(Pl. **P10,** figs. 11a–12b)

Theocyrtis sp(p).: Sanfilippo and Riedel, 1992, pl. 1, figs. 20–23.

Remarks: This form is distinguished from *T. tuberosa* group and *T.* (?) *tuberosa* form A by the large cephalis. Its shell size is smaller than that of typical *T.*

tuberosa (Pl. P10, figs. 6a, 6b). This form is same to *Theocyrtis* sp. B in Nigrini and Sanfilippo (this volume).

Family Theocotylidae Petrushevskaya, 1981

***Stichopilidium sphinx* Ehrenberg**
(Pl. P11, figs. 1a, 1b)

Stichopilidium sphinx, Ehrenberg, 1873, p. 255; 1875, pl. 17, fig. 5; Petrushevskaya and Kozlova, 1972, p. 552, pl. 27, fig. 1.

Theoperidae gen. A: Ling, 1975, p. 730, pl. 12, figs. 1, 2.

***Thyrsocyrtis* (*Pentalocorys*) *lochites* Sanfilippo and Riedel**
(Pl. P11, fig. 10)

Gen. et sp. indet.: Riedel and Sanfilippo, 1970, pl. 8, fig. 4.

Thyrsocyrtis sp.: Petrushevskaya and Kozlova, 1972, pl. 34, fig. 5.

Thyrsocyrtis triacantha (Ehrenberg): Johnson, 1974, p. 549, pl. 5, fig. 16

Thyrsocyrtis sp. form A: Holdsworth, 1975, p. 532, pl. 1, figs. 16, 17, 25.

Thyrsocyrtis (*Pentalocorys*) *lochites* Sanfilippo and Riedel, 1982, p. 175, pl. 1, fig. 13; pl. 3, figs. 5–9; Sanfilippo et al., 1985, p. 689, fig. 26.9; Nigrini and Sanfilippo, 2000, p. 74.

Thyrsocyrtis lochites Sanfilippo and Riedel: Sanfilippo and Riedel in Saunders et al., 1985, p. 413.

***Thyrsocyrtis* (*Pentalocorys*) *tetracantha* (Ehrenberg)**
(Pl. P11, figs. 9a, 9b)

Podocyrtis schomburgkii Ehrenberg: Bury, 1862, pl. 17, fig. 2.

Podocyrtis aculeata Ehrenberg, 1873, p. 248; 1875, pl. 13, fig. 3; Bütschli, 1881, p. 524, pl. 33, figs. 34a, 34b.

Podocyrtis parvipes Ehrenberg, 1873, p. 252; 1875, pl. 14, fig. 5; Haeckel, 1887, p. 1371.

Podocyrtis pentacantha Ehrenberg, 1873, p. 252; 1875, pl. 17, fig. 1.

Podocyrtis tetracantha Ehrenberg, 1873, p. 254; 1875, pl. 13, fig. 2.

Alacorys tetracantha (Ehrenberg): Haeckel, 1887, p. 1371; Riedel and Funnell, 1964, p. 310.

Alacorys pentacantha (Ehrenberg): Haeckel, 1887, p. 1371.

Alacorys aculeata (Ehrenberg): Haeckel, 1887, p. 1373.

Thyrsocyrtis tetracantha (Ehrenberg): Riedel and Sanfilippo, 1970, p. 527; 1971, p. 1596; 1973, p. 740; 1978, p. 80, pl. 10, figs. 8, 9; 1986, pl. 6, fig. 3; Moore, 1971, p. 741, pl. 4, fig. 8; 1973, p. 822; Petrushevskaya and Kozlova, 1972, p. 542; Dinkelmann, 1973, p. 787, pl. 2. figs. 4, 5; Foreman, 1973, p. 422; Johnson, 1974, p. 549, pl. 5, fig. 15; 1976, p. 436; 1978, p. 782; Nigrini, 1974, p. 1069, pl. 2E, fig. 2; Sanfilippo and Riedel, 1974, p. 1025; 1979, p. 507; Hold-

P11. *Stichopilidium, Thyrsocyrtis,* p. 68.

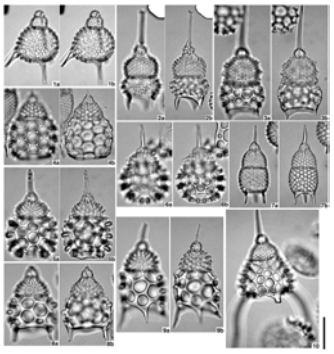

sworth, 1975, p. 531; Ling, 1975, p. 730, pl. 11, fig. 19; Renz, 1984, p. 460; Sanfilippo and Riedel in Saunders et al., 1985, p. 413.

Thyrsocyrtis cf. *T. triacantha* (Ehrenberg): Dinkelman, 1973, pl. 2, fig. 8.

Thyrsocyrtis sp. aff. *T. bromia* Ehrenberg: Dinkelman, 1973, pl. 3, fig. 5.

Thyrsocyrtis (*Pentalocorys*) *tetracantha* (Ehrenberg): Sanfilippo and Riedel, 1982, p. 176, pl. 1, figs. 11, 12; pl. 3, fig. 10; Sanfilippo et al., 1985, p. 690, figs. 26.8a, 26.8b; Nigrini and Sanfilippo, 2000, p. 74, pl. 1, fig. 2.

***Thyrsocyrtis* (*Pentalocorys*) *triacantha* (Ehrenberg)**
(Pl. **P11,** figs. 8a, 8b)

Podocyrtis schomburgkii Ehrenberg, 1847, p. 55, fig. 1 (plate opposite p. 60); 1854, pl. 36, fig. 22; 1873, p. 253; 1875, pl. 14, fig. 7; Haeckel, 1862, p. 339; 1887, p. 1343.

Podocyrtis cothurnata Ehrenberg, 1854, pl. 36, fig. B21; 1873, p. 250; 1875, pl. 14, fig. 1.

Anthocyrtis cothurnata (Ehrenberg): Haeckel, 1862, p. 310.

Podocyrtis centriscus Ehrenberg, 1873, p. 249; 1875, pl. 14, fig. 2; Haeckel, 1887, p. 1341.

Podocyrtis princepsi Ehrenberg, 1873, p. 252; 1875, pl. 13, fig. 1; Bütschli, 1881, p. 524, pl. 33, figs. 32a–32c; 1882, pl. 30, figs. 14a, 14b; Haeckel, 1887, p. 1342; Murray, 1895, p. 881.

Podocyrtis radicata Ehrenberg, 1873, p. 253; 1875, pl. 13, fig. 5.

Podocyrtis triacantha Ehrenberg, 1873, p. 254; 1875, pl. 13, fig. 4; Heckel, 1887, p. 1350; Riedel, 1957a, p. 260, pl. 63, fig. P; Wiseman and Riedel, 1960, p. 216; Riedel and Funnell, 1964, p. 311.

Podocyrtis ventricosa Ehrenberg, 1873, p. 254; 1875, pl. 16, fig. 3; Haeckel, 1887, p. 1341.

Dictyopodium moseleyi Haeckel, 1879, p. 706, pl. 16, fig. 10.

Thyrsocyrtis radicata (Ehrenberg): Haeckel, 1887, p. 1351.

Dictyopodium cothurnatum (Ehrenberg): Haeckel, 1887, p. 1353.

Dictyopodium scaphopodium Haeckel, 1887, p. 1353, pl. 73, fig. 8; Murray, 1895, p. 1042.

Dictyopodium thyrsolophus Haeckel, 1887, p. 1354, pl. 73, fig. 7.

Thyrsocyrtis triacantha (Ehrenberg): Riedel and Sanfilippo, 1970, p. 526, pl. 8, figs. 2, 3; 1971, p. 1596, pl. 3C, fig. 7; 1973, p. 740; 1978, p. 82, pl. 10, figs. 10, 11; 1986, pl. 6, fig. 2; Moore, 1971, p. 740, pl. 4, fig. 2; 1973, p. 822; Petrushevskaya and Kozlova, 1972, p. 542, pl. 32, fig. 9; pl. 34, fig. 6; Dinkelman, 1973, p. 787, pl. 2, fig. 7 (partim); Foreman, 1973, p. 442, pl. 12, figs. 9–11; Johnson, 1976, p. 436; 1978, p. 782; Nigrini, 1974, p. 1069, pl. 1J, figs. 5–7; pl. 2E, fig. 1; Sanfilippo and Riedel, 1974, p. 1025; 1979, p. 507; Holdsworth, 1975, p. 531, pl. 1, fig. 18; Ling, 1975, p. 730, pl. 11, fig. 20; Weaver and Dinkelman, 1978, p. 873; Renz, 1984, p. 460; Sanfilippo and Riedel in Saunders et al., 1985, p. 413.

Thyrsocyrtis (*Pentalocorys*) *triacantha* (Ehrenberg): Sanfilippo and Riedel, 1982, p. 176, pl. 1, figs. 8–10; pl. 3, figs. 3, 4; Sanfilippo et al., 1985, p. 690, figs. 26.7a, 26.7b; Hull, 1993, p. 13, pl. 7, fig. 12; pl. 8, fig. 2; Nigrini and Sanfilippo, 2000, p. 74, pl. 1, figs. 13, 16, 17.

Thyrsocyrtis (*Thyrsocyrtis*) *bromia* Ehrenberg
(Pl. **P11,** figs. 2a–3b)

Thyrsocyrtis bromia Ehrenberg, 1873, p. 260; 1875, pl. 12, fig. 12; Riedel and Sanfilippo, 1970, p. 526; Moore, 1971, p. 740, pl. 5, fig. 1 (partim); Dinkelman, 1973, p. 787, pl. 3, figs. 1, 2, 4 (partim); Johnson, 1974, p. 549, pl. 5, fig. 7; Nigrini, 1974, p. 1068, pl. 2D, fig. 6; Holdsworth, 1975, p. 531, pl. 1, figs. 14, 19–21 (partim).

Thyrsocyrtis ?*rhizodon* Ehrenberg: Holdsworth, 1975, pl. 1, fig. 24.

Thyrsocyrtis (*Thyrsocyrtis*) *bromia* Ehrenberg: Sanfilippo and Riedel, 1982, p. 172, pl. 1, fig. 17 (partim); Sanfilippo et al., 1985, p. 687, fig. 26.4a (partim).

It is not clear whether to cite the following synonymy as the typical form of T. bromia or following T. bromia group A in this study:

Podocyrtis bromia (Ehrenberg): Haeckel, 1887, p. 1349.

Thyrsocyrtis bromia Ehrenberg: Riedel and Sanfilippo, 1970, p. 526; 1973, p. 740; Moore, 1973, p. 822; Foreman, 1973, p. 441; Johnson, 1976, p. 436; 1978, p. 782; Sanfilippo and Riedel, 1974, p. 1025; 1979, p. 506; Petrushevskaya and Kozlova, 1972, p. 542; Renz, 1984, p. 460; Sanfilippo and Riedel in Saunders et al., 1985, p. 413; Caulet, 1991, p. 539; Nigrini and Sanfilippo, 2000, p. 75.

Thyrsocyrtis (*Thyrsocyrtis*) *bromia* Ehrenberg form A
(Pl. **P11,** figs. 4a–6b)

Thyrsocyrtis bromia Ehrenberg, Riedel and Sanfilippo, 1971, p. 1596, pl. 8, fig. 6; 1978, p. 78, pl. 10, figs. 4, 5; 1986, pl. 6, fig. 1; Moore, 1971, p. 740, pl. 5, figs. 2, 3 (partim); Dinkelman, 1973, p. 787, pl. 3, figs. 3, 6 (partim); Holdsworth, 1975, p. 531, pl. 1, figs. 12, 13 (partim); Ling, 1975, p. 730, pl. 11, figs. 15, 16.

Thyrsocyrtis sp. Dinkelman, 1973, pl. 3, figs. 7, 8.

Thyrsocyrtis (*Thyrsocyrtis*) *bromia* Ehrenberg: Sanfilippo and Riedel, 1982, p. 172, pl. 1, figs. 18–20 (partim); Sanfilippo et al., 1985, p. 687, fig. 26.4b (partim).

?*Theocorys sphaerophila* (Ehrenberg): Haeckel, 1887, p. 1418.

Remarks: Shell is composed of three segments. Cephalis is subspherical, perforated by small circular pores, and has rodlike apical horn with variable length. Collar stricture is distinct. Thorax is campanulate with tuberculate or smooth surface. Pores in thorax are circular to subcircular, aligned longitudinally. Lumbar stricture is distinct. Abdomen is inflated cylindrical with tuberculate or smooth surface. Pores in abdomen are very large, with roughly hexagonal framework. Distal end of abdomen is fully opened with internal ring. On peristome, if present, abdominal pore bars extend downward.

This form is distinguished from *T. bromia* by the internal ring at the distal end of the abdomen with or without differentiated peristome and by the strongly inflated abdomen with hexagonally framed large pores. This form is distinguished from *Thyrsocyrtis pinguisicoides* by the larger size of abdominal pores and inflated cylindrical abdomen.

***Thyrsocyrtis* (*Thyrsocyrtis*?) *pinguisicoides* O'Connor**
(Pl. **P4,** figs. 7a–12b)

Eucyrtidium apiculatum Ehrenberg, 1873, p. 225; 1875, pl. 10, fig. 10.

Eucyrtidium sphaerophilum Ehrenberg, 1873, p. 233; 1875, pl. 8, fig. 16.

?*Calocyclura sphaerophilum* (Ehrenberg): Kozlova, 1999, p. 154, pl. 31, figs. 7, 12, 17; pl. 46, fig. 19.

Thyrsocyrtis (*Thyrsocyrtis*?) *pinguisicoides* O'Connor, 1999, p. 29, pl. 4, figs. 28–32; pl. 7, figs. 28a–31.

Remarks: Cephalis is subspherical and perforated by subcircular pores. Apical horn is rodlike, bladed proximally in many specimens, and variable length. Collar stricture is distinct. Thorax is campanulate with circular to subcircular pores and thorny to tuberculate surface. Lumbar stricture is distinct. Abdomen is inflated subcylindrical to campanulate with subcircular to circular pores, which are larger than those in thorax. Abdominal surface is thorny to smooth. Distal end of abdomen is fully opened with internal ring. Distal appendages may be present or absent.

The earlier form of this species has a large inflated subcylindrical abdomen with a distal lattice appendage (Pl. **P4,** figs. 7a–8b) and resembles *Eucyrtidium sphaerophilum*, whereas the later one (Pl. **P4,** figs. 9a–12b) has a campanulate abdomen similar to *Eucyrtidium apiculatum*. The morphologic change between these two forms, mainly in abdominal size and shape, is gradual. This species is distinguished from *Artophormis barbadensis* by the inflated abdomen and from *A. gracilis* by a stout apical horn. The early form is distinguished from *Thyrsocyrtis bromia* form A by the relatively small size of abdominal pores and the distal lattice appendage (perhaps the remnant of post-abdominal segment) and from *T. bromia* by the internal ring at the distal end of the abdomen. Although the late form has similar shell to one of the later forms of *A. gracilis* (Pl. **P4,** figs. 3a, 3b), they are clearly distinguished by significantly different stratigraphic ranges; the former is extinct in the late Eocene and the latter appeared in the middle early Oligocene.

***Thyrsocyrtis* (*Thyrsocyrtis*) *rhizodon* Ehrenberg**
(Pl. **P11,** figs. 7a, 7b)

Thyrsocyrtis rhizodon Ehrenberg, 1873, p. 262; 1875, pl. 12, fig. 1; Haeckel, 1887, p. 1350; Riedel and Sanfilippo, 1970, p. 525, pl. 7, figs. 6, 7; 1971, p. 1596, pl. 3C, fig. 6; 1973, p. 740; Moore, 1971, p. 740, pl. 2, figs. 8, 9; 1973, p. 822; Petrushevskaya and Kozlova, 1972, p. 542; Dinkelman, 1973, p. 787; Foreman, 1973, p. 442, pl. 3, figs. 1, 2; Johnson, 1974, p. 549, pl. 4, figs. 6–9; 1976, p. 436; 1978, p. 782; Nigrini, 1974, p. 1069, pl. 1I, figs. 9–13; pl. 2D, fig. 7; Sanfilippo and Riedel, 1974, p. 1025; 1979, p. 507; Holdsworth, 1975, p. 531, pl. 1, figs. 15, 22, 23; Ling, 1975, p. 730, pl. 11, fig. 18; Weaver and Dinkelman, 1978, p. 873; Renz, 1984, p. 460; Sanfilippo and Riedel in Saunders et al., 1985, p. 413; Sanfilippo et al., 1985, p. 687, figs. 26.3a, 26.3b.

Podocyrtis rhizodon Haeckel, 1887, p. 1351.

Podocyrtis aff. *P. argus* Ehrenberg: Riedel, 1957a, p. 260, pl. 62, fig. 4; pl. 63, fig. 8.

Thyrsocyrtis argulus (Ehrenberg): Petrushevskaya and Kozlova, 1972, p.542, pl. 32, fig. 8.

Thyrsocyrtis hirsuta hirsuta (Krasheninnikov): Ling, 1975, p. 730, pl. 11, fig. 17.

Theocotyle (*Theocotyle*) *cryptocephala cryptocephala* (Ehrenberg): Ling, 1975, p. 730, pl. 11, fig. 14.

Thyrsocyrtis (*Thyrsocyrtis*) *rhizodon* Ehrenberg: Sanfilippo and Riedel, 1982, p. 173, pl. 1, figs. 14–16; pl. 3, figs. 12–17; Nigrini and Sanfilippo, 2000, p. 75, pl. 1, fig. 14.
?*Thyrsocyrtis* sp.: Weaver and Dinkelman, 1978, p. 873, pl. 6, fig. 3.

Family Theoperidae Haeckel, 1881

***Eusyringium fistuligerum* (Ehrenberg) group**
(Pl. **P12,** figs. 1a–3)

Eucyrtidium tubulus Ehrenberg, 1854, pl. 36, fig. 19; 1873, p. 233; 1875, pl. 9, fig. 6.

Eucyrtidium fistuligerum Ehrenberg, 1873, p. 229; 1875, pl. 9, fig. 3.

Eucyrtidium sipho Ehrenberg, 1873, p. 229; 1875, pl. 9, fig. 2.

Eusyringium fistuligerum (Ehrenberg): Haeckel, 1887, p. 1498; Riedel, 1957b, p. 94, pl. 4, fig. 8; Riedel and Sanfilippo, 1970, p. 527,pl. 8, figs. 8, 9; 1971, p. 1594, pl. 3B, fig. 14; 1973, p. 738; 1978, p. 68, pl. 5, figs. 6, 7; Moore, 1971, p. 741, pl. 4, figs. 10, 11; Petrushevskaya and Kozlova, 1972, p. 549, pl. 32, fig. 3; Foreman, 1973, p. 435, pl. 11, fig. 6; Dinkelman, 1973, p. 777; Nigrini, 1974, p. 1067, pl. 1F, figs. 9–12; pl. 2C, fig. 9; Johnson, 1974, p. 548, pl. 5, fig. 4; 1976, p. 435; 1978, p. 781; Sanfilippo and Riedel, 1974, p. 1022; Holdsworth, 1975, p. 530; Ling, 1975, p. 728, pl. 9, figs. 19, 20; Weaver, 1983, p. 676; Renz, 1984, p. 459; Sanfilippo and Riedel in Saunders et al., 1985, p. 412; Sanfilippo et al., 1985, p. 670, figs. 17.1a, 17.1b; Takemura, 1992, p. 746, pl. 7, figs. 5, 6; Takemura and Ling, 1997, p. 113; Nigrini and Sanfilippo, 2000, p. 73, pl. 2, figs. 2, 3.

Eusyringium tubulus (Ehrenberg): Petrushevskaya and Kozlova, 1972, p. 549, pl. 32, figs. 4, 5.

?*Eusyringium fistuligerum* (Ehrenberg): Chen, 1975, p. 461, pl. 3, fig. 3.

?*Eusyringium tubulus* (Ehrenberg): Ling, 1975, p. 729, pl. 9, fig. 22.

***Lychnocanoma amphitrite* Foreman**
(Pl. **P12,** figs. 8a, 8b)

Lychnocanium sp. aff. *L. bellum* Clark and Campbell: Riedel and Sanfilippo, 1971, p. 1595, pl. 3C, fig. 1 (partim).

Lychnocanoma amphitrite Foreman, 1973, p. 437, pl. 11, fig. 10; Riedel and Sanfilippo, 1973, p. 739; 1978, p. 70, pl. 7, figs. 2, 3; 1986, pl. 1, fig. 13; Nigrini, 1974, p. 1067, pl. 2D, figs. 2, 3; Sanfilippo and Riedel, 1974, p. 1022; Chen, 1975, p. 462, pl. 2, fig. 7; Holdsworth, 1975, p. 530; Weaver, 1983, p. 678; Renz, 1984, p. 459; Sanfilippo and Riedel in Saunders et al., 1985, p. 412; Caulet, 1991, p. 538; Takemura, 1992, p. 747, pl. 2, figs. 13, 14; Takemura and Ling, 1997, p. 114, pl. 1, fig. 21; Nigrini and Sanfilippo, 2000, p. 73.

***Lychnocanoma babylonis* (Clark and Campbell) group**
(Pl. **P13,** figs. 1a, 1b)

Dictyophimus (*Dictyophimium*) *babylonis* Clark and Campbell, 1942, p. 67, pl. 9, figs. 32, 36; Riedel, 1957b, p. 81, pl. 1, fig. 6.

P12. *Eusyringium, Lychnocanoma,* p. 69.

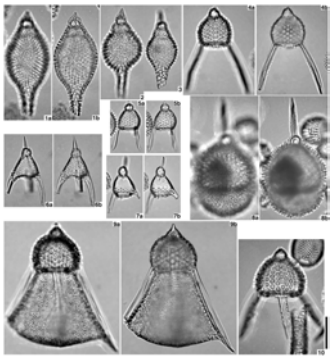

P13. *Lychnocanoma, Stichopilium*?, *Anthocyrtis, Pterocodon, Cycladophora, Eurystomoskevos, Thecospharella, Thecosphaera, Axoprunum, Stylosphaera,* p. 70.

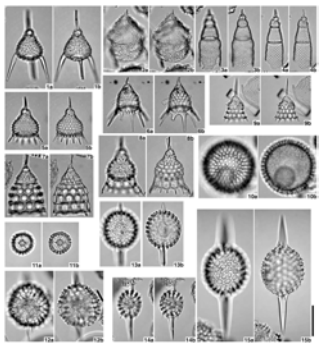

Dictyophimus (*Dictyophimium*) cf. *babylonis* Clark and Campbell: Clark and Campbell, 1945, p. 38, pl. 6, fig. 2.

Sethocytris babylonis (Clark and Campbell) group: Riedel and Sanfilippo, 1970, p. 528, pl. 9, figs. 1–3; 1971, p. 1595, pl. 3B, fig. 13; Moore, 1971, p. 741, pl. 3, figs. 9, 10; Dinkelman, 1973, p. 780; Johnson, 1974, p. 548, pl. 2, fig. 13; Sanfilippo and Riedel, 1974, p. 1023; Holdsworth, 1975, p. 531; Renz, 1984, p. 460; Sanfilippo et al., 1985, figs. 17.8a, 17.8b, 22.2.

Lychnocanoma babylonis (Clark and Campbell) group: Foreman, 1973, p. 437, pl. 2, fig. 1; Riedel and Sanfilippo, 1973, p. 739; Weaver, 1983, p. 678; Caulet, 1991, p. 538.

Lychnocanoma babylonis (Clark and Campbell): Nigrini, 1974, p. 1068, pl. 1G, figs. 9–14; pl. 2D, fig. 4; Chen, 1975, p. 462, pl. 2, fig. 8; Johnson, 1976, p. 436; 1978, p. 781; Riedel and Sanfilippo, 1986, pl. 2, fig. 17; Nigrini and Sanfilippo, 2000, p. 73.

Lychnocanella babylonis (Clark and Campbell): Shilov, 1995, p. 126.

Lychnocanoma (?) *babylonis* (Clark and Campbell): Kozlova, 1999, pl. 27, fig. 12.

?*Lychnocanoma babylonis–turgidulum* group: Ling, 1975, p. 729, pl. 10, figs. 8, 9 (partim).

?*Lychnocanoma* sp. aff. *L. babylonis* (Clark and Campbell): Nishimura, 1987, p. 727, pl. 3, figs. 3–5.

***Lychnocanoma tripodium* (Ehrenberg) form A**
(Pl. **P12,** figs. 4a, 4b)

Lychnocanium tripodium Ehrenberg, 1873, p. 245; 1875, pl. 6, fig. 2; Petrushevskaya and Kozlova, 1972, p. 553, pl. 29, fig. 2.

Lychnocanoma tripodium (Ehrenberg): Haeckel, 1887, p. 1229; Caulet, 1991, p. 538.

Lychnocanium grande Campbell and Clark: Petrushevskaya and Kozlova, 1972, p. 553, pl. 29, fig. 6.

Lychnocanoma sp. B: Ling, 1975, p. 729, pl. 10, fig. 14.

Theoperid gen. et sp. indet.: Sanfilippo et al., 1985, fig. 19.6.

Lychnocanium sp. aff. *L. tripodium* Ehrenberg: Kozlova, 1999, p. 130, pl. 24, fig. 12 (partim).

Lychnocanium separatum Moksjakova: Kozlova, 1999, p. 129, pl. 26, fig. 14; pl. 27, fig. 10; pl. 45, figs. 10, 11.

?*Lychnocanium hirundo* Ehrenberg, 1854, pl. 36, fig. 6; 1875, pl. 7, fig. 8; Petrushevskaya and Kozlova, 1972, p. 553, pl. 29, fig. 3.

?*Dictyophimus* (*Dictyophimium*) *splendens* Clark and Campbell, 1942, p. 66, pl. 9, fig. 34.

***Lychnocanoma tripodium* (Ehrenberg) form B**
(Pl. **P12,** figs. 5a, 5b)

Lychnocanium sp. aff. *L. tripodium* Ehrenberg: Kozlova, 1999, p. 130, pl. 45, figs. 15, 16 (partim).

Remarks: This form is distinguished from *L. tripodium* by smaller shell size.

***Lychnocanoma tripodium* (Ehrenberg) form C**
(Pl. **P12,** figs. 9a–10)

Remarks: Shell is composed of two segments. Hemispherical cephalis us hyaline, has rough surface without pores, and a conical tiny apical horn, which is shorter than the height of cephalis. Collar stricture is distinct. Thorax is globular, with rough surface and numerous tiny thorns. Thoracic pores are subcircular with rough hexagonal framework. Three long and solid feet arise from distal end of thorax and are three-bladed and curve outward. Thin porous plates with very small circular to subcircular pores connect each foot and form basal cap.

This form is distinguished from *L. tripodium* and *L. tripodium* form B by its large globular thorax with outwardly curved feet.

***Lychnocanium continuum* Ehrenberg**
(Pl. **P12,** figs. 7a, 7b)

Lychnocanium continuum Ehrenberg, 1873, p. 243; 1875, pl. 7, fig. 11.

***Lychnocanium tridentatum* Ehrenberg**
(Pl. **P12,** figs. 6a, 6b)

Lychnocanium tridentatum Ehrenberg, 1873, p. 244; 1875, pl. 6, fig. 4.

Gen. et sp. indet., cf. *Lychnodictyum tridentatum* (Ehrenberg): Sanfilippo et al., 1985, fig. 21.6.

***Stichopilium* ? sp. B**
(Pl. **P13,** figs. 2a, 2b)

Remarks: Shell surface is somewhat thorny and composed of conical cephalothorax and cylindrical post-thoracic segments. Cephalis is semispherical with circular to subcircular pores and three-bladed apical horn longer than cephalis. Collar stricture is indistinct. Conical thorax is somewhat triangular in cross section with three ridges extending to three-bladed lateral wings from its lower part, with transversely aligned circular pores. Lumbar stricture is indistinct. Abdomen and post-abdominal segments are somewhat inflated cylindrical with transversely aligned or irregularly distributed circular to subcircular pores. Distal end of shell is opened.

***Stichopodium ?microporum* (Ehrenberg)**
(Pl. **P13,** figs. 3a–4b)

Eucyrtidium microporum Ehrenberg, 1873, p. 230; 1875, pl. 11, fig. 20.

Stichopodium ?microporum (Ehrenberg): Petrushevskaya and Kozlova, 1972, p. 548, pl. 25, figs. 4–6.

Remarks: Earlier form has wider abdomen and post-abdominal segment than the later form.

Family Theopiliidae Haeckel, 1881

***Anthocyrtis furcata* Ehrenberg**
(Pl. **P13,** figs. 5a, 5b)

Anthocyrtis furcata Ehrenberg, 1873, p. 216; 1875, pl. 6, fig. 2.

Anthocyrtella sp.: Petrushevskaya and Kozlova, 1972, pl. 33, fig. 10.

Diplocyclas spp.: Ling, 1975, p. 728, pl. 9, figs. 1, 2.

Theoperid gen. et sp. indet.: Sanfilippo et al., 1985, fig. 15.4.

***Cycladophora spatiosa* Ehrenberg group**
(Pl. **P13,** figs. 7a–8b)

Cycladophora spatiosa Ehrenberg, 1873, p. 222; 1875, pl. 18, figs. 5, 6.

Anthocyrtella spatiosa (Ehrenberg) group: Petrushevskaya and Kozlova, 1972, p. 541, pl. 33, figs. 1–3; Petrushevskaya, 1975, pl. 15, fig. 6.

Theoperid gen. et sp. indet.: Sanfilippo et al., 1985, fig. 15.3.

Anthocyrtella spatiosa (Ehrenberg): Caulet, 1991, p. 537.

***Eurystomoskevos petrushevskaae* Caulet**
(Pl. **P13,** figs. 9a, 9b)

Diplocyclas sp. A group: Petrushevskaya and Kozlova, 1972, p. 541, pl. 33, figs. 15, 16 (partim).; Petrushevskaya, 1975, p. 587, pl. 24, fig. 4; Chen, 1975, p. 460, pl. 7, figs. 4, 5.

Eurystomoskevos petrushevskaae Caulet, 1991, p. 536, pl. 3, figs. 14, 15.

Diplocyclas sp.: Takemura, 1992, p. 746, pl. 13, fig. 16; Takemura and Ling, 1997, p. 113.

***Pterocodon campanella* Ehrenberg**
(Pl. **P13,** figs. 6a, 6b)

Pterocodon campanella Ehrenberg, 1873, p. 256; 1875, pl. 19, fig. 2.

Order SPUMELLARIA Ehrenberg, 1875, emend. De Wever et al., 2001
Family Actinommidae Haeckel, 1862, emend. De Wever et al., 2001

***Thecospharella ptomatus* Sanfilippo and Riedel**
(Pl. **P13,** figs. 10a, 10b)

Thecospharella ptomatus Sanfilippo and Riedel, 1973, p. 521, pl. 2, figs. 14–18; pl. 26, fig. 2; Riedel and Sanfilippo, 1973, p. 740; Kozlova, 1999, p. 70, pl. 8, figs. 4,5.

***Thecosphaera* sp. A**
(Pl. **P12,** figs. 11a, 11b)

?*Carposphaera* (*Melittosphaera*) *magnaporulosa* Clark and Campbell, 1942, p. 21, pl. 5, figs. 15, 17, 21, 23.

Remarks: Outer cortical shell is spherical to somewhat irregular. Pores are circular to subcircular and hexagonally arranged. Internal shell is spherical. This species is distinguished from *T. ptomatus* by its smaller cortical shell.

Family Saturnalidae Deflandre, 1953

***Axoprunum* sp. aff. *A. irregularis* Kozlova**
(Pl. **P12,** figs. 12a, 12b)

aff. *Axoprunum irregularis* Kozlova, 1983, p. 88, pl. 1, fig. 4; 1999, p. 69, pl. 2, fig. 7; pl. 5, fig. 1; pl. 38, fig. 14.

?*Axoprunum* (?) *irregularis* Kozlova: Takemura, 1992, p. 742, pl. 3, figs. 8–11; Takemura and Ling, 1997, p. 111, pl. 1, fig. 2.

Remarks: This species has a relatively smaller shell with longer polar spines than the Antarctic form reported by Takemura (1992) and Takemura and Ling (1997). Connecting bars between outer cortical shell and inner sphere are not concentrated in the equatorial horizon of shell.

***Axoprunum pierinae* (Clark and Campbell)**
(Pl. **P13,** figs. 15a, 15b)

Dorylonchidium (*Dorylonchella*) *monoxyphos monoxyphos* Clark and Campbell, 1942, p. 23, pl. 5, fig. 10.

Lithatractus (*Lithatractona*) *pierinae* Clark and Campbell, 1942, p. 34, pl. 5, fig. 25.

Axoprunum carduum (Ehrenberg): Petrushevskaya and Kozlova, 1972, p. 521, pl. 10, fig. 1.

Axoprunum liostylum (Ehrenberg) group: Petrushevskaya and Kozlova, 1972, p. 521, pl. 10, fig. 3; Petrushevskaya, 1975, p. 571, pl. 2, fig. 22.

Axoprunum pierinae (Clark and Campbell) group: Sanfilippo and Riedel, 1973, p. 488, pl. 1, figs. 6–12; pl. 23, fig. 3; Riedel and Sanfilippo, 1973, p. 737; Petrushevskaya, 1975, p. 571; Caulet, 1991, p. 537.

Axoprunum pierinae (Clark and Campbell): Dzinoridze et al., 1978, pl. 22, fig. 19; Nishimura, 1987, p. 720, pl. 1, fig. 9; Takemura, 1992, p. 742, pl. 6, figs. 3–6; Takemura and Ling, 1997, p. 111, pl. 1, fig. 1.

Axoprunum venustum (Borisenko): Kozlova, 1999, p. 70, pl. 33, fig. 10; pl. 38, fig. 2.

?*Stylosphaera carduum* Ehrenberg, 1873, p. 258; 1875, pl. 25, fig. 7.

Family Stylosphaeridae Haeckel, 1881

***Stylosphaera coronata laevis* Haeckel**
(Pl. **P13,** figs. 13a, 13b)

Stylosphaera laevis Ehrenberg. 1873, p. 259; 1875, pl. 25, fig. 6.

Druppatractus (*Druppatractaria*) *polycentrus* Clark and Campbell, 1942, p. 35, pl. 5, fig. 19.

Ellipsostylus (*Ellipsostyletta*) *anisoxyphos* Clark and Campbell, 1942, p. 32, pl. 5, figs. 7, 11.

Lithatractus (*Lithatractaria*) *hederae* Clark and Campbell, 1942, p. 33, pl. 5, fig. 3.

Druppatractus (*Druppatractaria*) *trichopterus* Clark and Campbell, 1942, p. 34, pl. 5, fig. 4.

Stylatractus coronatus (Ehrenberg): Petrushevskaya and Kozlova, 1972, p. 520, pl. 11, fig. 9.

Stylosphaera ?*laevis* Ehrenberg: Petrushevskaya and Kozlova, 1972, p. 520, pl. 11, fig. 8.

Axoprunum polycentrum (Clark and Campbell): Petrushevskaya and Kozlova, 1972, p. 521, pl. 10, figs. 11, 12.

Stylosphaera coronata laevis Ehrenberg: Sanfilippo and Riedel, 1973, p. 520, pl. 1, fig. 19; pl. 25, figs. 5, 6; Riedel and Sanfilippo, 1973, p. 740; Johnson, 1978, p. 782.

Druppatractus coronata laevis (Ehrenberg): Ling, 1975, p. 717, pl. 1, fig. 16.

?*Druppatratus* sp.: Ling, 1975, p. 717, pl. 1, fig. 19, pl. 2, fig. 1.

***Stylosphaera goruna* Sanfilippo and Riedel**
(Pl. **P13,** figs. 14a, 14b)

Stylosphaera goruna Sanfilippo and Riedel, 1973, p. 521, pl. 1, figs. 20–22; pl. 25, figs. 9, 10; Riedel and Sanfilippo, 1973, p. 740; Nishimura, 1987, p. 729, pl. 1, fig. 3.

?*Stylatractus spinulosus* (Ehrenberg) group: Petrushevskaya and Kozlova, 1972, p. 519, pl. 11, figs. 2–4.

Family Coccodiscidae Haeckel, 1862, Sanfilippo and Riedel, 1980
Subfamily Artiscinae Haeckel, 1881, emend. Riedel, 1967

***Didymocyrtis prismatica* (Haeckel)**
(Pl. **P14,** figs. 1a, 1b)

P14. *Didymocyrtis, Lithocyclia,* p. 71.

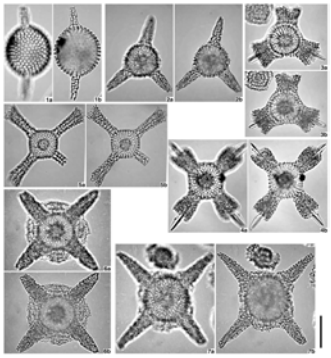

Pipettella prismaticus Haeckel, 1887, p. 305; Riedel, 1959, p. 289, pl. 1, fig. 2.

Pipettella tuba Haeckel, 1887, p. 337, pl. 39, fig. 7; Dreyer, 1889, pl. 10, fig. 72.

Cannartiscus canavarii Vinassa de Regny, 1900, p. 236, pl. 1, fig. 45; Lucchese, 1927, p. 94, pl. 5, fig. 13.

Cannartus prismaticus (Haeckel): Riedel and Sanfilippo, 1970, p. 520, pl. 15, fig. 1; 1971, p. 1588, pl. 2C, figs. 11–13; pl. 4, fig. 5; 1973, p. 738; Kling, 1971, p. 1086, pl. 3, fig. 2; Moore, 1971, p. 736, pl. 12, figs. 1, 2; Goll, 1972, p. 956, pl. 3, figs. 1–3; pl. 4, figs. 1, 2; Petrushevskaya and Kozlova, 1972, p. 521; Dinkelman, 1973, p. 765, pl. 5, fig. 5; Nigrini, 1974, p. 1064, pl. 2A, figs. 1, 2; Johnson, 1974, p. 545; 1976, p. 435; 1978, p. 781; Holdsworth, 1975, p. 519; Ling, 1975, p. 717, pl. 2, figs. 7, 8; Theyer et al., 1978, pl. 1, fig. 14.

Ommatartus prismaticus (Haeckel): Kellogg, 1980, fig. 1.1.

Didymocyrtis prismatica (Haeckel): Sanfilippo and Riedel, 1980, p. 1010; Renz, 1984, p. 459; Sanfilippo et al., 1985, p. 659, fig. 8.1; Nigrini, 1985, p. 520; Sanfilippo and Nigrini, 1995, p. 275; Nigrini and Sanfilippo, 2000, p. 72.

?*Doryphacus bergontianus* Carnevale, 1908, p. 22, pl. 3, fig. 14.

?*Cannartus prismaticus* (Haeckel): Petrushevskaya, 1975, p. 577, pl. 7, figs. 5–7.

?*Cannartus* sp. aff. *C. prismaticus* (Haeckel): Chen, 1975, p. 453, pl. 20, fig. 7.

Subfamily Coccodiscinae Haeckel, 1862

***Lithocyclia angusta* (Riedel)**
(Pl. **P14,** figs. 2a, 2b)

Trigonactura ?*angusta* Riedel, 1959, p. 292, pl. 1, fig. 6.

Lithocyclia angustum (Riedel): Riedel and Sanfilippo, 1970, p. 522, pl. 13, figs. 1, 2; 1971, p. 1588, pl. 3A, figs, 1, 3; 1978, p. 70, pl. 6, fig. 5; Moore, 1971, p. 737, pl. 6, figs. 5, 6; Goll, 1972, p. 957, pl. 11, fig. 1; Dinkelman, 1973, p. 768, pl. 5, figs. 7, 8; Nigrini, 1974, p. 1065, pl. 2A, figs. 4–6; 1985, p. 523; Johnson, 1974, p. 545, pl. 6, fig. 4; 1976, p. 435; 1978, p. 781; Sanfilippo and Riedel, 1974, p. 1022; Ling, 1975, p. 725, pl. 3, figs. 5, 6.

Lithocyclia angusta (Riedel): Sanfilippo and Riedel, 1973, p. 523; Riedel and Sanfilippo, 1973, p. 739; Holdsworth, 1975, p. 528; Renz, 1984, p. 459; Sanfilippo and Riedel in Saunders et al., 1985, p. 412; Sanfilippo et al., 1985, p. 653, figs. 7.3a–7.3c; Sanfilippo and Nigrini, 1995, p. 279, pl. 3, figs. 7–9; Nigrini and Sanfilippo, 2000, p. 73.

?*Lithocyclia angusta* (Riedel) Form A: Holdsworth, 1975, p. 528, pl. 1, figs. 7, 8.

***Lithocyclia aristotelis* (Ehrenberg) group**
(Pl. **P14,** figs. 3a–4b)

Astromma aristotelis Ehrenberg, 1847, p. 55, fig. 10; 1873, p. 217; 1875, pl. 30, figs. 3, 4.

Hymeniastrum pythagorae Ehrenberg, 1854, pl. 36, fig. 31; 1873, p. 237; 1875, pl. 30, fig. 5.

Astromma pythagorae Ehrenberg, 1873, p. 217; 1875, pl. 30, fig. 2.

Astractinium aristotelis (Ehrenberg) group: Petrushevskaya and Kozlova, 1972, p. 524, pl. 16, figs. 1–5.

Trigonactinium pythagorae (Ehrenberg): Petrushevskaya and Kozlova, 1972, p. 524, pl. 17, fig. 1.

Lithocyclia aristotelis (Ehrenberg): Riedel and Sanfilippo, 1970, p. 522, pl. 13, figs. 1, 2.

Lithocyclia aristotelis (Ehrenberg) group: Riedel and Sanfilippo, 1971, p. 1588, pl. 3A, figs. 4, 5; 1973, p. 739; 1978, p. 70, pl. 6, fig. 6; 1986, pl. 2, figs. 23, 24; Moore, 1971, p. 737, pl. 4, figs. 4, 5; Sanfilippo and Riedel, 1973, p. 523; 1974, p. 1022; Dinkelman, 1973, p. 768; Johnson, 1974, p. 545, pl. 5, figs. 13, 14; 1976, p. 435; 1978, p. 781; Nigrini, 1974, p. 1065, pl. 2A, fig. 7; Holdsworth, 1975, p. 528; Ling, 1975, p. 725, pl. 3, figs. 7, 8; Renz, 1984, p. 459; Sanfilippo and Riedel in Saunders et al., 1985, p. 412; Sanfilippo et al., 1985, p. 653, figs. 7.2a–7.2c (partim); Nigrini and Sanfilippo, 2000, p. 73.

***Lithocyclia aristotelis* (Ehrenberg) group form A**
(Pl. **P14,** figs. 5a, 5b)

Astractinium sp. A: Petrushevskaya and Kozlova, 1972, pl. 16, fig. 6.

Astractinium spp. aff. *Lithocyclia crux* Moore: Petrushevskaya and Kozlova, 1972, p. 524, pl. 16, fig. 8 (partim).

Lithocyclia aristotelis (Ehrenberg) group: Sanfilippo et al., 1985, p. 653, fig. 7.2d (partim).

Remarks: Phacoid cortical shell, rounded quadrangular in section, without patagium and spongy meshwork, with four arms. Proximal part of arms with pores aligned along rough longitudinal ridges. This form is distinguished from *L. aristotelis* group by the porous arms in its proximal part.

***Lithocyclia crux* Moore**
(Pl. **P14,** figs. 6a–7b)

Lithocyclia crux Moore, 1971, p. 737, pl. 6, fig. 4; Sanfilippo and Riedel, 1973, p. 523; Riedel and Sanfilippo, 1973, p. 739; 1978, p. 70, pl. 6, fig. 7; Dinkelman, 1973, p. 768, pl. 5, fig. 9; Johnson, 1974, p. 545, pl. 6, fig. 5; 1976, p. 435; 1978, p. 781; Holdsworth, 1975, p. 528; Ling, 1975, p. 725, pl. 3, fig. 9; Weaver, 1983, p. 678; Renz, 1984, p. 459; Sanfilippo and Riedel in Saunders et al., 1985, p. 412; Nigrini, 1985, p. 523; Sanfilippo et al., 1985, p. 655, figs. 7.4a, 7.4b; Sanfilippo and Nigrini, 1995, p. 279.

Lithocyclia sp. cf. *L. angustum* (Riedel): Riedel and Sanfilippo, 1971, pl. 3A, fig. 2.

Astractinium sp. C: Petrushevskaya and Kozlova, 1972, p. 524, pl. 16, fig. 10.

***Lithocyclia ocellus* Ehrenberg group**
(Pl. **P15,** figs. 1a, 1b)

P15. *Lithocyclia, Periphaena,* p. 72.

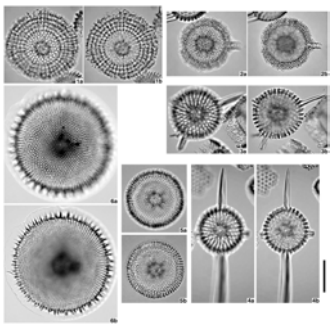

Lithocyclia ocellus Ehrenberg, 1854, pl. 36, fig. 30; 1873, p. 240; 1875, pl. 29, fig. 3; Petrushevskaya and Kozlova, 1972, p. 523, pl. 15, figs. 1, 2.

Lithocyclia ocellus Ehrenberg group: Riedel and Sanfilippo, 1971, p. 1588, pl. 3A, fig. 6; 1973, p. 739, pl. 2, figs. 7, 8; 1978, p. 70, pl. 6, fig. 8; 1986, pl. 3, figs. 4, 5; Moore, 1971, p. 737, pl. 4, fig. 1; Sanfilippo and Riedel, 1973, p. 523, pl. 10, figs. 1, 2; 1974, p. 1022; Dinkelman, 1973, p. 768; Nigrini, 1974, p. 1065, pl. 1D, figs. 3–6; Johnson, 1974, p. 545; 1978, p. 781; Holdsworth, 1975, p. 528; Ling, 1975, p. 725, pl. 3, fig. 10; Sanfilippo and Riedel in Saunders et al., 1985, p. 412; Sanfilippo et al., 1985, p. 655, figs. 7.1a, 7.1b; Nigrini and Sanfilippo, 2000, p. 73, pl. 2, figs. 14–17.

***Lithocyclia* sp. aff. *L. stella* Ehrenberg**
(Pl. **P15,** figs. 2a, 2b)

aff. *Lithocyclia stella* Ehrenberg, 1873, p. 240; 1875, pl. 29, fig. 2.
Remarks: This species is distinguished from *L. stella* by the spongy meshwork surrounding phacoid cortical shell and from *L. ocellus* by the absence of patagium in spongy part surrounding phacoid shell.

***Periphaena decora* Ehrenberg**
(Pl. **P15,** figs. 5a–6b)

Periphaena decora Ehrenberg, 1873, p. 246; 1875, pl. 6, fig. 2; Riedel, 1957a, p. 258, pl. 62, fig. 1; Petrushevskaya and Kozlova, 1972, p. 523, pl. 14, figs. 1, 2; Sanfilippo and Riedel, 1973, p. 523, pl. 8, figs. 8–10; pl. 27, figs. 2–4 (partim);

Riedel and Sanfilippo, 1973, p. 739; Nigrini, 1974, p. 1065, pl. 1C, figs. 1, 2, 4, 6 (partim); Ling, 1975, p. 725, pl. 3, figs. 1, 2; Weaver, 1983, p. 678; Caulet, 1991, p. 538; Takemura, 1992, p. 743, pl. 6, fig. 8; Takemura and Ling, 1997, p. 114.

Periphaena cincta Haeckel, 1887, p. 426, pl. 33, fig. 4.

Perizona scutella Haeckel, 1887, p. 427, pl. 32, fig. 7.

Heliodiscus cingillum Haeckel, 1887, p. 448, pl. 33, fig. 7.

***Periphaena triactis* (Ehrenberg)**
(Pl. **P15,** figs. 3a–4b)

Haliomma triactis Ehrenberg, 1873, p. 236; 1875, pl. 28, fig. 4.

Sethostylus sp. aff. *Phacostylus amphistylus* Haeckel: Petrushevskaya and Kozlova, 1972, p. 522, pl. 13, fig. 1.

?*Triactis triactis* (Ehrenberg): Petrushevskaya and Kozlova, 1972, p. 523, pl. 13, fig. 2; Kozlova, 1999, pl. 28, fig. 8; pl. 29, fig. 5; Popova et al., 2002, p. 50, fig. 8A.

?*Triactis tripyramis* Haeckel, 1887, p. 432, pl. 33, fig. 6.

?*Triactis tripyramis tripyramis* Haeckel: Riedel and Sanfilippo, 1970, p. 521, pl. 4, fig. 8; Moore, 1971, p. 737, pl. 1, fig. 8; Dinkelman, 1973, p. 767; Ling, 1975, p. 725, pl. 3, fig. 4.

***Rhopalastrum* sp. A**
(Pl. **P16,** figs. 1a–2b)

Euchitonia furcata Ehrenberg: Ling, 1975, p. 725, pl. 4, fig. 3.

?*Histiastrum ternarium* Ehrenberg, 1873, p. 237; 1875, pl. 24, fig. 2.

?*Rhopalastrum profunda* (Ehrenberg) group: Petrushevskaya and Kozlova, 1972, p. 529, pl. 20, fig. 8 (partim).

Remarks: This species is distinguished from *L. aristotelis* group by the smaller phacoid cortical shell and from *L. aristotelis* form A group by three spongy arms.

***Rhopalastrum* sp. B**
(Pl. **P16,** figs. 3a, 3b)

Astractinium sp. B: Petrushevskaya and Kozlova, 1972, pl. 16, fig. 7.

Astractinium spp. aff. *Lithocyclia crux* Moore: Petrushevskaya and Kozlova, 1972, p. 524, pl. 16, fig. 9 (partim).

Lithocyclia aff. *crux* Moore: Nigrini, 1974, p. 1065, pl. 2A, fig. 8.

Remarks: This species is mostly similar to *Rhopalastrum* sp. A and is distinguished from it by four spongy arms. This species is distinguished from *L. aristotelis* group and *L. crux* by the smaller phacoid cortical shell.

***Rhopalastrum* (?) sp. C**
(Pl. **P16,** figs. 4, 5)

Remarks: Phacoid cortical shell is subcircular to irregular in horizontal cross section and is approximately twice as broad as medullary shell. Medullary shell is subcircular to irregular in cross section. Rounded quadrangular spongy mesh-

P16. *Rhopalastrum*, p. 73.

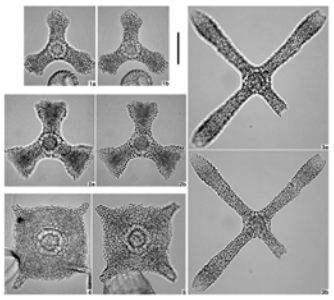

work surrounds cortical shell, with four spongy tubules extending from the corners. Patagium may be present or absent at the most inner part of the spongy meshwork.

This species is distinguished from *Lithocyclia* sp. aff. *L. stella* by the quadrangular-shaped spongy meshwork surrounding a smaller phacoid cortical shell. The small phacoid shell is same as those of *Rhopalastrum* sp. A and *Rhopalastrum* sp. B; this species is distinguished from them by the spongy meshwork surrounding the phacoid shell.

Family Collosphaeridae Müller 1858

Collosphaera sp. A

(Pl. P17, figs. 1a–2b)

Polysolenia sp.: Sanfilippo and Riedel, 1973, p. 485, pl. 22, fig. 1.

Remarks: Shell is spherical to somewhat irregular spherical with subcircular pores.

Collosphaera sp. B

(Pl. P17, figs. 3a–4)

Remarks: Shell is spherical to irregular spherical with polygonal pores. This species is distinguished from *Collosphaera* sp. A by the smaller polygonal pores and narrower pore bars.

Family Entapiidae Dumitrica, 2001

Zealithapium mitra (Ehrenberg) group

(Pl. P17, figs. 5a, 5b)

Cornutella mitra Ehrenberg, 1873, p. 221; 1875, pl. 2, fig. 8.

Lithapium mitra (Ehrenberg): Riedel and Sanfilippo, 1970, p. 520, pl. 4, figs. 6, 7; 1973, p. 516; 1978, p. 69, pl. 6, figs. 1, 2; Moore, 1971, p. 736, pl. 3, fig. 1; Sanfilippo and Riedel, 1974, p. 1022; Weaver, 1983, p. 678; Sanfilippo and Riedel in Saunders et al., 1985, p. 412.

Lithapium ?*mitra* (?): Petrushevskaya and Kozlova, 1972, pl. 34, fig. 3; Dinkelman, 1973, p. 764.

Lithapium cf. *mitra* (Ehrenberg): Takemura, 1992, p. 742, pl. 7, fig. 2.

Zealithapium mitra (Ehrenberg): O'Connor, 1999, p. 5.

Zealithapium anoectum (Ehrenberg) group

(Pl. P17, figs. 6a, 6b)

Lithapium (?) *anoectum* Riedel and Sanfilippo, 1970, p. 520, pl. 4, figs. 4, 5.

Lithapium anoectum Sanfilippo and Riedel, 1973, p. 516, pl. 24, figs. 6, 7; 1974, p. 1022; Riedel and Sanfilippo, 1973, p. 739; Nigrini, 1974, p. 1064, pl. 1A, figs. 1, 2; Holdsworth, 1975, p. 521; Takemura, 1992, p. 742, pl. 7, fig. 1; Kozlova, 1999, p. 125, pl. 32, fig. 19.

Zealithapium anoectum (Ehrenberg): O'Connor, 1999, p. 5.

Remarks: Because of the common occurrence of broken specimens missing the distal part of the shell, *Zealithapium mitra* (Pl. P17, figs. 5a, 5b) and *Zealithapium anoectum* (Pl. P17, figs. 6a, 6b) are counted together with the *Z. mitra* group.

P17. *Collosphaera, Zealithapium, Lithelius, Rhopalodictyum,* p. 74.

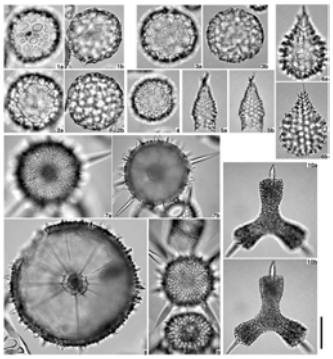

Family Litheliidae Haeckel, 1862

Lithelius hexaxyphophorus (Clark and Campbell)

(Pl. P17, figs. 7a–9)

Lithelius hexaxyphophorus (Clark and Campbell): Sanfilippo and Riedel, 1973, p. 522, pl. 7, figs. 7–9; pl. 26, figs. 6, 7; Riedel and Sanfilippo, 1973, p. 739, pl. 3, fig. 6.

Remarks: Cortical shell, spherical and large. Numerous spines extend from cortical shell rodlike or bladed proximally, variable in length and breadth. Pores in cortical are shell small, circular to subcircular, and randomly distributed with high pore bars. Internal shell is roughly spiral and connected to cortical shell by numerous radial beams.

Family Spongodiscidae Haeckel, 1862

Rhopalodictyum californicum Clark and Campbell

(Pl. P17, figs. 10a, 10b)

Rhopalodictyum (*Rhopalodictya*) *californicum* Clark and Campbell, 1942, p. 49, pl. 1, fig. 13.

APPENDIX B

Radiolarian species and species group stratigraphy, Hole 1218A. (This table is available in an **oversized format.**)

APPENDIX C

Radiolarian species and species group stratigraphy, Hole 1219A. (This table is available in an **oversized format.**)

APPENDIX D

Radiolarian species and species group stratigraphy, Hole 1220A. (This table is available in an **oversized format.**)

Figure F1. Map of the Central Pacific showing examined Leg 199 sites and DSDP sites (after Shipboard Scientific Party, 2002a).

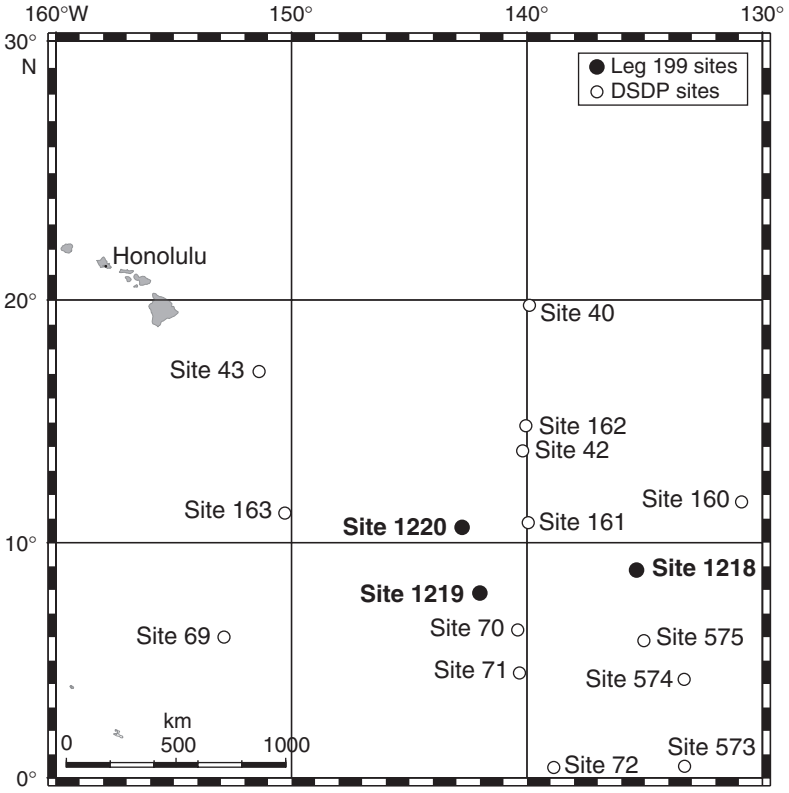

Figure F2. Stratigraphic distribution of selected radiolarian species and species groups in Hole 1218A. Event numbers shown in Table T1, p. 57.

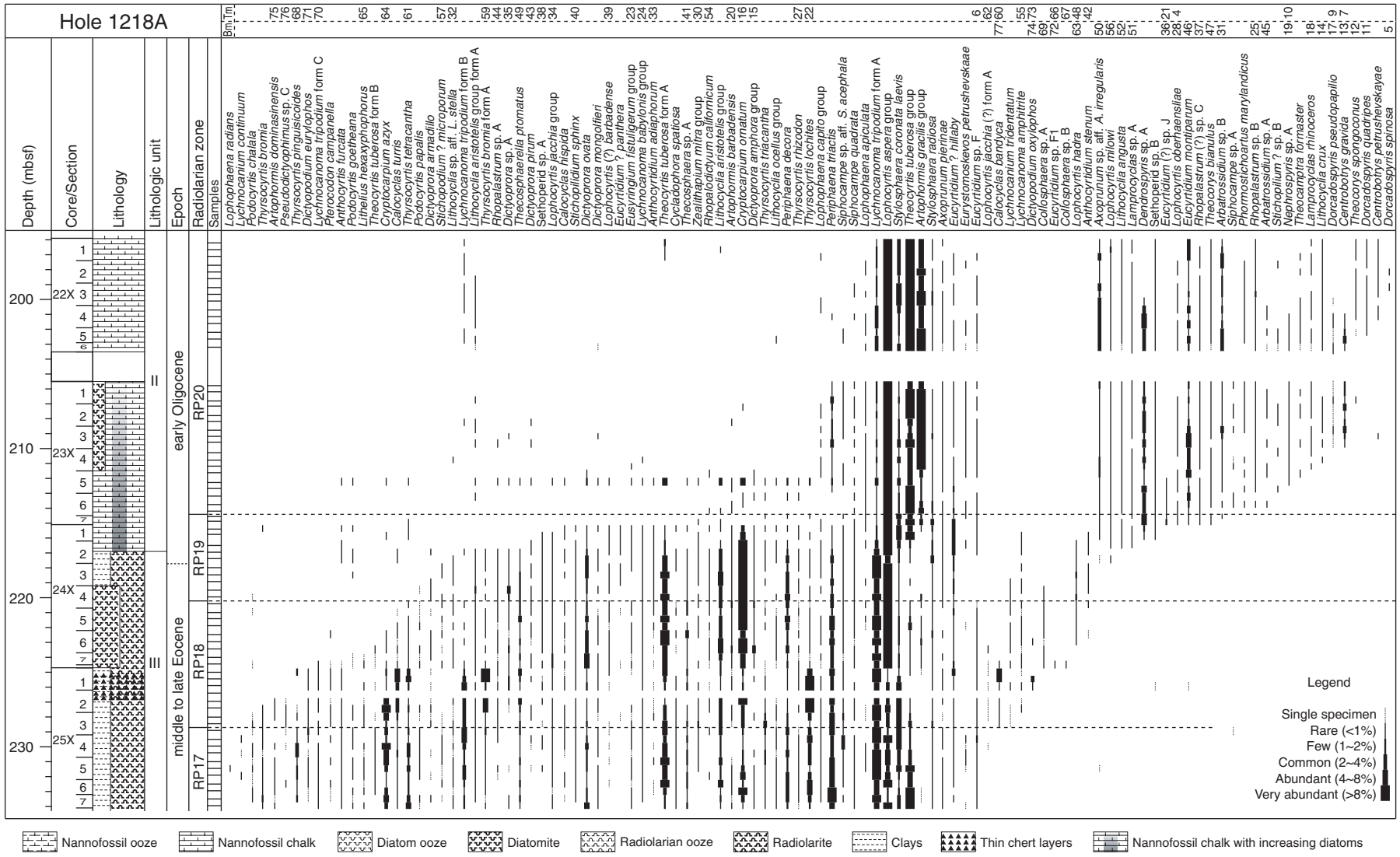

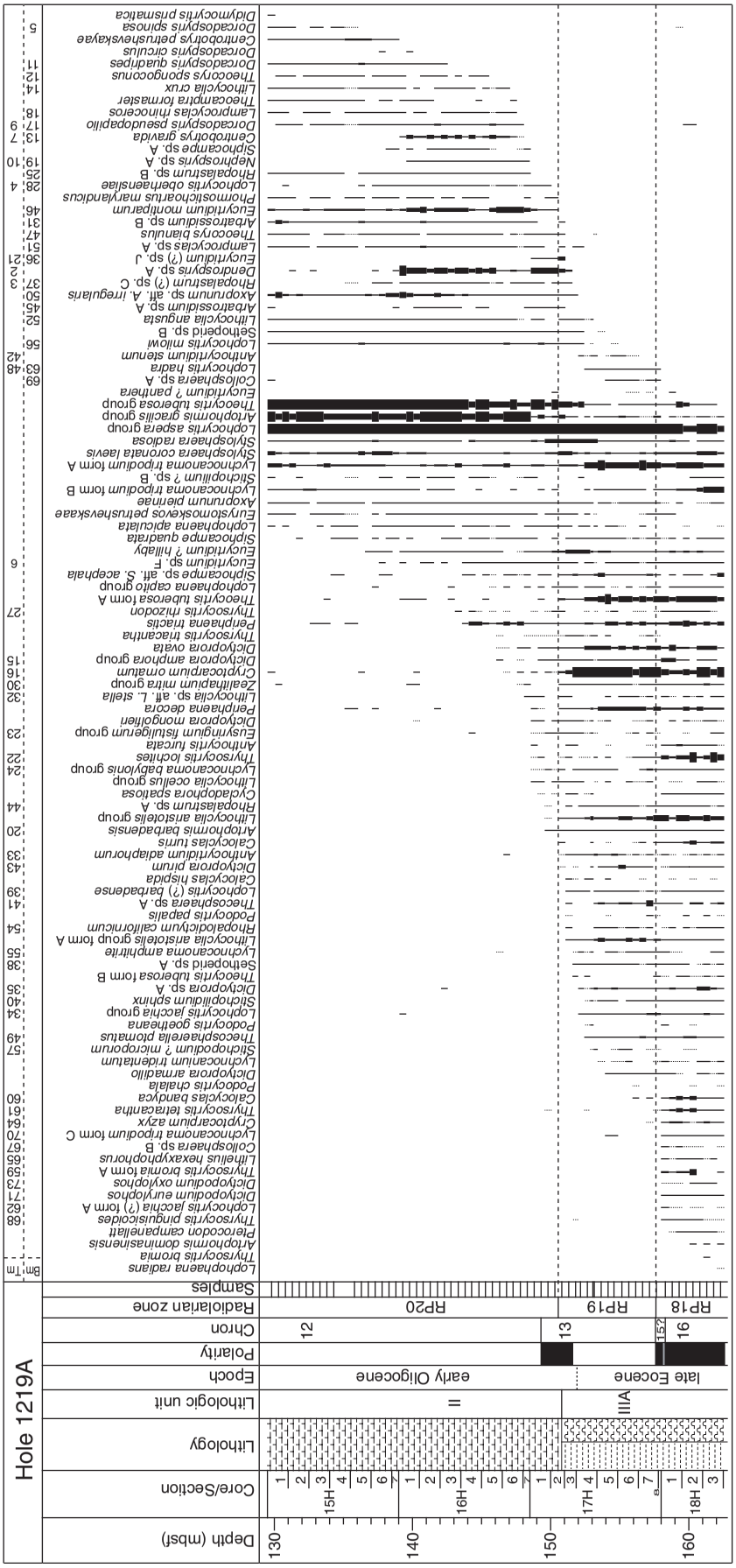

Figure F3. Stratigraphic distribution of selected radiolarian species and species groups in Hole 1219A. Event numbers shown in Table T1, p. 57.

Figure F4. Stratigraphic distribution of selected radiolarian species and species groups in Hole 1220A. Event numbers shown in Table T1, p. 57.

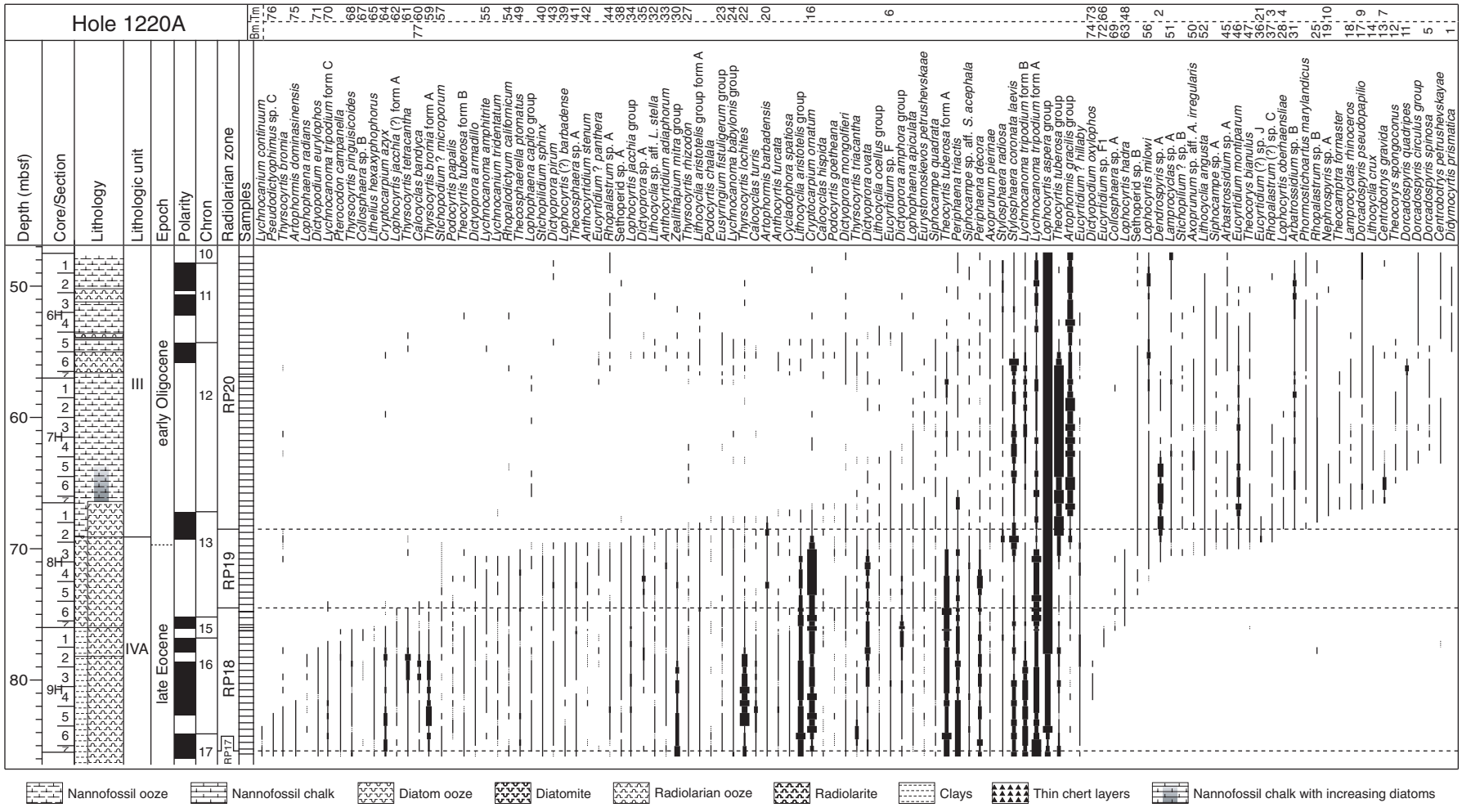

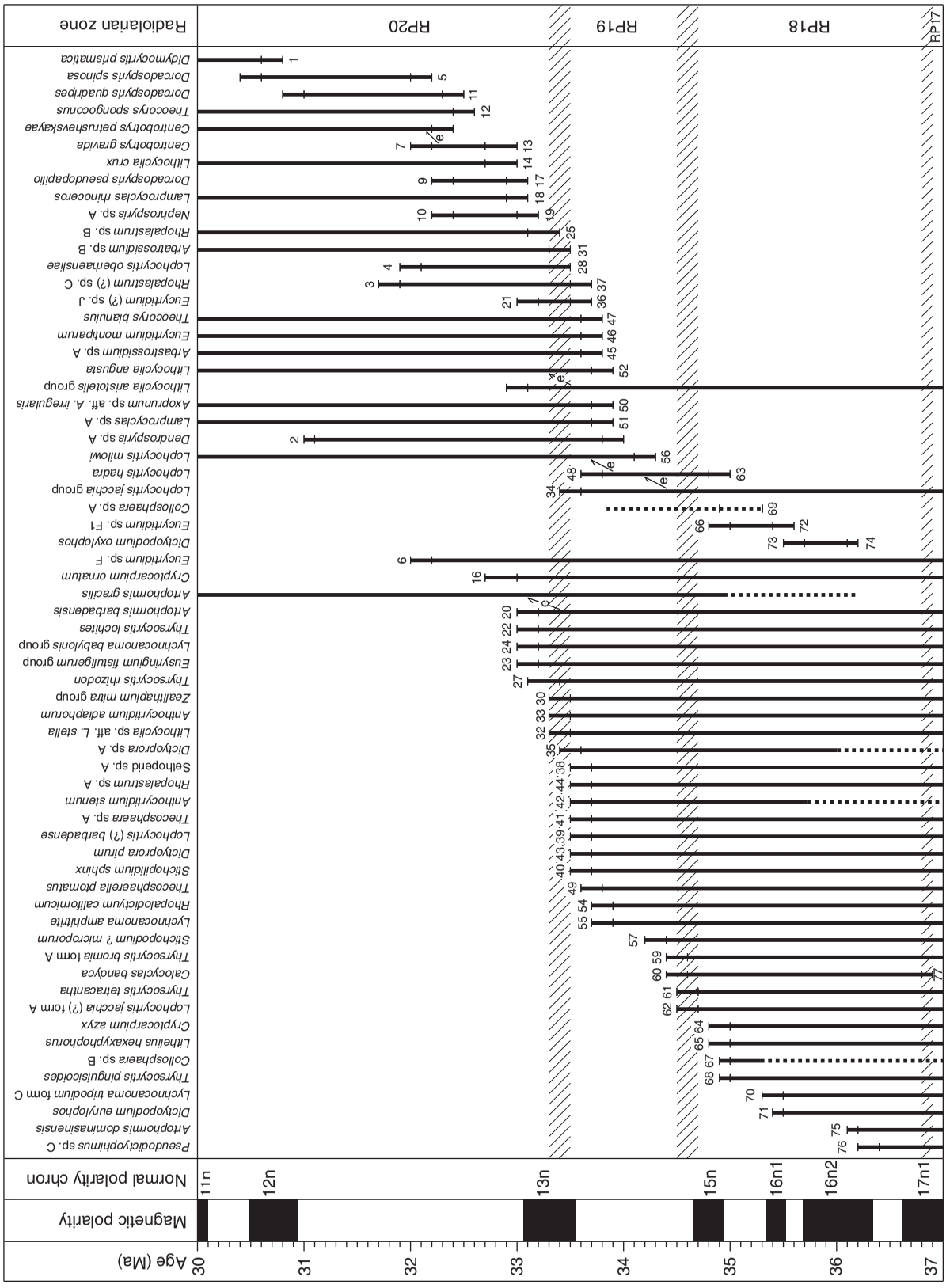

Figure F5. Radiolarian zones and ranges of stratigraphic valuable species and species groups in Hole 1220A. Top and bottom lines mark the lower and upper limits of the location of datum levels, respectively. Event numbers shown in Table T1, p. 57.

Figure F6. Stratigraphic distribution of radiolarian events in Hole 1218A. Event numbers shown in Table T1, p. 57. Tm = top morphotypic appearance, Bm = bottom morphotypic appearance.

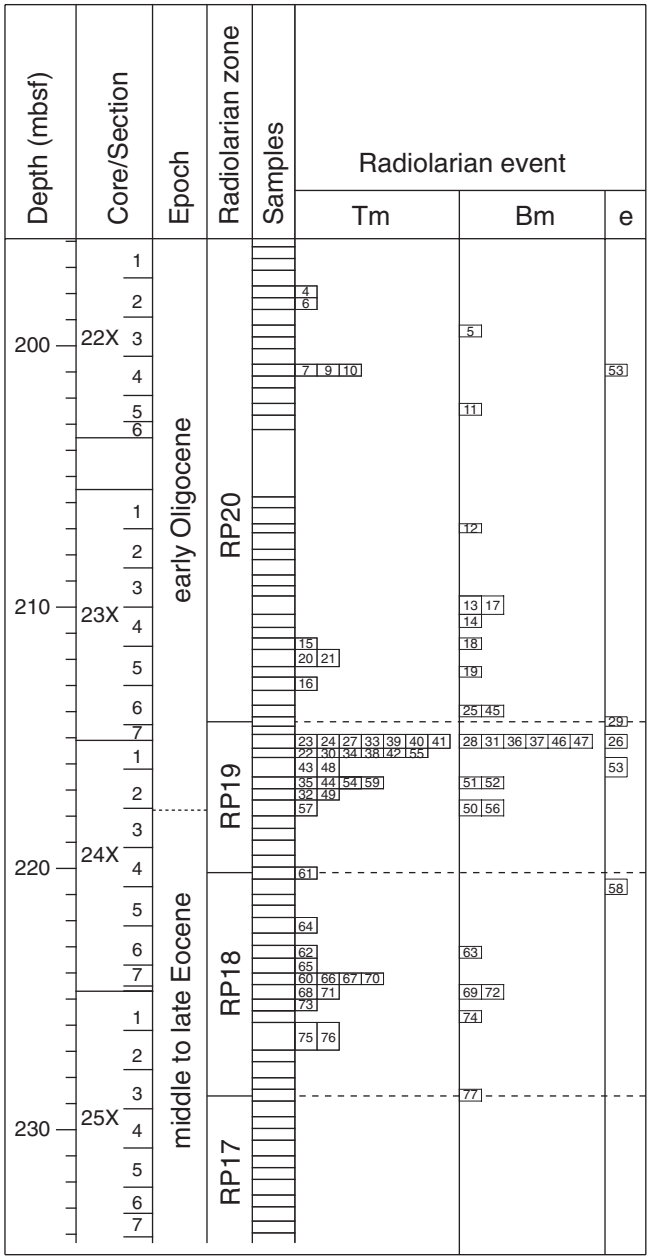

Figure F7. Stratigraphic distribution of radiolarian events in Hole 1219A. Event numbers shown in Table T1, p. 57. Tm = top morphotypic appearance, Bm = bottom morphotypic appearance.

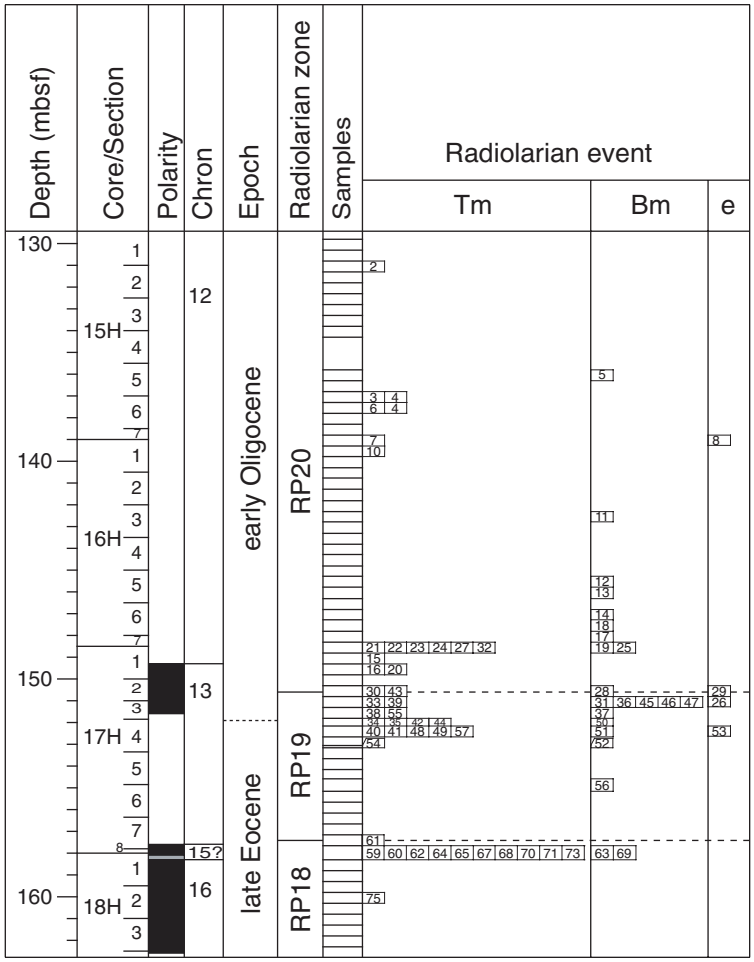

Figure F8. Stratigraphic distribution of radiolarian events in Hole 1220A. Event numbers shown in Table T1, p. 57. Tm = top morphotypic appearance, Bm = bottom morphotypic appearance.

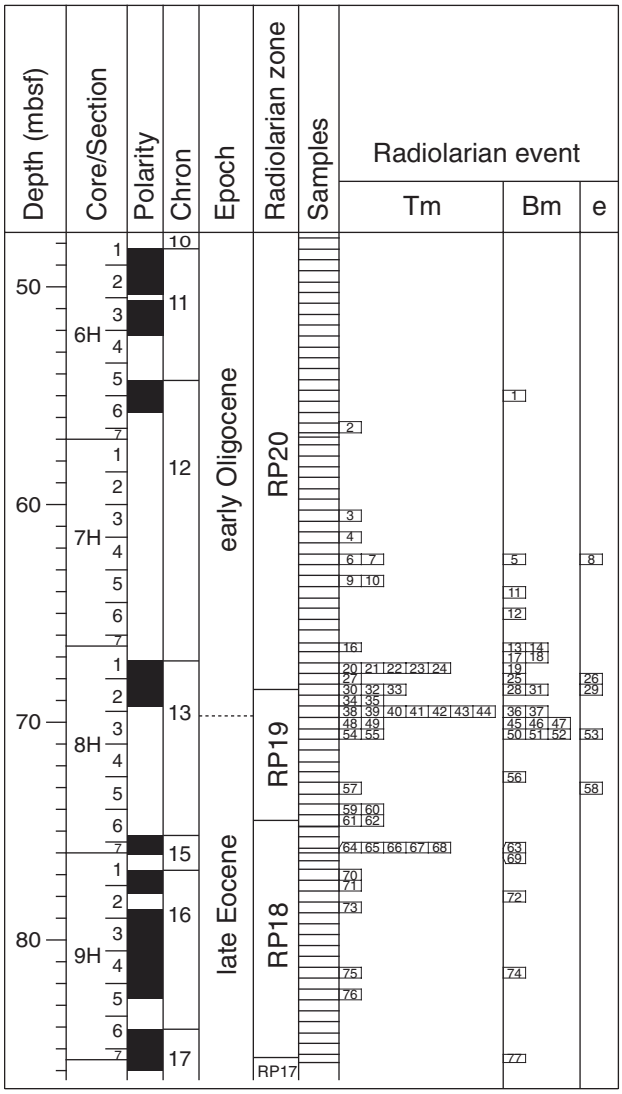

Table T1. Late middle Eocene–early Oligocene radiolarian events, Holes 1218A, 1219A, and 1220A. (This table is available in an **oversized format.**)

Plate P1. Transmitted light microphotographs of radiolarians from Holes 1218A, 1219A, and 1220A. Scale bar = 100 µm for all figures except for figures 4, 5, 6, 8, and 9 scale bar = 200 µm. **1–3.** *Dendrospyris* sp. A. (Sample 199-1220A-7H-7, 35–37 cm); (1) B27/1, (2) D14/2, (3) S29/0, basal view showing fine primary lateral spines. One of them does not reach at shell wall. **4, 5.** *Dorcadospyris circulus* (Sample 199-1220A-6H-3, 125–127 cm); (4) E18/4, (5) C26/0, without apical horn. **6.** *Dorcadospyris quadripes* (Sample 199-1220A-7H-2, 77–79 cm), K50/4. **7.** *Dorcadospyris spinosa* (Sample 199-1220A-7H-3, 125–127 cm), K23/1. **8, 9.** *Dorcadospyris pseudopapilio* (Sample 199-1220A-7H-7, 35–37 cm); (8) B24/0, (9) D36/1. **10.** *Nephrospyris* sp. A (Sample 199-1220A-7H-7, 35–37 cm), H14/2.

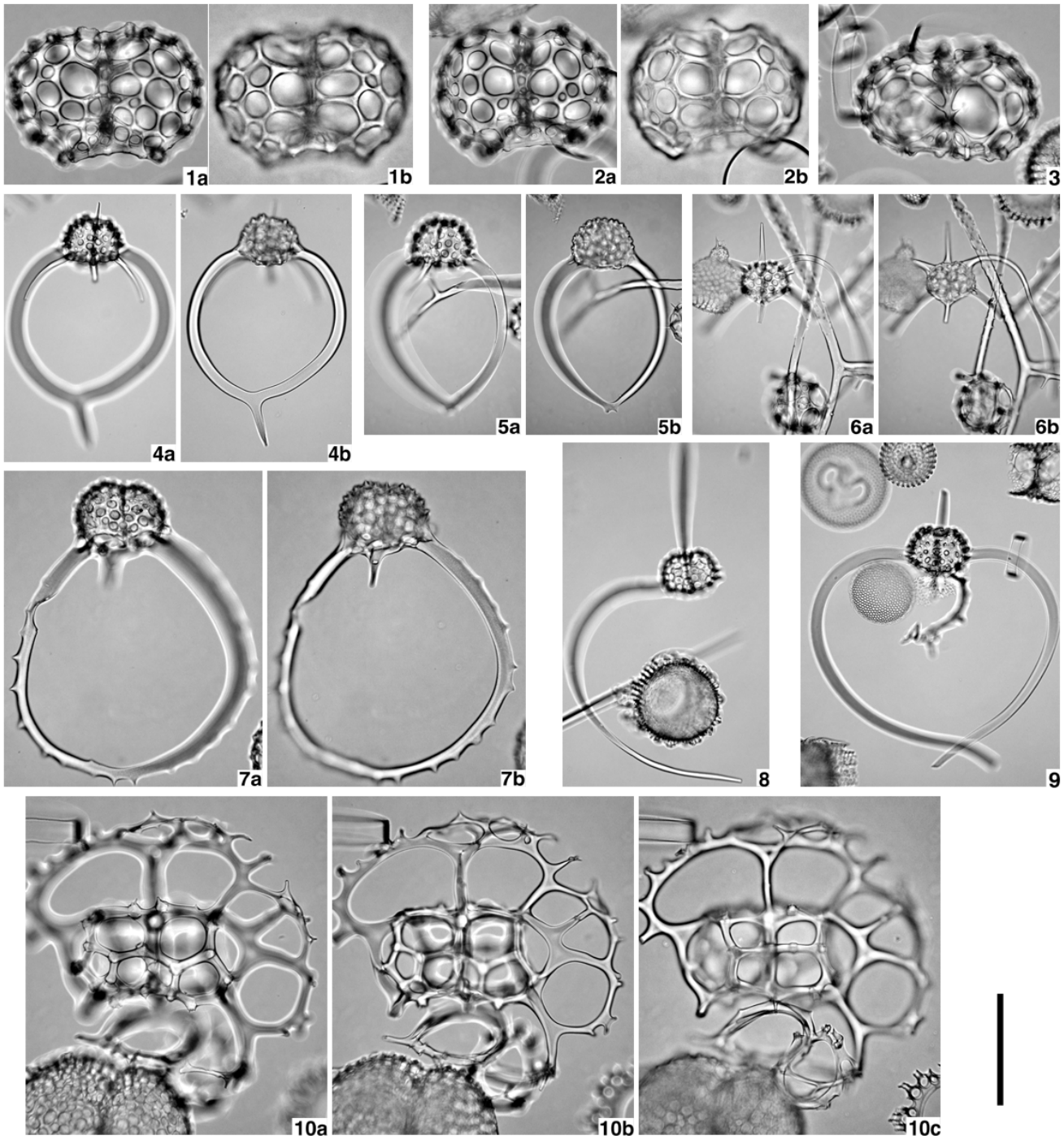

Plate P2. Transmitted light microphotographs of radiolarians from Holes 1218A, 1219A, and 1220A. Scale bar = 100 µm. **1, 2.** *Dictyoprora amphora* group; (1) Sample 199-1220A-8H-7, 50–52 cm (F36/0), (2) Sample 199-1220A-9H-3, 125–127 cm (N41/0). **3, 4.** *Dictyoprora armadillo;* (3) Sample 199-1220A-9H-6, 25–27 cm (K37/3), (4) Sample 199-1218A-25X-7, 75–77 cm (O49/2). **5, 6.** *Dictyoprora mongolfieri;* (5) Sample 199-1220A-9H-7, 63–65 cm (G27/2). (6) Sample 199-1220A-8H-5, 125–127 cm (O32/0). **7.** *Dictyoprora ovata* (Sample 199-1220A-9H-7, 63–65 cm), L25/3. **8, 9.** *Dictyoprora pirum;* (8) Sample 199-1219A-17H-6, 130–132 cm (K35/0), (9) Sample 199-1220A-9H-7, 63–65 cm (S40/3). **10.** *Dictyoprora* sp. A (Sample 199-1220A-8H-4, 127–129 cm), N20/3. **11, 12.** *Phormostichoartus marylandicus* (Sample 199-1220A-6H-1, 77–79 cm); (11) L33/3, (12) L50/1. **13.** *Siphocampe* sp. aff. *S. acephala* (Sample 199-1220A-9H-7, 63–65 cm), B29/0. **14, 15.** *Siphocampe quadrata* (Sample 199-1218A-25X-7, 75–77 cm); (14) J43/3, (15) B46/2. **16, 17.** *Siphocampe* sp. A; (16) Sample 199-1220A-7H-6, 125–127 cm (K28/0), (17) Sample 199-1220A-6H-4, 25–27 cm (X17/3). **18.** *Theocamptra formaster* (Sample 199-1220A-7H-7, 35–37 cm), V14/4. **19.** *Centrobotrys gravida* (Sample 199-1220A-7H-7, 35–37 cm), A14/4. **20.** *Centrobotrys petrushevskayae* (Sample 199-1220A-6H-1, 77–79 cm), B21/1.

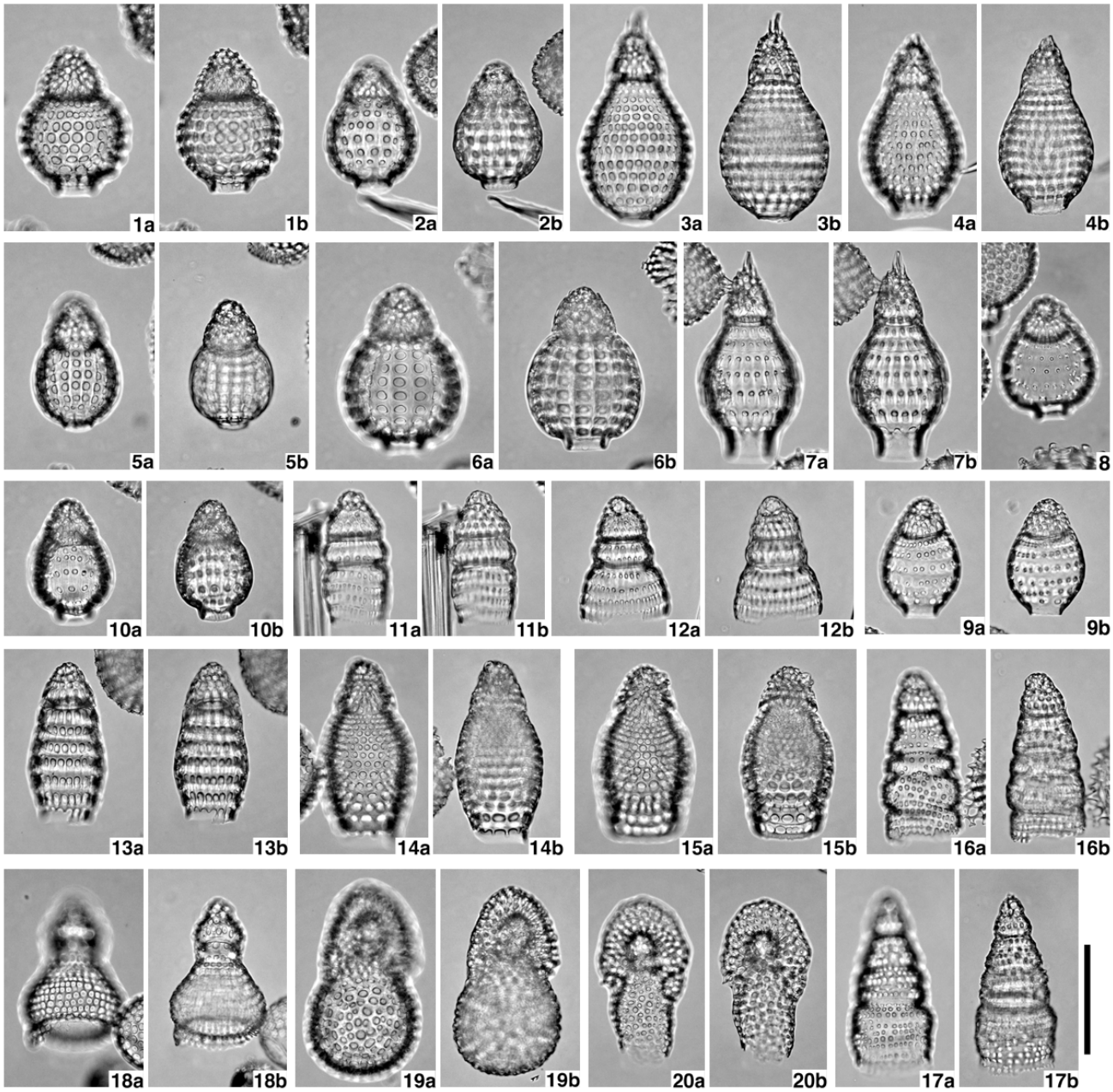

Plate P3. Transmitted light microphotographs of radiolarians from Holes 1218A, 1219A, and 1220A. Scale bar = 100 µm. **1, 2.** *Lophophaena apiculata;* (1) Sample 199-1220A-9H-7, 63–65 cm, (L40/0), (2) Sample 199-1220A-6H-3, 125–127 cm (B53/1). **3, 4.** *Lophophaena capito* group; (3) Sample 199-1220A-9H-7, 63–65 cm (O51/3), (4) Sample 199-1220A-9H-3, 125–127 cm (R40/1). **5, 6.** *Lophophaena radians;* (5) Sample 199-1220A-9H-3, 125–127 cm (J39/0), (6) Sample 199-1220A-9H-2, 75–77 cm (U34/4). **7–9.** *Pseudodictyophimus* sp. C; (7) Sample 199-1218A-25X-4, 30–32 cm (K40/0), (8a–9b) Sample 199-1220A-9H-5, 75–77 cm (K51/0). **10–12.** Sethoperid sp. A (Sample 199-1220A-9H-3, 125–127 cm; (10) N28/2, (11) F52/0, (12) B20/0. **13–15.** Sethoperid sp. B; (13) Sample 199-1220A-7H-3, 125–127 cm (L23/3), (14) Sample 199-1218A-25X-1, 120–122 cm (P27/0), (15) Sample 199-1220A-6H-3, 125–127 cm (A49/4).

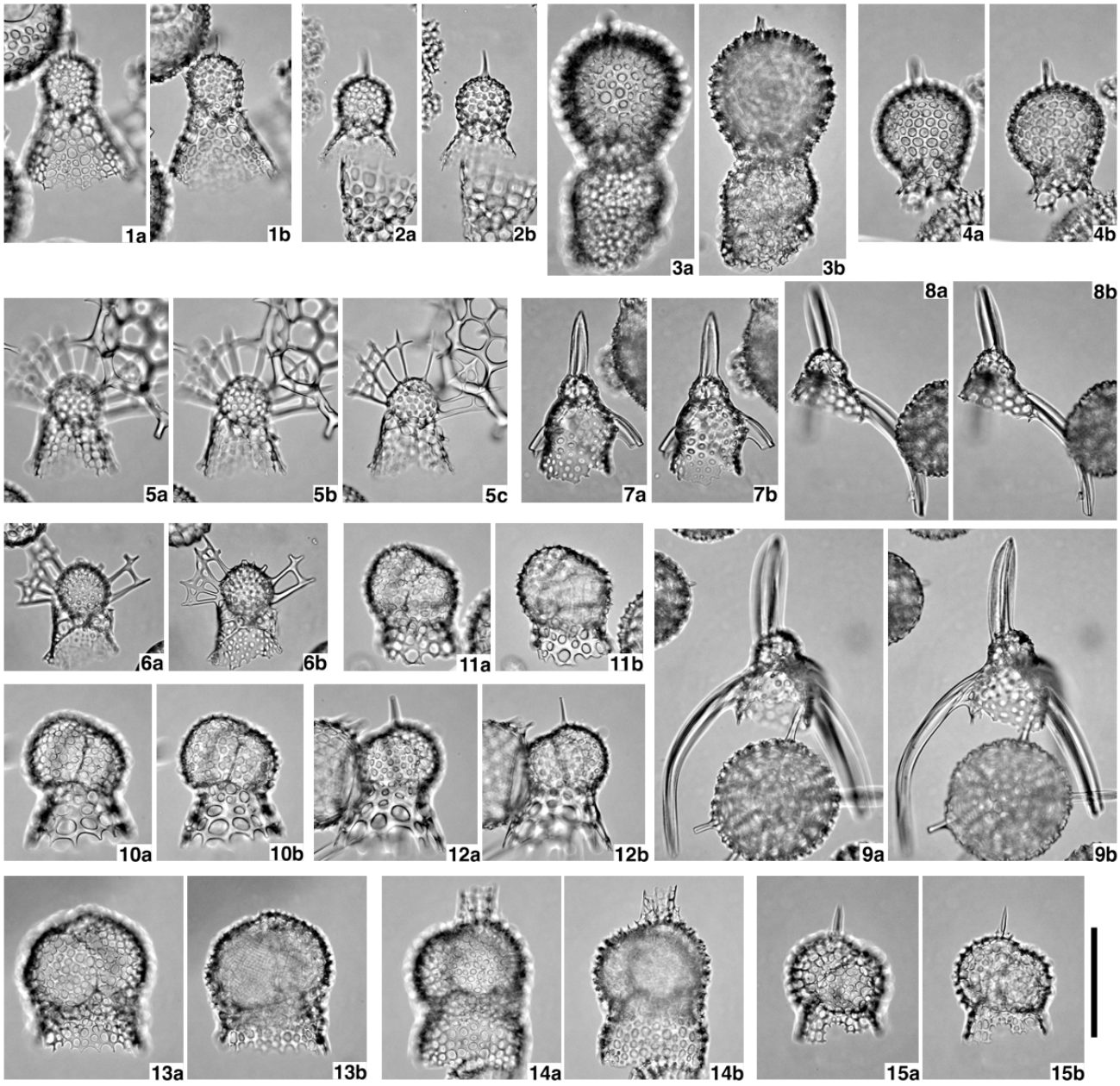

Plate P4. Transmitted light microphotographs of radiolarians from Holes 1218A, 1219A, and 1220A. Scale bar = 100 µm. **1.** *Artophormis barbadensis* (Sample 199-1218A-24X-1, 65–67 cm), W28/0. **2–6.** *Artophormis gracilis* group; (2) Sample 199-1220A-8H-1, 25–27 cm (F32/0), (3) Sample 199-1220A-7H-4, 125–127 cm (D23/2), (4) Sample 199-1218A-24X-7, 67–69 cm (R36/4), (5) Sample 199-1220A-6H-2, 125–127 cm (K44/4), (6) Sample 199-1220A-7H-3, 80–82 cm (Q26/4). **7–12.** *Thyrsocyrtis* (*Thyrsocyrtis*) *pinguisicoides* O'Connor; (7) earlier form (Sample 199-1218A-25X-6, 30–32 cm), O23/1, (8) earlier form (Sample 199-1218A-25X-5, 120–122 cm), D35/0, (9) Sample 199-1220A-9H-1, 75–77 cm), O49/1, (10) Sample 199-1220A-9H-3, 75–77 cm (X48/1), (11) Sample 199-1220A-25X-4, 30–32 cm (U15/0), (12) Sample 199-1220A-9H-2, 25–27 cm (V19/0).

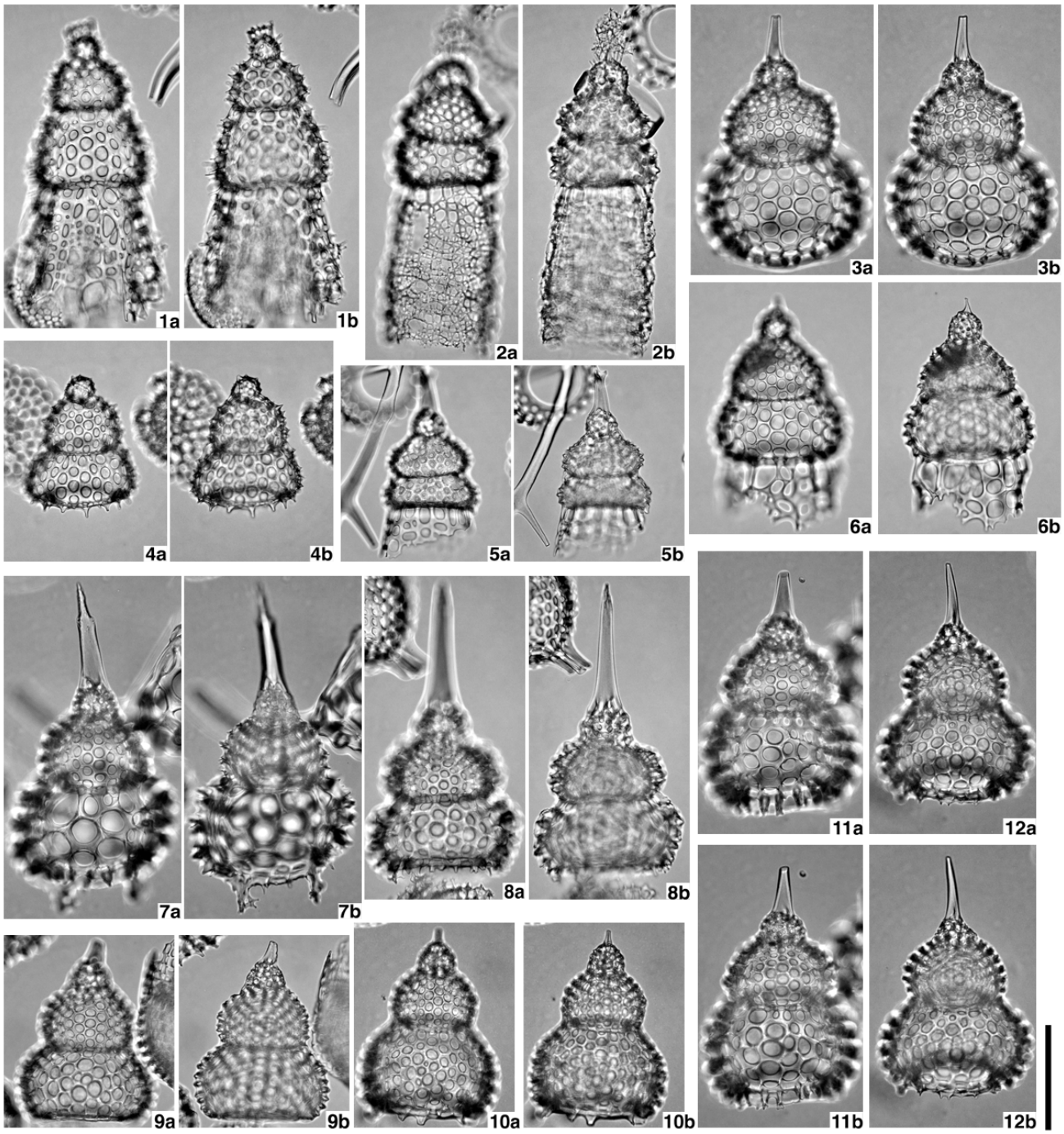

Plate P5. Transmitted light microphotographs of radiolarians from Holes 1218A, 1219A, and 1220A. Scale bar = 100 µm. **1–3**: *Calocyclas bandyca;* (1) Sample 199-1218A-25X-1, 120–122 cm (J46/4), (2) Sample 199-1220A-9H-7, 25–27 cm (X44/3), (3) Sample 199-1220A-9H-2, 125–127 cm (O46/1). **4.** *Calocyclas hispida* (Sample 199-1218A-25X-5, 120–122 cm), K24/0. **5.** *Calocyclas turris* (Sample 199-1218A-25X-5, 120–122 cm), F34/3. **6–8.** *Eucyrtidium ?hillaby;* (6) Sample 199-1218A-25X-5, 120–122 cm (X49/4), (7) Sample 199-1218A-25X-5, 120–122 cm (H52/0), (8) Sample 199-1220A-9H-2, 25–27 cm (U40/0). **9.** *Eucyrtidium ?panthera* (Sample 199-1220A-8H-4, 27–29 cm), K16/4. **10.** *Eucyrtidium montiparum* (Sample 199-1218A-22X-5, 30–32 cm) F38/0. **11, 12.** *Eucyrtidium* sp. F1 (Sample 199-1220A-9H-1, 25–27 cm); (11) E33/0, (12) G16/0.

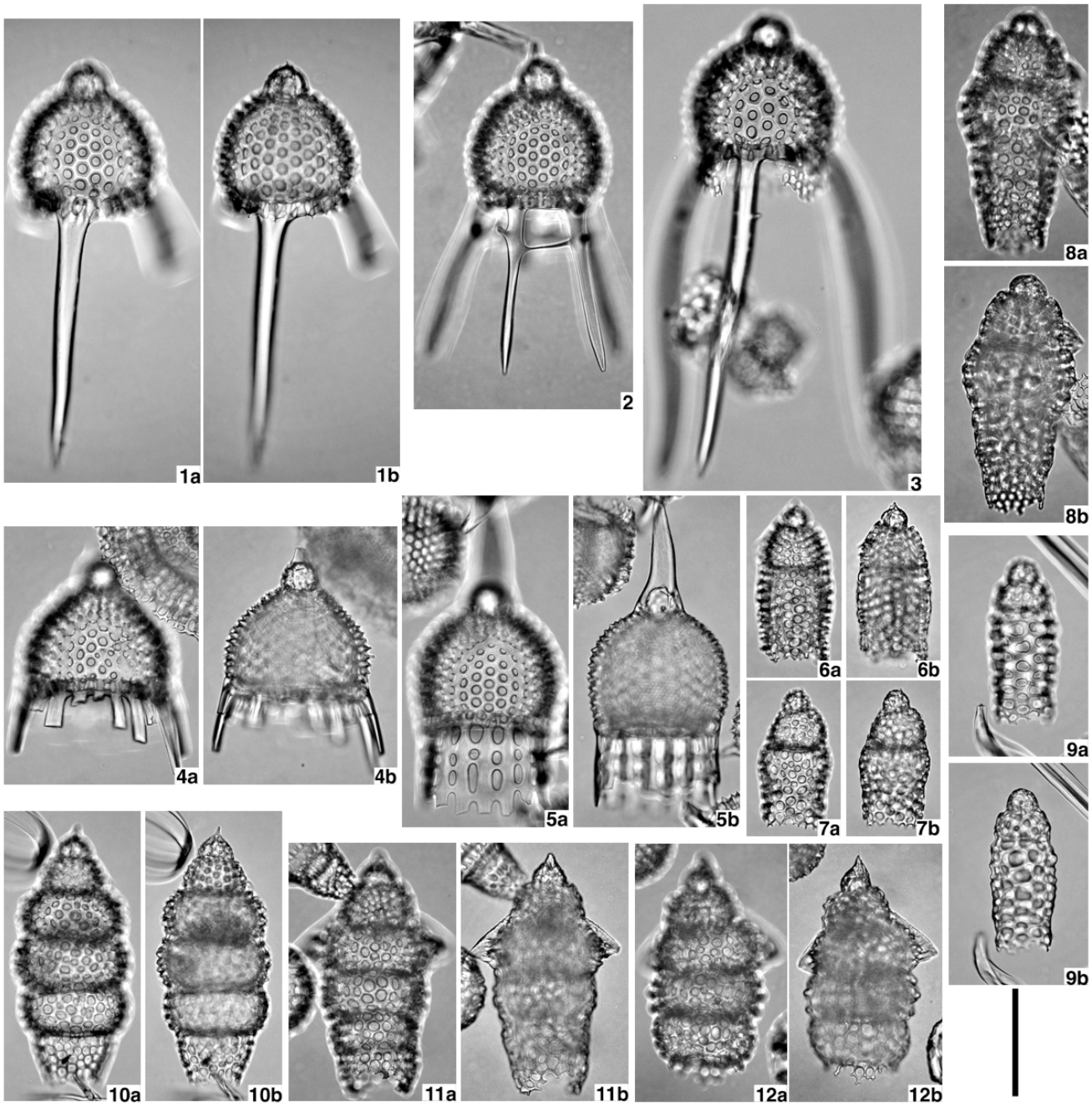

Plate P6. Transmitted light microphotographs of radiolarians from Holes 1218A, 1219A, and 1220A. Scale bar = 100 µm. **1–3.** *Eucyrtidium* sp. F; (1) Sample 199-1218A-25X-1, 120–122 cm (X29/4), (2) Sample 199-1218A-25X-7, 75–77 cm (J50/4), (3) Sample 199-1218A-22X-5, 30–32 cm (B41/0). **4.** *Eucyrtidium* sp. J. (Sample 199-1220A-8H-2, 75–77 cm), O54/1. **5, 6.** *Artophormis dominasinensis;* (5) Sample 199-1220A-9H-5, 125–127 cm (E54/1), (6) Sample 199-1218A-25X-7, 75–77 cm (A52/0). **7.** *Theocorys bianulus* (Sample 199-1218A-22X-5, 30–32 cm), H30/3. **8–10.** *Dictyopodium eurylophus,* (8) Sample 199-1220A-9H-2, 75–77 cm (O47/4), (9) Sample 199-1218A-25X-3, 120–122 cm (L36/0), (10) Sample 199-1220A-9H-3, 75–77 cm (W46/4).

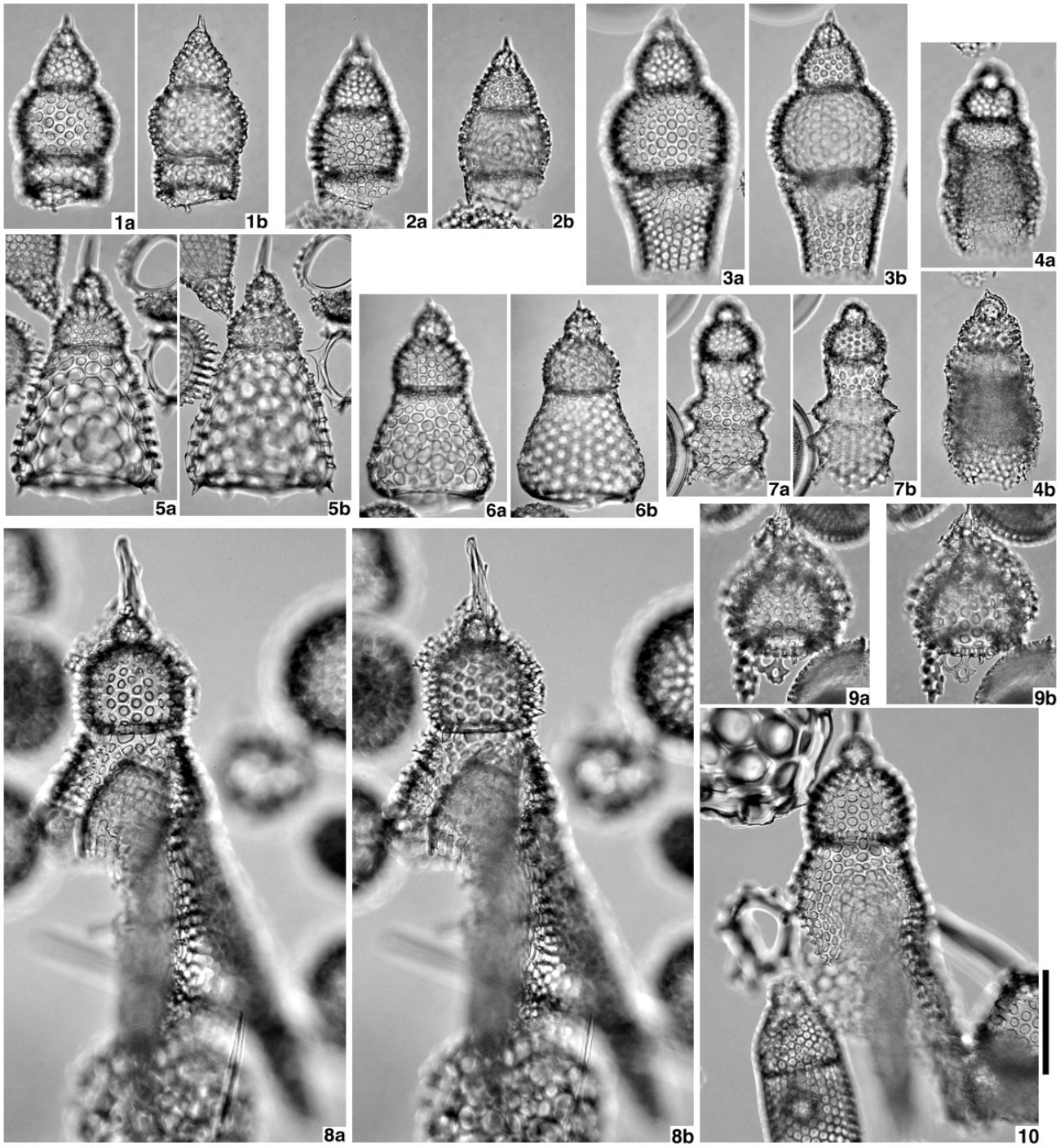

Plate P7. Transmitted light microphotographs of radiolarians from Holes 1218A, 1219A, and 1220A. Scale bar = 100 µm. **1–3.** *Dictyopodium oxylophus;* (1) Sample 199-1220A-9H-3, 125–127 cm (G45/3), (2) Sample 199-1220A-9H-3, 125–127 cm (O19/1), (3) Sample 199-1220A-9H-3, 75–77 cm (S30/4). **4–7.** *Lophocyrtis* (*Apoplanius*) *aspera;* (4) Sample 199-1218A-25X-7, 75–77cm (L26/0), (5) Sample 199-1218A-25X-7, 75–77 cm (E53/0), (6) Sample 199-1218A-22X-5, 30–32 cm (F40/1), (7) Sample 199-1218A-24X-7, 67–69 cm (U30/3). **8, 9.** *Lophocyrtis* (*Apoplanius*) *nomas;* (8) Sample 199-1220A-8H-1, 25–27 cm (K46/0), (9) Sample 199-1218A-22X-5, 30–32 cm (A38/0).

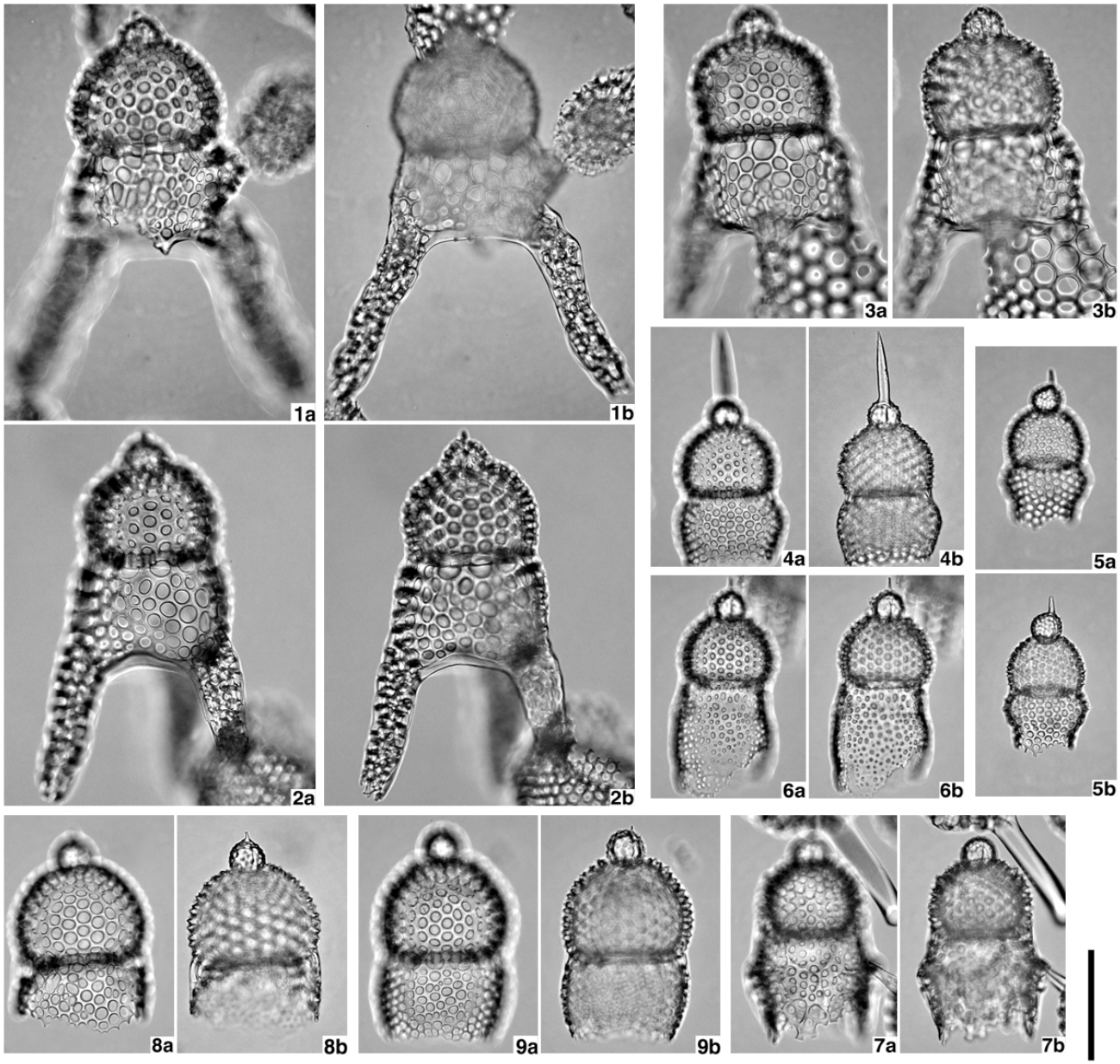

Plate P8. Transmitted light microphotographs of radiolarians from Holes 1218A, 1219A, and 1220A. Scale bar = 100 µm for all figures except figures 3 and 10a scale bar = 200 µm. **1, 2.** *Lophocyrtis* (*Cyclampterium*) *hadra;* (1) Sample 199-1219A-17H-5, 123–125 cm (A43/0), (2) Sample 199-1218A-24X-5, 71–73 cm (D36/3). **3.** *Lophocyrtis* (*Cyclampterium*) *milowi* (Sample 199-1218A-22X-5, 30–32 cm), W51/0. **4, 5.** *Lophocyrtis* (*Lophocyrtis*?) *barbadense;* (4) Sample 199-1218A-24X-5, 71–73 cm (M18/4), (5) Sample 199-1218A-24X-7, 67–69 cm (D16/0). **6, 7.** *Lophocyrtis* (*Lophocyrtis*) *jacchia;* (6) Sample 199-1218A-25X-1, 120–122 cm (Q35/4), (7) Sample 199-1218A-24X-5, 71–73 cm (V37/0). **8, 9.** *Lophocyrtis* (*Lophocyrtis*) *jacchia* group A; (8) Sample 199-1218A-24X-7, 67–69 cm (E49/1), (9) Sample 199-1218A-25X-7, 75–77 cm (W41/2). **10.** *Lophocyrtis* (*Sciadiapeplus*) *oberhaensliae* (Sample 199-1220A-7H-7, 35–37 cm), H30/4. **11.** *Theocorys spongoconus* (Sample 199-1218A-22X-2, 120–122 cm), K46/0.

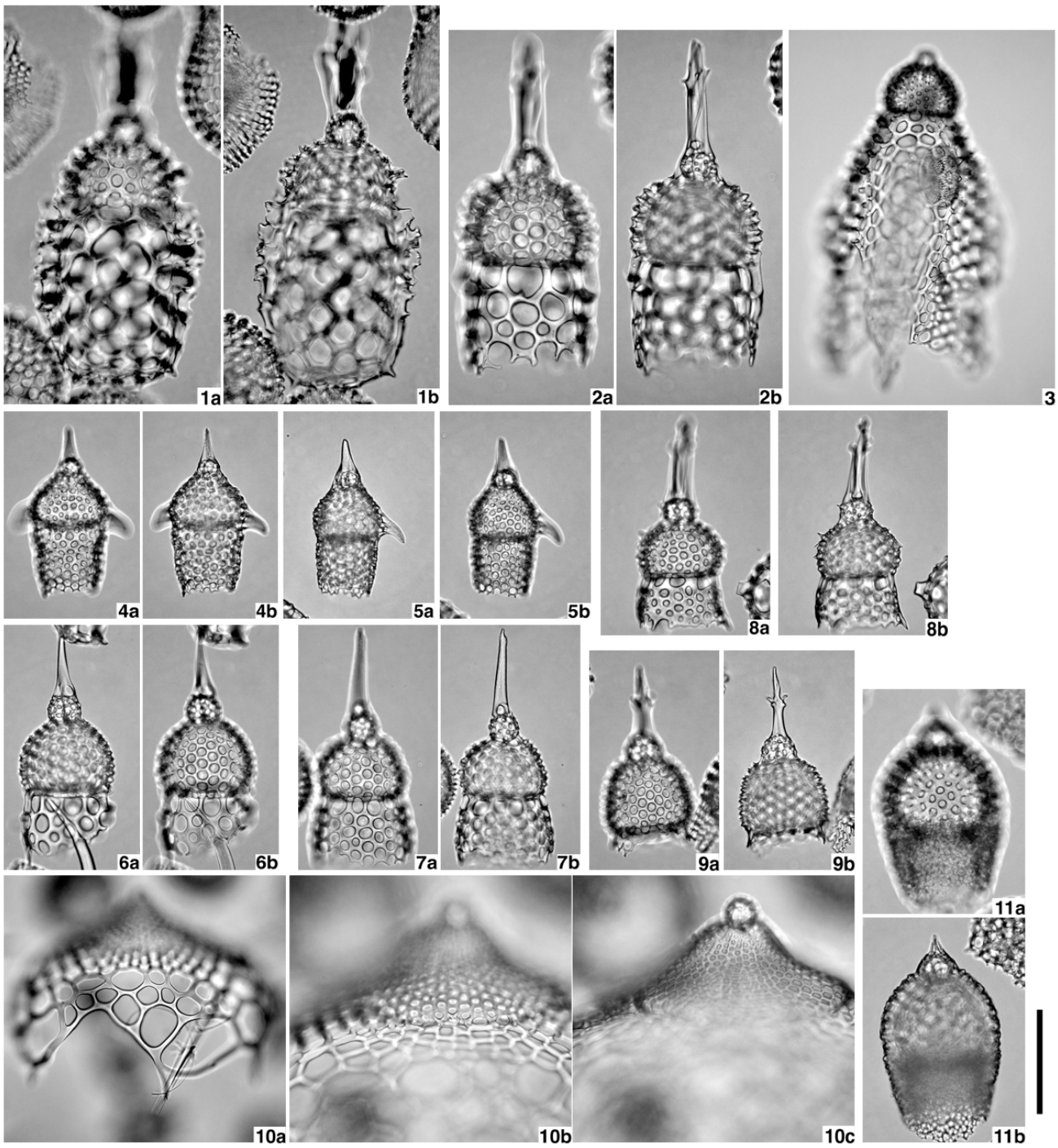

Plate P9. Transmitted light microphotographs of radiolarians from Holes 1218A, 1219A, and 1220A. Scale bar = 100 µm. **1.** *Anthocyrtidium adiaphorum* (Sample 199-1218A-24X-5, 71–73 cm), A16/4. **2.** *Anthocyrtidium stenum* (Sample 199-1220A-8H-6, 25–27 cm), K14/4. **3.** *Arbatrossidium* sp. B (Sample 199-1220A-6H-2, 78–80 cm), M47/0. **4.** *Arbatrossidium* sp. A (Sample 199-1220A-7H-6, 125–127 cm), S41/2. **5.** *Cryptocarpium azyx* (Sample 199-1220A-8H-6, 25–27 cm), V30/1. **6–8.** *Cryptocarpium ornatum;* (6) Sample 199-1220A-9H-5, 25–27 cm (F32/0), (7) Sample 199-1218A-25X-7, 75–77 cm (A44/0), (8) Sample 199-1218A-25X-3, 75–77 cm (E21/4). **9.** *Lamprocyclas rhinoceros* (Sample 199-1218A-22X-3, 120–122 cm), N23/4. **10.** *Lamprocyclas* sp. A (Sample 199-1220A-8H-1, 25–27 cm), O17/2. **11.** *Podocyrtis* (*Lampterium*) *chalala* (Sample 199-1220A-9H-7, 25–27 cm), G21/0. **12.** *Podocyrtis* (*Lampterium*) *goetheana* (Sample 199-1218A-24X-2, 75–77 cm), V25/1. **13.** *Podocyrtis* (*Podocyrtis*) *papalis* (Sample 199-1220A-8H-7, 50–52 cm), D50/2.

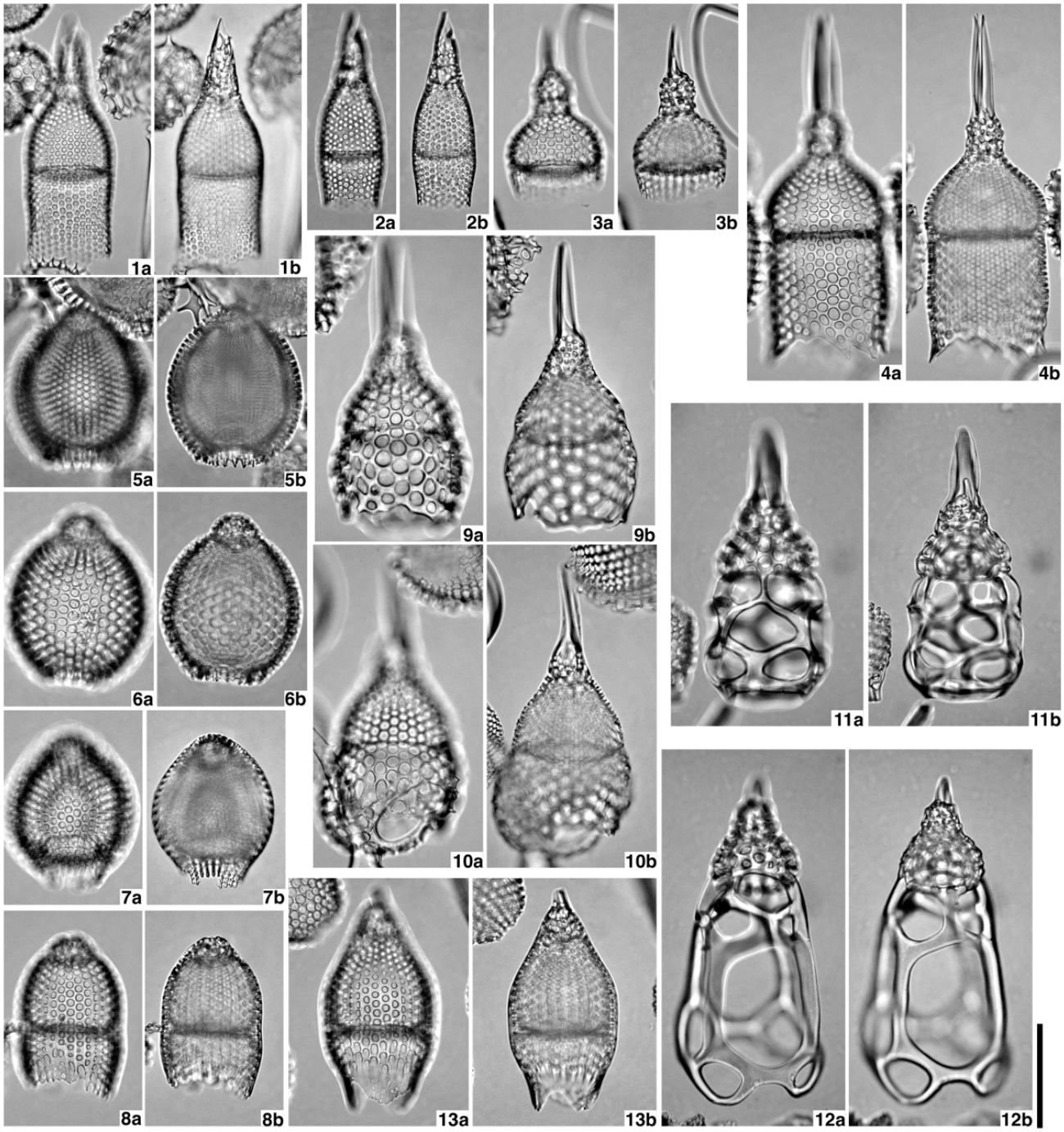

Plate P10. Transmitted light microphotographs of radiolarians from Holes 1218A, 1219A, and 1220A. Scale bar = 100 µm. **1–6.** *Theocyrtis tuberosa* group; (1) Sample 199-1218A-25X-7, 75–77 cm (H51/3), (2) Sample 199-1218A-25X-5, 120–122 cm (L18/0), (3) Sample 199-1218A-25X-7, 75–77 cm (A44/3), (4) Sample 199-1218A-25X-7, 75–77 cm (L36/2), (5) Sample 199-1218A-25X-1, 120–122 cm (C51/2), (6) Sample 199-1218A-22X-5, 30–32 cm (A48/0). **7–10.** *Theocyrtis tuberosa* form A; (7) Sample 199-1218A-25X-5, 120–122 cm (F41/4), (8) Sample 199-1218A-25X-5, 120–122 cm (W40/2), (9) Sample 199-1218A-25X-5, 120–122 cm (L39/4), (10) Sample 199-1218A-24X-5, 71–73 cm (N34/4). **11, 12.** *Theocyrtis tuberosa* form B; (11) Sample 199-1220A-9H-7, 63–65 cm (P43/2), (12) Sample 199-1218A-24X-1, 65–67 cm (H43/3).

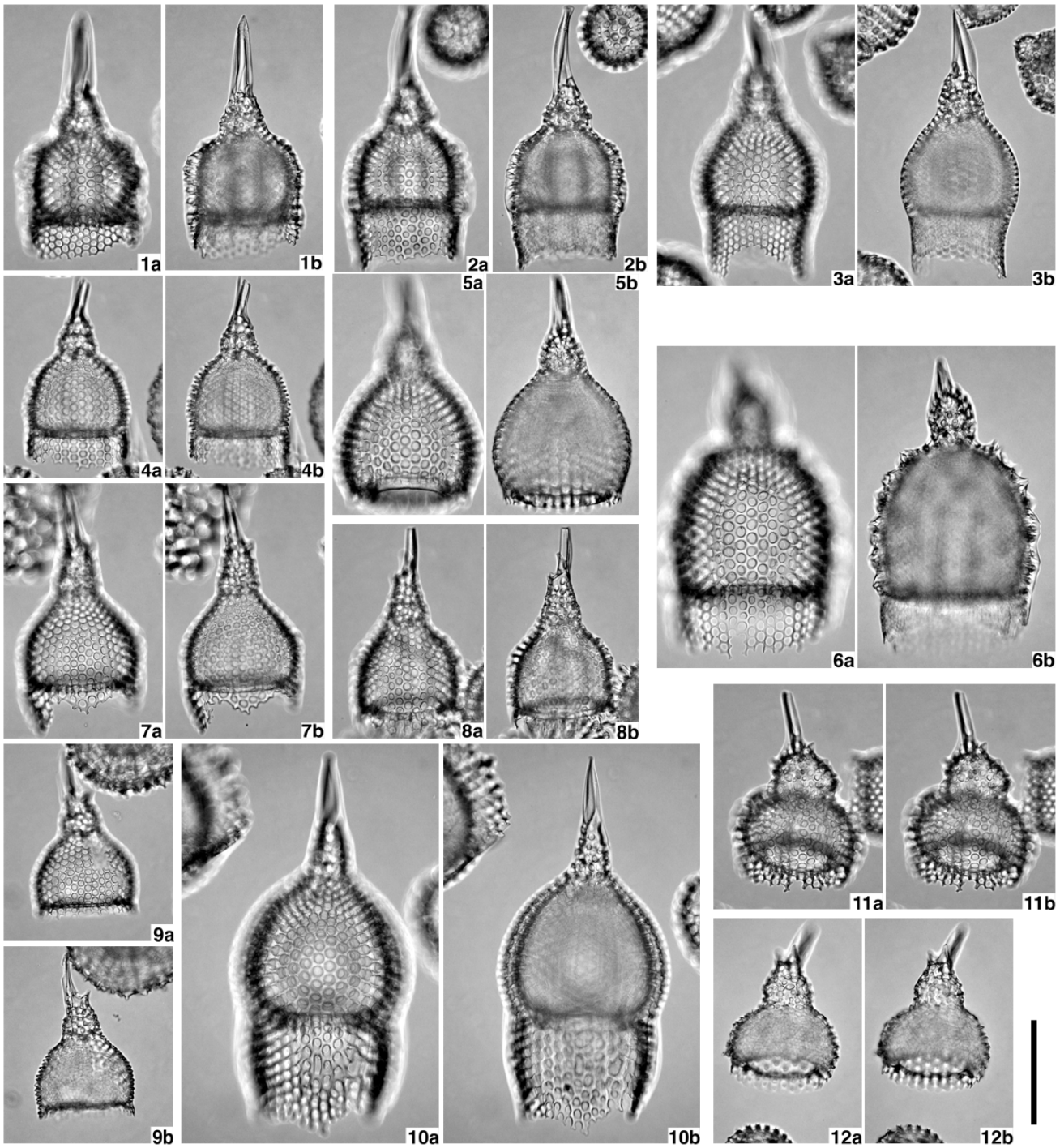

Plate P11. Transmitted light microphotographs of radiolarians from Holes 1218A, 1219A, and 1220A. Scale bar = 100 µm. **1.** *Stichopilidium sphinx* (Sample 199-1218A-24X-7, 67–69 cm), X40/1. **2, 3.** *Thyrsocyrtis bromia;* (2) Sample 199-1218A-25X-7, 75–77 cm (H25/1), (3) Sample 199-1218A-25X-6, 30–32 cm (O28/2). **4–6.** *Thyrsocyrtis bromia* group A; (4) Sample 199-1220A-9H-2, 125–127 cm (K37/1), (5) Sample 199-1220A-9H-2, 125–127 cm (T42/1), (6) Sample 199-1218A-25X-3, 31–33 cm (D24/0). **7.** *Thyrsocyrtis rhizodon* (Sample 199-1220A-8H-6, 77–79 cm), G47/4. **8.** *Thyrsocyrtis triacantha* (Sample 199-1218A-25X-5, 120–122 cm), A23/1. **9.** *Thyrsocyrtis tetracantha* (Sample 199-1218A-25X-7, 75–77 cm), A29/2. **10.** *Thyrsocyrtis lochites* (Sample 199-1220A-9H-5, 125–127cm), G34/0.

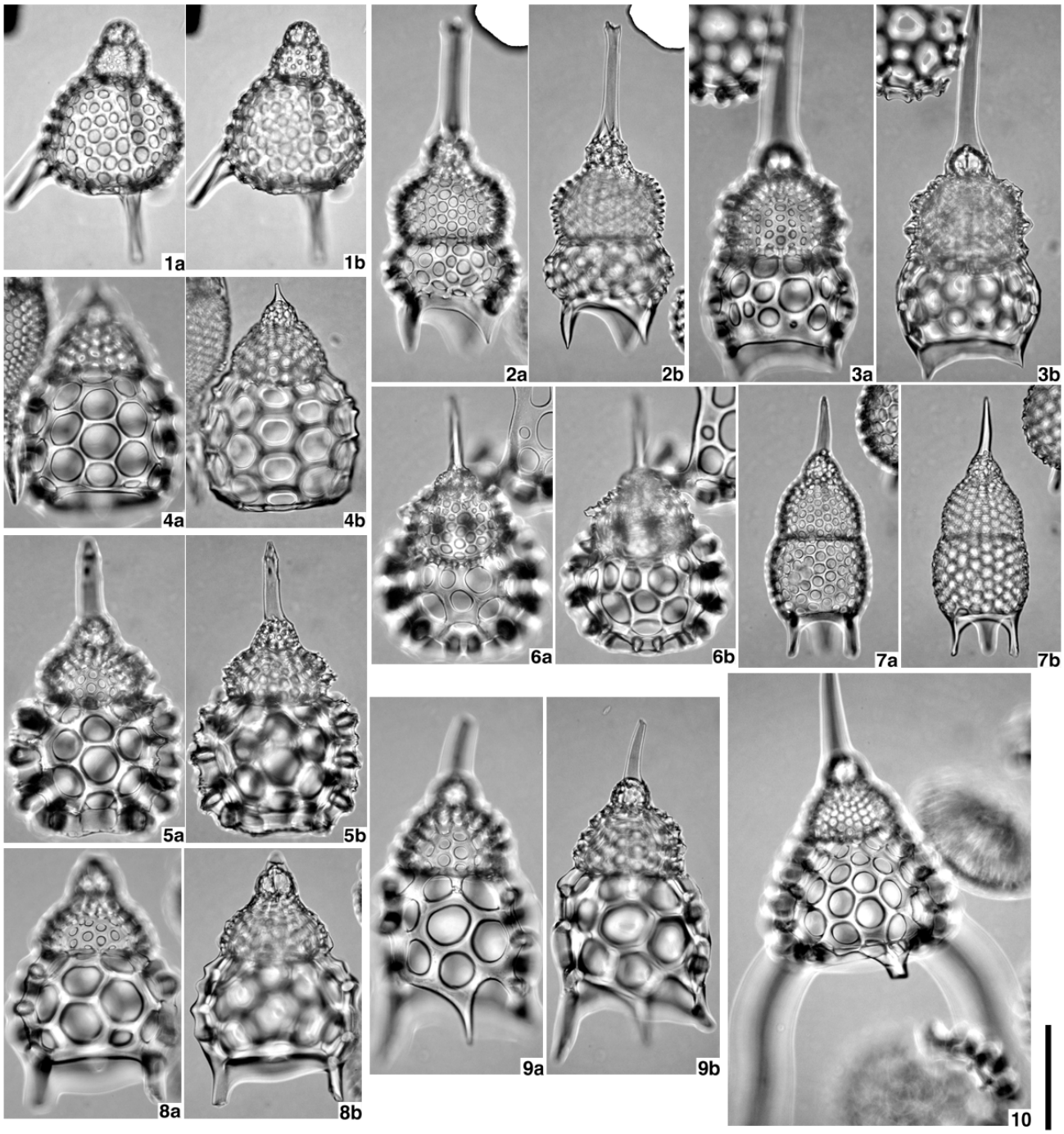

Plate P12. Transmitted light microphotographs of radiolarians from Holes 1218A, 1219A, and 1220A. Scale bar = 100 µm. **1–3.** *Eusyringium fistuligerum* group; (1) Sample 199-1220A-8H-7, 28–30 cm (E34/0), (2) Sample 199-1220A-9H-2, 75–77 cm (M16/4), (3) Sample 199-1218A-25X-7, 75–77 cm (L51/1). **4.** *Lychnocanoma tripodium* form A (Sample 199-1218A-25X-7, 75–77 cm), M24/2. **5.** *Lychnocanoma tripodium* form B (Sample 199-1218A-25X-7, 75–77 cm), Q52/0. **6.** *Lychnocanoma tridentatum* (Sample 199-1220A-9H-7, 25–27 cm), L52/0. **7.** *Lychnocanoma continuum* (Sample 199-1218A-25X-5, 120–122 cm), D48/0. **8.** *Lychnocanoma amphitrite* (Sample 199-1220A-8H-6, 25–27 cm), Q37/4. **9, 10.** *Lychnocanoma tripodium* form C; (9) Sample 199-1220A-9H-6, 125–127 cm (B27/1), (10) Sample 199-1220A-9H-2, 125–127 cm (O42/2).

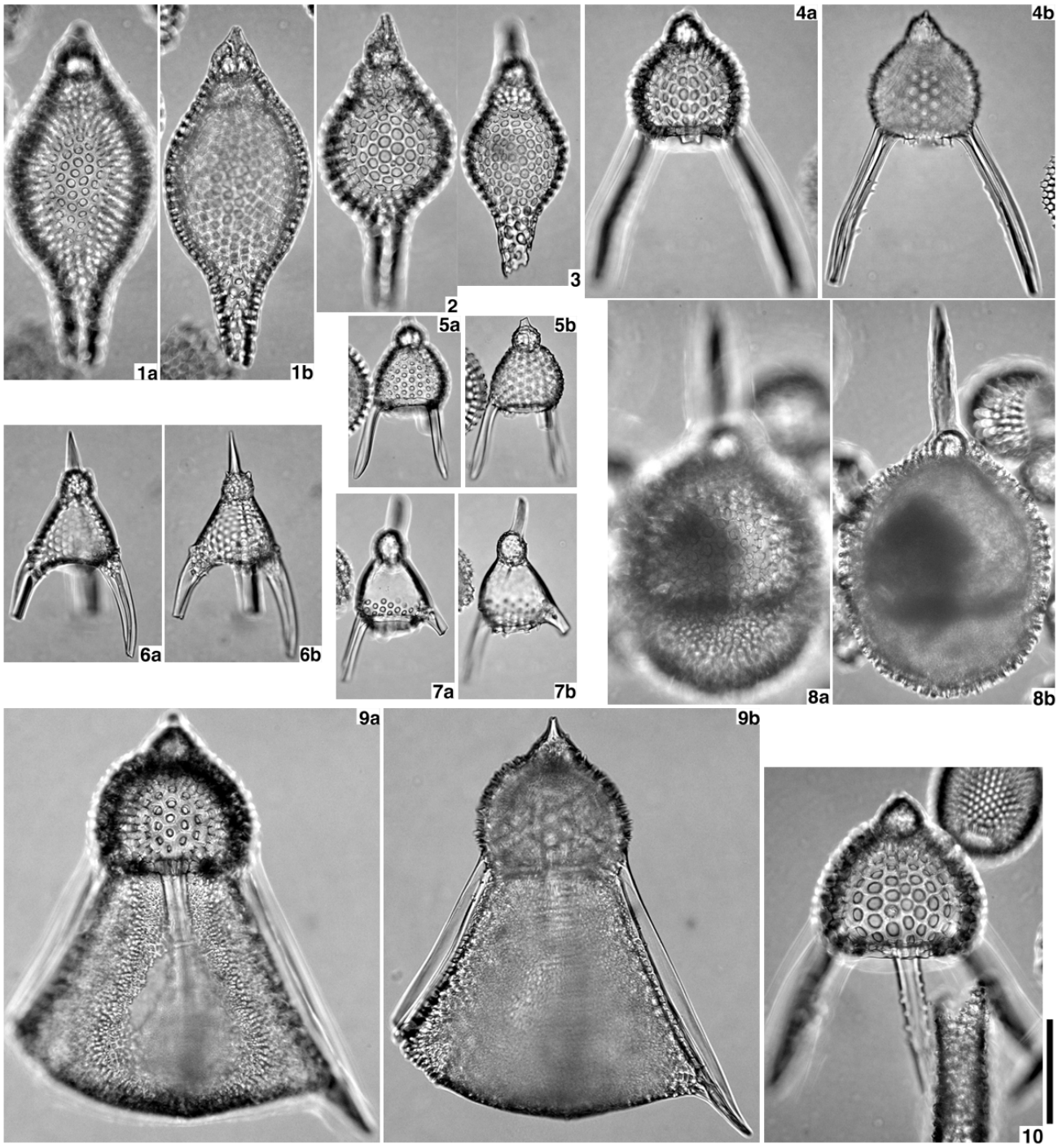

Plate P13. Transmitted light microphotographs of radiolarians from Holes 1218A, 1219A, and 1220A. Scale bar = 100 µm. **1.** *Lychnocanoma babylonis* group (Sample 199-1218A-25X-5, 120–122 cm), V28/2. **2.** *Stichopilium*? sp. B (Sample 199-1220A-7H-7, 35–37 cm), T30/2. **3–4.** *Stichopodium* ?*microporum;* (3) Sample 199-1219A-17H-7, 130–132 cm (G45/4), (4) Sample 199-1220A-9H-1, 125–127 cm (K50/4). **5.** *Anthocyrtis furcata* (Sample 199-1220A-9H-6, 125–127 cm), K36/1. **6.** *Pterocodon campanella* (Sample 199-1218A-25X-3, 31–33 cm), J34/0. **7, 8.** *Cycladophora spatiosa* group; (7) Sample 199-1220A-9H-2, 25–27 cm (Q27/4), (8) Sample 199-1218A-25X-7, 75–77 cm (L22/2). **9.** *Eurystomoskevos petrushevskaae* (Sample 199-1218A-22X-5, 30–32 cm), P23/3. **10.** *Thecospharella ptomatus* (Sample 199-1218A-25X-7, 75–77 cm), C27/0. **11.** *Thecosphaera* sp. A (Sample 199-1218A-25X-7, 75–77 cm), P24/0. **12.** *Axoprunum* sp. aff. *A. irregularis* (Sample 199-1220A-7H-4, 125–127 cm), K46/0. **13.** *Stylosphaera coronata laevis* (Sample 199-1218A-25X-7, 75–77 cm), N21/2. **14.** *Stylosphaera goruna* (Sample 199-1218A-25X-5, 120–122 cm), H41/0. **15.** *Axoprunum pierinae* (Sample 199-1218A-25X-5, 120–122 cm), A18/1.

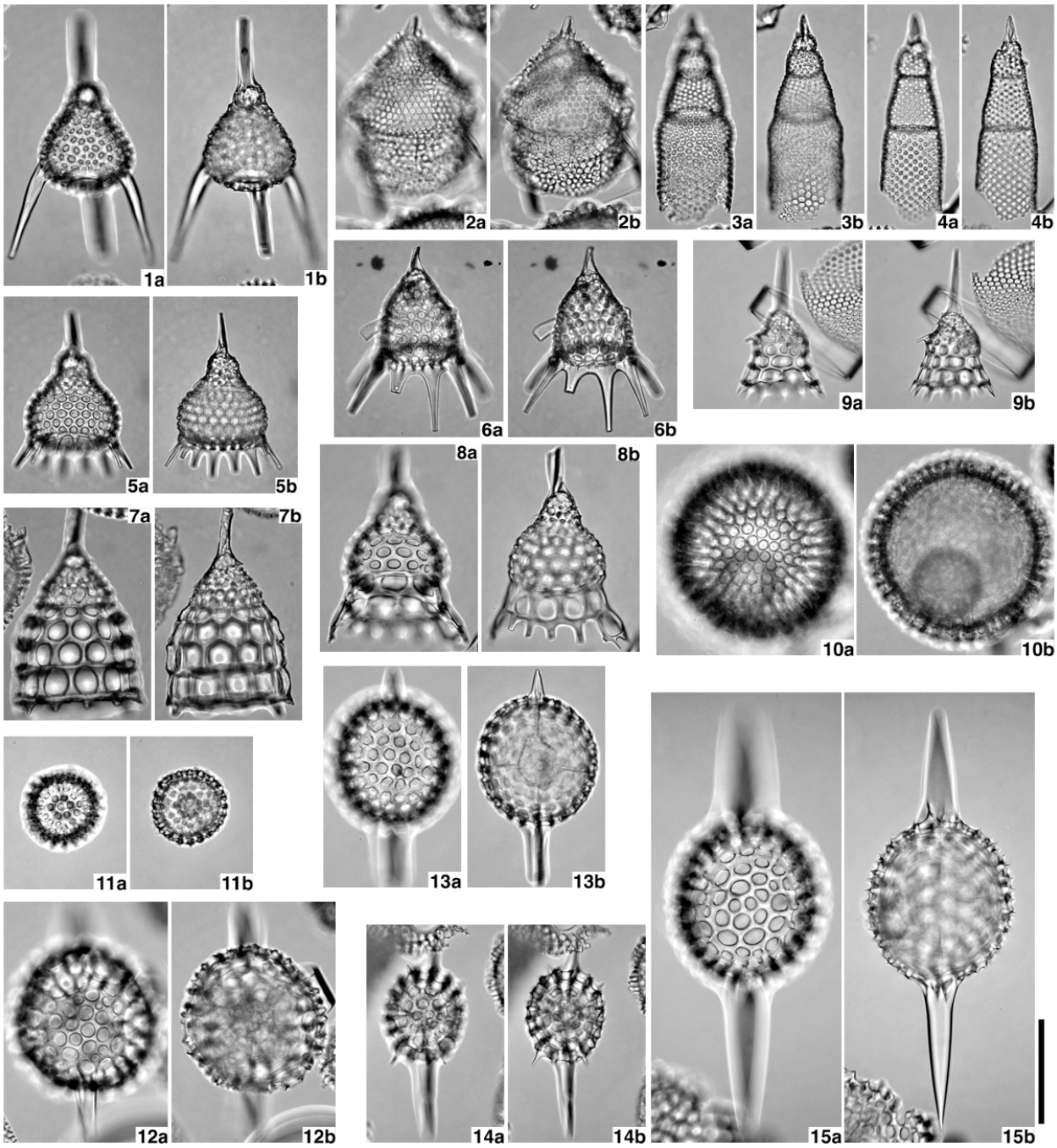

Plate P14. Transmitted light microphotographs of radiolarians from Holes 1218A, 1219A, and 1220A. Scale bar = 100 µm. **1.** *Didymocyrtis prismatica* (Sample 199-1220A-6H-2, 125–127 cm), K42/1. **2.** *Lithocyclia angusta* (Sample 199-1218A-22X-3, 120–122 cm), E29/0. **3, 4.** *Lithocyclia aristotelis* group; (3) Sample 199-1218A-25X-7, 75–77 cm (F51/2), (4) Sample 199-1218A-25X-3, 75–77 cm (R32/0). **5.** *Lithocyclia aristotelis* group form A (Sample 199-1220A-9H-6, 125–127 cm), O14/2. **6, 7.** *Lithocyclia crux;* (6) Sample 199-1218A-22X-4, 120–122 cm (Q48/2), (7) Sample 199-1218A-22X-3, 120–122 cm (L44/3).

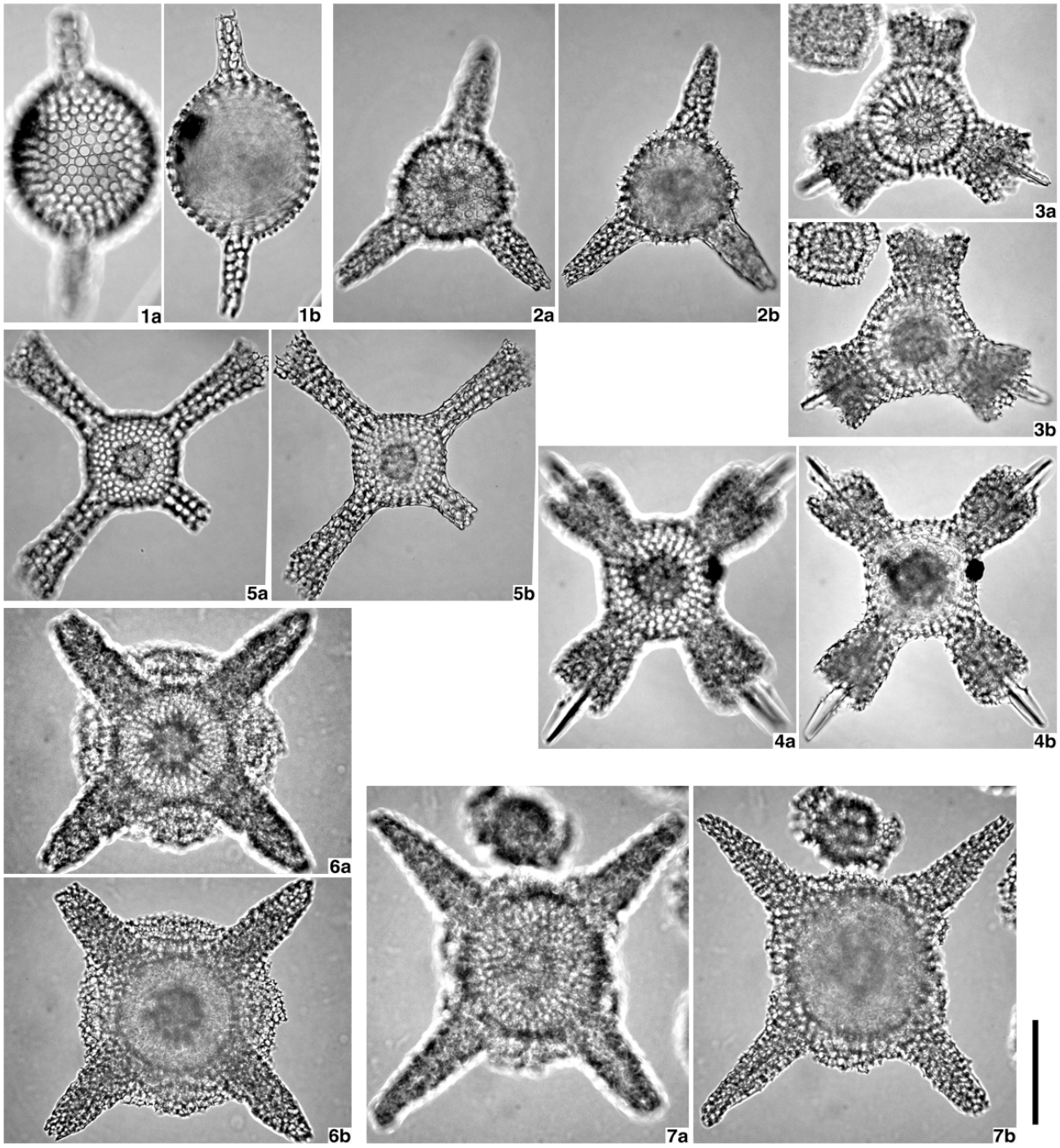

Plate P15. Transmitted light microphotographs of radiolarians from Holes 1218A, 1219A, and 1220A. Scale bar = 100 µm. **1.** *Lithocyclia ocellus* group (Sample 199-1218A-25X-7, 75–77 cm), G48/3. **2.** *Lithocyclia* sp. aff. *L. stella* (Sample 199-1218A-25X-7, 75–77 cm), L46/3. **3, 4.** *Periphaena triactis* (Sample 199-1218A-24X-5, 71–73 cm); (3) P47/3, (4) T19/2. **5, 6.** *Periphaena decora* (Sample 199-1218A-25X-7, 75–77 cm); (5) A34/3, (6) W40/0.

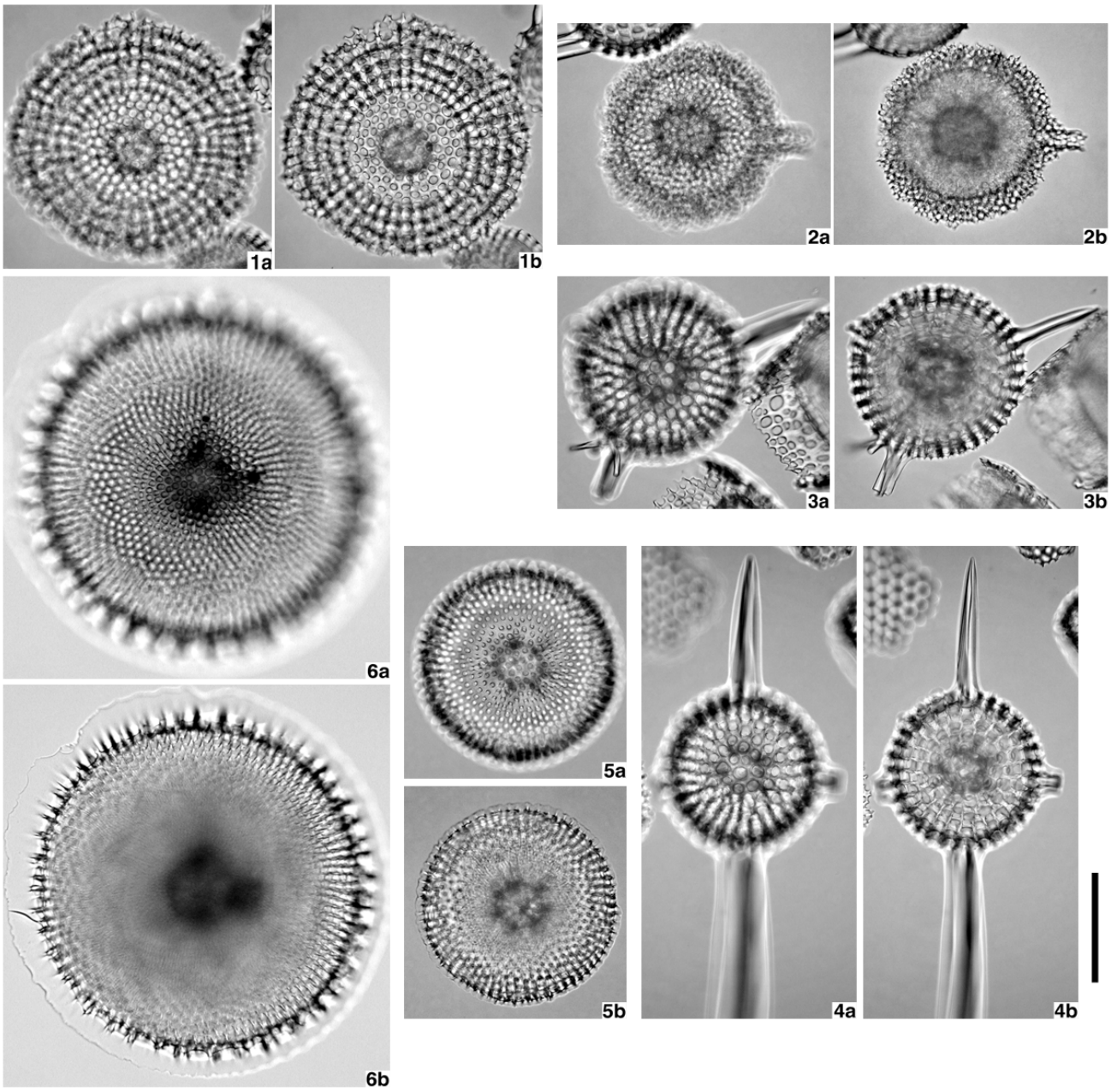

Plate P16. Transmitted light microphotographs of radiolarians from Holes 1218A, 1219A, and 1220A. Scale bar = 100 µm. **1, 2.** *Rhopalastrum* sp. A.; (1) Sample 199-1218A-24X-5, 71–73 cm (Y28/1), (2) Sample 199-1220A-6H-4, 77–79 cm (M38/1). **3.** *Rhopalastrum* sp. B (Sample 199-1220A-6H-7, 40–42 cm), O52/3. **4, 5.** *Rhopalastrum* (?) sp. C; (4) Sample 199-1218A-22X-5, 30–32 cm (H17/4), (5) Sample 199-1220A-7H-5, 77–79 cm (N36/0).

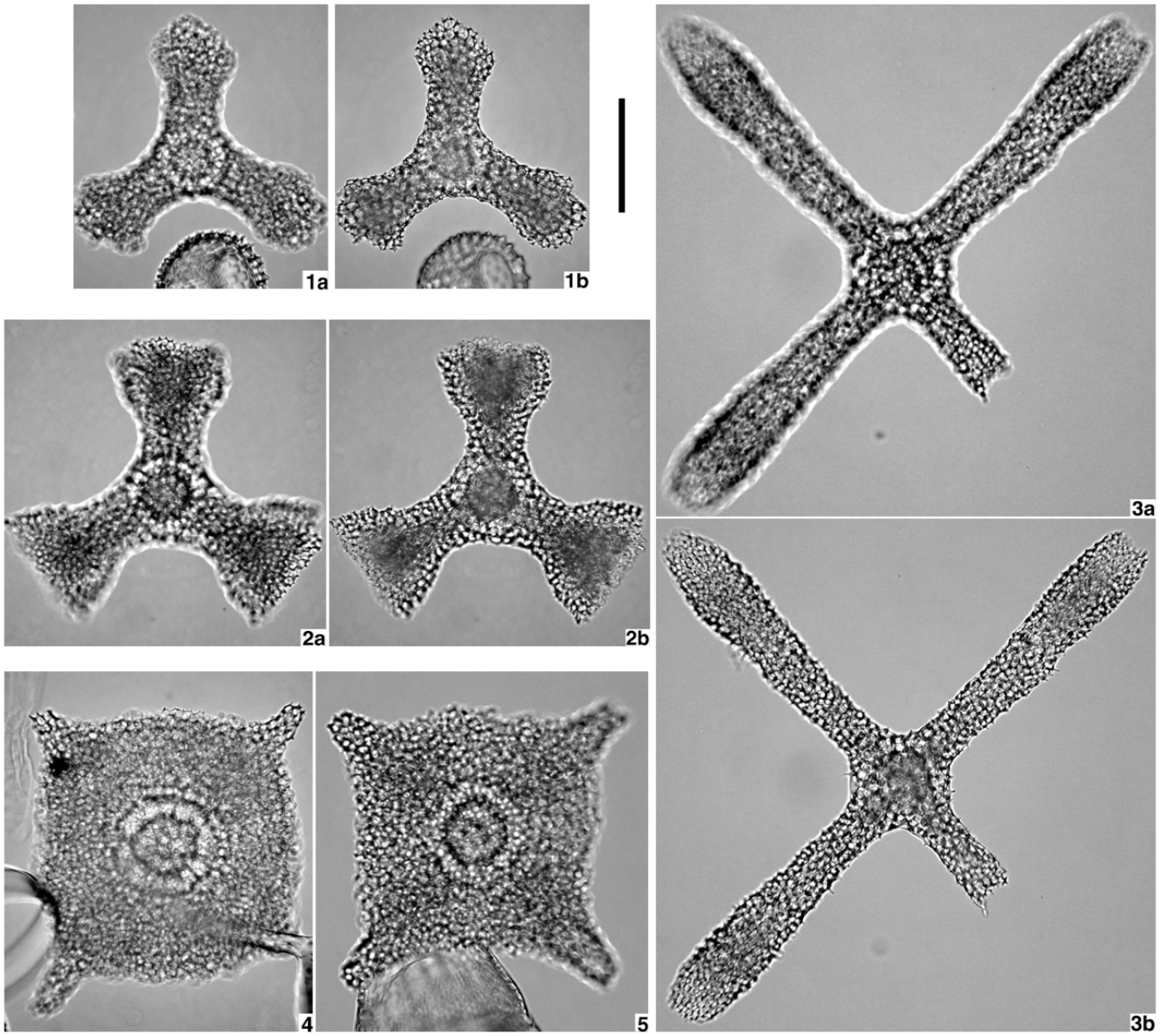

Plate P17. Transmitted light microphotographs of radiolarians from Holes 1218A, 1219A, and 1220A. Scale bar = 100 µm for all figures except for fig. **9** (= 200 µm). **1, 2.** *Collosphaera* sp. A; (1) Sample 199-1218A-24X-5, 71–73 cm (H21/3), (2) Sample 199-1220A-8H-7, 50–52 cm (N18/1). **3, 4.** *Collosphaera* sp. B; (3) Sample 199-1220A-9H-1, 25–27 cm (Y39/1), (4) Sample 199-1220A-9H-3, 25–27 cm (Q24/0). **5.** *Zealithapium mitra* (Sample 199-1218A-22X-3, 120–122 cm), N51/1. **6.** *Zealithapium anoectum* (Sample 199-1218A-25X-3, 31–33 cm), C16/4. **7–9.** *Lithelius hexaxyphophorus;* (7) Sample 199-1218A-25X-5, 120–122 cm (C27/0), (8) Sample 199-1220A-8H-3, 80–82 cm (U35/0), (9) Sample 199-1220A-9H-2, 25–27 cm (C33/4). **10.** *Rhopalodictyum californicum* (Sample 199-1220A-9H-7, 25–27 cm), K25/1.